# The Development of an Inducible Akt as a Potential Gene Therapy for Parkinson's Disease

Soyeon Park

Submitted in partial fulfillment of the
requirements for the degree of
Doctor of Philosophy
in the Graduate School of Arts and Sciences

COLUMBIA UNIVERSITY

2017

**ABSTRACT**

The Development of an Inducible Akt System as a Therapeutic Tool in Parkinson's Disease

Soyeon Park

Parkinson's disease remains a major neurodegenerative disease with prevalence that is second only to Alzheimer's disease. Despite much advancement in the understanding of the pathogenesis of Parkinson's disease, current therapeutic options are limited to those that are only symptomatic and are not disease-modifying. Furthermore, due to what seems to be increasingly complex underlying mechanisms of the disease, identifying a broadly applicable therapeutic strategy is difficult.

There is much evidence surrounding the role of apoptosis and conversely, dysfunction of anti-apoptotic signaling in the progressive neurodegeneration that causes Parkinson's disease. In particular, suppressed PI3K signaling has been implicated in the literature as a key event that occurs during neurodegeneration. Thus, regardless of the diverse upstream mechanisms that may lead to the disease, targeting a downstream effector of neuronal survival presents a therapeutic strategy that may be broadly effective against Parkinson's disease.

For this dissertation, we have developed a method to control the levels of active Akt, the main mediator of the PI3K signaling pathway, using an innovative protein destabilizing technique to create an inducible Akt, DD-Akt(E40K). This method permits the control of active Akt levels through a commonly used and blood-brain barrier permeable antibiotic, Trimethoprim.

We have successfully established the inducibility of DD-Akt(E40K) across various cellular contexts, including neuronal cell types and conditions with suppressed PI3K signaling.

This inducibility was found to be dose-responsive to Trimethoprim, reversible, and able to induce a known downstream substrate, FoxO4, that is an important regulator of cell survival.

Importantly, DD-Akt(E40K) was found to inducibly protect neuronal PC12 cells against Parkinson's disease mimetic toxins as well as growth-factor removal, indicating a proof of principle for the targeting of Akt activity as a protective strategy against Parkinson's disease. The reported trophic effects of active Akt were also corroborated using our inducible DD-Akt(E40K) system *in vivo*, demonstrating significant increases in neuronal cell size within the substantia nigra of mice.

Intriguingly, the inducibility of DD-Akt(E40K) was found to be dependent on the region of expression in the brain of mice such that the levels of this protective protein were not controllable by Trimethoprim in the substantia nigra but were controllable in the striatum.

Taken together, the studies presented in this dissertation establish a new tool for the study of Akt signaling in various cellular and disease contexts and validate Akt as a promising therapeutic target in Parkinson's disease. Our results also suggest an intriguing mechanism for the underlying pathology and selective degeneration observed in the disease.

## TABLE OF CONTENTS

## LIST OF FIGURES

### Chapter 1



### Chapter 3

**Chapter 4**



**Chapter 5**

## LIST OF ABBREVIATIONS & ACRONYMS

| | |
|---|---|
| 6-OHDA | 6-hydroxydopamine |
| AAV | Adeno-associated virus |
| ATP13A2 | Gene encoding ATPase 13A2 |
| BDNF | Brain derived neurotrophic factor |
| CNS | Central nervous system |
| COMTI | Catechol-O-methyltransferase inhibitor |
| DBS | Deep brain stimulation |
| DD | Destabilizing domain |
| DHFR | Dihydrofolate reductase |
| DJ-1 | Gene encoding protein deglycase DJ-1 |
| DNAJC6 | Gene encoding auxilian |
| Endo-Akt | Endogenous Akt |
| FDA | US Food and Drug Administration |
| FKBP12 | FK506 binding protein 12 |
| GBA | Gene encoding glucocerebrosidase |
| GDNF | Glial cell line derived neurotrophic factor |
| GSK3 | Glycogen synthase kinase 3 |
| HA | Hemagglutinin |
| HEK293 | Human embryonic kidney cells 293 |
| LC | Locus ceruleus |
| L-DOPA | L-3,4-dihydroxyphenylalanine |

| | |
|---|---|
| LRRK2 | Gene encoding leucine-rich repeat kinase 2 |
| MAOBI | Monoamine oxidase type B inhibitor |
| MAPT | Gene encoding microtubule-associated protein tau |
| $MPP^+$ | 1-methyl-4-phenylpyridinium |
| MPTP | 1-methyl-4-phenyl-1,2,3,6-tetrahydropyridine |
| mTORC | Mammalian target of rapamycin complex |
| Myr-Akt | Myristoylated Akt |
| NGF | Nerve growth factor |
| pAkt | Phosphorylated Akt |
| PC12 | Pheochromocytoma of the rat adrenal medulla 12 |
| PD | Parkinson's disease |
| PDK1 | Phosphoinositide-dependent protein kinase 1 |
| PH | Pleckstrin homology |
| $PI3,4P_2$ | Phosphatidylinositol 3,4 bisphosphate |
| PINK1 | Gene encoding PTEN-induced putative kinase 1 |
| $PIP_3$ | Phosphatidylinositol 3,4,5 triphosphate |
| PKB | Protein kinase B |
| PRAS40 | Proline-rich Akt substrate of 40 kDa |
| Shld1 | Shield-1 |
| SN | Substantia nigra |
| SNpc | Substantia nigra pars compacta |
| SYNJ1 | Gene encoding synaptojanin 1 |
| TMP | Trimethoprim |

| | |
|---|---|
| TSC2 | Tuberous sclerosis complex 2 |
| VPS35 | Gene encoding vacuolar protein sorting associated protein 35 |
| VTA | Ventral tegmental area |

**ACKOWLEDGEMENTS**

First and foremost, I would like to thank my advisor, Lloyd Greene, for accepting me into his lab and trusting me with this exciting translational project. I do not know if it was intentionally matched to my interests, but the potential clinical implications of this project hooked me right from the start. Project aside, thank you for your dependable guidance throughout this long journey – I certainly would not have made it this far without your quiet patience and nudges in the right direction along the way. I look back at the incredible growth I have had as a person and critical thinker and cannot imagine that I would have been able to accomplish this without your mentorship.

I would also like to give special thanks to Oren Levy, for being my first mentor in the lab and continually providing great insights and friendly support even as you have gone on to start your own lab and take on other mentees.

I owe a great amount of gratitude to my many collaborators who have provided me materials and scientific support throughout this project.

First, major thanks go to Bob Burke and all former and current members of his lab for adopting me into your scientific family for a good couple of years and providing me with all the support I could ever hope for in my training. Bob, I have learned a great deal from you about the merits of rigorous science and hold an incredible amount of respect for you as a mentor, scientist, and person. Adriana, thank you for patiently teaching me all the necessary techniques to complete my *in vivo* studies. Marla, thank you for providing unquestionable support whenever I needed (and thank you for all delicious food you've cooked for me). Nick, thank you for your help in creating my constructs and cloning advice thereafter. Tanya, thank you for always being so willing to work with my schedule and working to make such incredibly consistent injections

each time.

Second, thank you to Dr. Thomas Franke for lending crucial advice with your Akt expertise and providing the Akt(E40K) construct, without which this project would not have been possible.

Third, thank you to Roger Lefort, for being so flexible and generous with your animal protocol. Without that, I would not have been able to complete my critical animal experiments on time.

Finally, thank you to Pascaline Aimé for supplying me with valuable and hard-earned ventral midbrain cultures. I know how difficult and time-consuming those cultures can be, so thank you for so generously donating them for my project. Cultures aside, thanks for being a great role model and friend, always knowing when to provide advice when I needed it.

I would also like to thank the other members of my lab for always being supportive and creating a real second home away from home. Everyone has been so great to work with and I could not have asked for a better lab environment. Special thanks go to Lyuda for being such a dependable friend and fellow PhD student. Your presence has made this experience so much more fun during the good times and bearable during the difficult times – I can't wait to see you take your turn in earning your PhD.

Thank you to all my friends outside of science bubble, including those from college and those in the taekwondo club. You guys provided me sanity and perspective, two things that are sometimes forgotten in the world of academia.

Lastly, I need to thank my family, particularly my parents. Both have a PhD under their belt, something that they earned after having just immigrated, while learning English, adjusting to American culture, and raising a child and an infant. I cannot imagine how difficult that was,

and my appreciation only grows as time goes on. Thank you, for cultivating my curiosity from a young age and teaching me that asking questions and thinking critically are important skills to be proud of, not shy away from, even if society expects less.

## DEDICATION

I would like to dedicate my thesis to my parents, for loving and supporting unconditionally, and providing me with the foundation and belief that I can be ambitious and achieve whatever I strive for.

I would also like to dedicate my thesis to Chinweike Okegbe. I wish I had expressed this while you were still here, but Chinwe, I hope you know the kind of impact you had on your fellow graduate students. Your willingness to go beyond what was expected and found the Biological Sciences Career Initiative is the only reason I was prepared enough to make the right decision for my career going forward. I regret that your opportunity to continue making impact in the future was taken away by your passing, but I and others in the program will continue to be inspired by you and strive to better our community.

# Chapter 1: General Introduction

## 1.1: Parkinson's Disease

### 1.1.1 Etiology and Pathogenesis

Parkinson's disease (PD) is the second most common progressive neurodegenerative disease, affecting 2-3% of the population ages 65 and older [1]. The principal risk factor for PD is considered to be increasing age, with incidence of PD being rare before 50 years of life but increasing 5-10 fold between ages 60-90 [2-4]. Typically thought of as a movement disorder, clinical diagnosis currently includes identification of cardinal motor symptoms such as tremor at rest, rigidity of limbs, slowness of movement or "bradykinesia", and postural instability, along with responsiveness to levodopa. However, a majority of PD patients also experience a variety of non-motor symptoms including sleep-wake cycle dysfunction, cognitive impairment, mood disorders, autonomic dysfunction, and hyposmia [5] .

Hallmark pathological features of PD include the loss of dopaminergic neurons within the substantia nigra pars compacta (SNpc) and deposition of α-synuclein in the form of Lewy bodies and neurites [6, 7]. Although neither of these features are unique to PD, the combination of both is still currently used for conclusive diagnosis of idiopathic PD [1, 7].

Dopaminergic degeneration within the SNpc is progressive and leads to subsequent loss of dopaminergic signaling within the nigrostriatal pathway, manifesting as the cardinal motor symptoms of the disease. The progression of this degeneration is reported to begin with loss of axonal projections and progress to death of SNpc dopaminergic neurons such that by the time of disease onset or diagnosis, it is believed that there has been approximately 50-60% loss of dopaminergic terminals within the striatum and 30% loss of SN dopaminergic neurons [8]. In addition to loss of dopaminergic innervation to the striatum, there are reports of degenerative

loss in other regions, including the peripheral nervous system, which often correlate with non-motor symptoms of the disease. For instance, degeneration of postganglionic sympathetic neurons that innervate the heart has been reported in patients that exhibit orthostatic hypotension [9]. Similarly, drastic loss of dopaminergic enteric neurons within the myenteric plexus is widely believed to underlie symptoms of gastrointestinal dysfunction, such as constipation [10, 11]. There also exist reports of neuronal loss within the central nervous system outside of the SN, often correlating with the presence of high neuromelanin levels [12]. These regions of degeneration include the cholinergic neurons within the dorsal motor nucleus of the vagus, noradrenergic neurons of the locus ceruleus (LC), serotonergic neurons of the raphe nuclei, and cholinergic neurons of the nucleus basalis of Meynert [12]. As mentioned above, although various areas within the peripheral and central nervous system may exhibit neurodegeneration in PD, neuronal loss in the SNpc remains the defining pathological feature of PD and thus is exhibited in nearly all PD patients. Interestingly, loss of noradrenergic neurons within the LC also appears in all PD patients [12]; however, the functional significance of this is yet to be fully elucidated.

The presence of abnormal intracellular protein deposits that aggregate within the SNpc and other brain regions affected in PD are termed Lewy bodies and Lewy neurites, collectively termed Lewy pathology [13, 14]. Although Lewy pathology consists of a variety of intracellular proteins including parkin, ubiquitin, and neurofilaments, the most abundant component is the protein α-synuclein [6, 15]. Initial thoughts within the field supported the belief that these aggregates were themselves toxic; however, more recent hypotheses suggest that Lewy pathology represents aggresomes that form as part of cellular processes to clear accumulation of misfolded proteins [16]. Although the field has not been able to fully elucidate the precise role of

Lewy pathology or α-synuclein in the disease, nor conclusively validate any causal role of Lewy pathology in disease etiology, research studies have provided insight into potential physiological functions and corresponding dysfunctions of α-synuclein within PD. These include evidence of α-synuclein involvement with synaptic dysfunction, vesicular release, axonal transport deficits, and ER-Golgi stress [17-25]. In further support of the hypothesis that α-synuclein dysfunction plays a role in the disease, studies have found that duplication or triplication in the α-synuclein gene can also lead to familial PD [26].

An interesting paradigm that has been the cause of scientific debate within the field is the potential prion-like behavior of α-synuclein. Traditional Braak staging of the neuropathological changes in PD has suggested that there is pathological spreading of α-synuclein aggregates that begins in the lower brain stem and olfactory bulb and eventually spreads to areas of the midbrain, including the SNpc, finally reaching the basal forebrain and neocortex. Furthermore, this spread of α-synuclein pathology has also been suggested to correlate with disease progression [13]. However, this scheme for Braak staging of PD is a contentious topic, with evidence to show that there is no correlation between Braak stage and clinical severity of PD, and there exist cases of aged individuals who exhibit no neurological symptoms but have brain synucleinopathy that would be characterized as late Braak stage [27]. Review of more recent literature suggests that Braak staging may in fact apply to a specific subset of PD patients with young onset and long disease duration, but indeed may not describe generalized PD pathogenesis [28].

Nevertheless, the prion hypothesis was first thrust into the spotlight of PD research when autopsy studies of patients who had received nigral neuron grafts revealed Lewy pathology present in the grafted neurons, thus suggesting a host-to-graft propagation of disease pathology

[29, 30]. Furthermore, recent research has implicated the presence of toxic α-synuclein strains in the form of fibrils that are capable of seeding α-synuclein pathology throughout the central nervous system [31]. Research surrounding the spread of α-synuclein pathology eventually led to the development of both *in vitro* and *in vivo* α-synuclein fibril-based PD models that demonstrate the spread of α-synuclein aggregation and corresponding neuronal degeneration [32-34]. In further support of the prion hypothesis, a recent study discovered a putative receptor that is sufficient for pathological transmission of α-synuclein, thus providing a mechanism for the potential spread of α-synuclein pathology within the disease [35].

The large majority of PD cases are idiopathic or sporadic, with estimates ranging from 90-95% of all PD cases [7, 36]. The remaining 5-10% are considered to be caused by inherited genetic abnormalities, termed familial PD [36]. Genetic studies of such cohorts have resulted in the discovery of various forms of monogenic PD, the first of which was autosomal-dominant PD caused by mutations within the *SNCA* gene, encoding α-synuclein [37]. Five other monogenic forms of PD have since been conclusively linked to classic Mendelian PD, caused by mutations within *LRRK2*, *Parkin*, *PINK1*, *DJ-1*, and *VPS35* [37, 38]. Additionally, there exist a number of genes linked to atypical forms of PD, such as *ATP13A2*, *SYNJ1*, and *DNAJC6*, as well as many reported genetic risk factors, those of note including associations with *GBA* and *MAPT* [38]. Combined, mutations in the six confirmed monogenic forms of classic PD only account for an estimated 30% of familial PD cases and 3-5% of sporadic PD cases, highlighting the complexity of PD etiology and importance of continued efforts to further elucidate genetic causes of PD.

In addition to genetic causes, there also exist various environmental factors that have been associated with susceptibility to PD, the most infamous of which is the synthetic neurotoxin 1-methyl-4-phenyl-1,2,3,6-tetrahydropyridine (MPTP). MPTP was discovered as a contaminant

in illicitly synthesized drugs, causing Parkinsonism in unknowing drug users in 1983 [39]. Other environmental risk factors of PD that have been the subject of discussion within the field include exposure to pesticides [40, 41], traumatic brain injury [42], and endogenous cellular factors, such as the loss of trophic support or the formation of endogenous toxins or reactive oxygen species during the metabolism of endogenous dopamine [43]. In support of the endogenous toxin hypothesis, there have been various reports of genetic susceptibility to PD associated with cytochrome P450-enzyme polymorphisms [44, 45]. Cytochrome P450 is believed to have potential detoxifying functions within the substantia nigra. However, further studies and meta-analyses of this association have resulted in conflicting conclusions, making the role of cytochrome P450 in PD unclear [46-49]. Additionally, there have been reports of polymorphisms in other genes that may have functions in detoxification of metabolites, such as *NAT2* encoding N-Acetyltransferase 2 and *GSTP1* encoding Glutathione S-Transferase Pi 1, but meta-analyses of these associations also have led to conflicting conclusions on their significance to the disease [50, 51].

### 1.1.2 Current Therapies and Treatments

Current approved treatments for PD rely on addressing the symptoms of the disease, with particular emphasis on the motor symptoms, but not necessarily the mechanism or cause of disease. The most ubiquitous methods of treatment remain pharmacological. Of these, levodopa (L-3,4-dihydroxyphenylalanine), a precursor to dopamine, is most effective at alleviating the symptoms caused by depletion of dopaminergic signaling within the nigrostriatal pathway [52]. Levodopa (L-DOPA) treatments are often administered as a formulation with carbidopa, an inhibitor of DOPA decarboxylase, to prevent the peripheral conversion of levodopa to dopamine

[52]. However, L-DOPA treatment is associated with increasing motor complications with increasing treatment time – these include dyskinesias or motor fluctuations with L-DOPA wear-off [53]. Alternatively, dopamine agonists can also provide efficacious motor symptom management in PD patients, particularly in younger patients, and have a lower risk for dyskinesia development [54].

There also exist pharmacological treatments outside of dopamine-based drugs that are used as alternatives or as combination therapies depending on patient needs. Anticholinergic medications comprise the oldest class of drugs approved for use in PD and have been shown to improve motor function in PD patients [55]. Additionally, the antipsychotic clozapine, although rarely used, has been reported to improve tremors in PD patients [56]. Amantadine, a compound used as an antiviral drug, has also been approved by the FDA as an antiparkinsonian drug and is recommended by both the International Parkinson and Movement Disorder Society and the European Federation of Neurological Societies as an efficacious symptomatic therapy [57, 58]. Finally, patients with mild motor symptoms may be prescribed monoamine oxidase type B inhibitors (MAOBI), such as selegiline or rasagiline, to augment L-DOPA function [52].

In practice, multiple pharmacological drugs are often used in combination to manage motor symptoms for each patient. As alluded to above, some of the major complications of dopamine-based treatments are motor fluctuations that are triggered as the medication wears off as well as management of motor symptom reemergence during “off” time. Strategies to combat these side effects focus on methods for continuous dopaminergic stimulation. These include the use of MAOBIs or catechol-O-methyltransferase inhibitors (COMTIs) to inhibit the metabolism of dopamine [52, 59], improved sustained-release formulations of L-DOPA, as well as dopamine agonists as an adjunctive therapy with L-DOPA to prolong its effects and minimize “off” time.

In addition, amantadine has reported anti-dyskinetic effects and is also used to combat motor fluctuations from wear-off and dyskinesia in PD patients [60]. There also exist alternative delivery strategies for prolonged or rapid acting drug action such as continuous duodenal infusion (Duodopa), and administration of dopamine agonists through rectal, intranasal, sublingual, subcutaneous, and transdermal routes [61].

For patients who develop severe dyskinesias and motor fluctuations enough to impair quality of life, there also exist surgical interventions, the most common of which is deep brain stimulation (DBS). Pioneered as a PD therapy nearly three decades ago, DBS has been shown to effectively reduce levodopa-responsive symptoms, dyskinesia, and tremor [62]. In this treatment, an electrode to deliver stimulation is surgically placed into one of two conventional target areas: the subthalamic nucleus or the internal segment of the globus pallidus [63]. As with any treatment, there are limitations to DBS including reports of complications with targeting the subthalamic nucleus which may lead to increased depression and cognitive impairment [62]. An alternative surgical intervention that has been proposed is ablative surgery, such as pallidotomy and thalamotomy; however, this surgery carries additional risks that come with open-brain surgery and mistargeted lesions [62]. With the recent advent of high-intensity focused ultrasound as a surgical technique that, combined with MRI for target guidance, allows for incision-less lesions, lesion therapy may in the near future provide a viable alternative to DBS [64].

Unfortunately, PD remains thus far an incurable disease. As the disease progresses, both motor and nonmotor symptoms increase in severity such that patients become less responsive to medication, and standard surgical interventions carry risks as discussed above [52, 62]. Additionally, almost all currently approved therapeutics are purely symptomatic and not disease-modifying, with potential exceptions being MAOBIs and DBS of the subthalamic nucleus.

Rasagiline, a MAOBI, has shown evidence of neuroprotection in preclinical studies, but phase III clinical trial results were inconclusive [65]. Additional studies have suggested that subthalamic nucleus DBS is neuroprotective in animal models, potentially through BDNF-trkB signaling [66]. However, no putative neuroprotective therapy has yet been able to demonstrate clear benefit in clinical trials; therefore, there is much room for improved therapies for PD, particularly ones that may be disease-modifying.

### 1.1.3 Models of Parkinson's Disease

There are a large variety of models and research tools that have been developed to study the pathogenesis of PD. These can be separated into two main categories: toxin models and genetic models. Although no one model perfectly recapitulates all features of the disease, a select few models have proven valuable for studying different aspects of the disease. Here, we will discuss the features of major PD models and their relevant advantages and disadvantages.

Pharmacological agents and toxins that lead to mitochondrial dysfunction have been widely used as classical models of PD, particularly as mitochondrial dysfunction has been implicated as a contributor to the accumulation of misfolded proteins and neuronal degeneration [7]. The two most common such models are 6-hydroxydopamine (6-OHDA) and 1-methyl-4-phenyl-1,2,3,6-tetrahydropyridine (MPTP).

6-OHDA is a hydroxylated analogue of dopamine and was the first such toxin used to create animal models of PD. It is extensively used as a PD mimetic neurotoxin because it is selectively taken up by catecholaminergic neurons and causes their rapid death [67]. Although the complete mechanism of degeneration is unclear, oxidative stress is a major, if not main, component of 6-OHDA-induced death and is believed to result from disruption of mitochondrial

complex I [68]. 6-OHDA has been used for both *in vitro* and *in vivo* models, although it must be directly injected into the brain of intact animals as it is not able to cross the blood brain barrier [7, 68].

MPTP was first discovered for its neurotoxic effects when young drug users developed Parkinsonism after having used illicitly synthesized drugs with MPTP as an unfortunate contaminant [39]. MPTP leads to selective degeneration of dopaminergic pathways with higher sensitivity to the toxin found in the SNpc than the ventral tegmental area (VTA), thus mimicking the specific regional pattern of degeneration seen in PD [69, 70]. MPTP can cross the blood brain barrier and thus can be systemically administered in animals, whereupon it is converted by monoamine oxidase B in astrocytes and serotonergic neurons into 1-methyl-4-phenylpyridinium ($MPP^+$). $MPP^+$ then is selectively taken up by catecholaminergic neurons and leads to impairment of mitochondrial respiration through the inhibition of mitochondrial complex I [68].

The major advantages of these toxin-based models include the reproducibility and reliability of degeneration as well as the relevance as a PD model for oxidative stress and mitochondrial dysfunction. MPTP has the unique advantage among PD mimetic toxins of causing the formation of intraneuronal inclusions similar to Lewy bodies within monkeys [7, 71]. However, studies have found that these inclusions may indeed be distinct from classic Lewy bodies [72]. Furthermore, MPTP exhibits much decreased toxicity in rodent models, with no toxicity at all in the rat, thus limiting its utility as a widely usable *in vivo* PD model [7]. Reported evidence of 6-OHDA as an endogenous toxin within dopaminergic neurons presents support for the 6-OHDA-based model as one that may replicate certain contributory aspects of PD pathogenesis [73]. The 6-OHDA toxin model also allows for the use of an excellent experimental control *in vivo* due to the availability of the hemisphere contralateral to the injection site as an

internal control. In contrast, MPTP is a systemic toxin that would lead to degeneration in both hemispheres and thus lacks a suitable control within each animal. Despite the reported relevance of these toxin models to PD pathogenesis, it is true that they do not replicate all features of PD, thus creating an overarching disadvantage and is exemplified by the numerous clinical trial failures with therapies that had showed great potential in these models [74].

Although there have been significant efforts to develop genetic models of PD based on major genes linked to the disease, these efforts have been met with difficulty because the majority of these genetic animal models lack significant degeneration within the SNpc [75]. Following the discovered importance of α-synuclein in the disease, various transgenic mouse models expressing the two major α-synuclein mutants (A53T and A30P) as well as WT human α-synuclein have been developed and tested. Although most of the earlier A53T and A30P mouse lines did not exhibit significant loss of dopaminergic cells within the SN, the use of the different promoters (murine Thy-1 or Pitx3) was found to induce more robust neurodegeneration and loss of DA release [75]. As an alternative to transgenic models, viral vectors that deliver and overexpress α-synuclein have been used to create rodent models that exhibit progressive degeneration of nigral neurons [75]. In contrast to the α-synuclein transgenic mouse models, virally-delivered α-synuclein models exhibited clearer pathology and dopaminergic degeneration [76-79]. More recently, several studies have demonstrated the use of α-synuclein fibrils in rodents as a model of transmissible α-synuclein pathology and progressive degeneration, including the development of motor deficits [32-34, 80].

Other mouse models based on knowledge of genetic risk factors for PD have also been developed, but to minimal success. Mutations of LRRK2 have been identified to cause a late-onset autosomal dominant form of PD [81]. Corresponding LRRK2 knockout and LRRK2

mutant (G2019S and R1441C) mouse models have been developed but show mild to no neurodegeneration, pathological features of PD, or behavioral deficits [75]. An exception was found with a mouse model overexpressing G2019S LRRK2, which exhibits up to 20% degeneration of dopaminergic neurons in the SNpc, but an interesting reversal of degeneration of dopaminergic nerve terminals in the striatum at 19-20 months [82, 83]. Similarly, PINK1 knockout mice do not show major abnormalities in the nigrostriatal dopaminergic pathway in terms of striatal signaling or SNpc degeneration, although there was detectable, age-dependent loss of striatal dopamine levels [84]. Knockout mouse models of parkin and DJ-1 likewise exhibited minor reductions in dopaminergic signaling but without loss of SNpc neurons [75]. Inactivation of multiple genes in double and triple knockout mouse models (*parkin* (-/-); *DJ-1* (-/-) or *parkin* (-/-); *DJ-1* (-/-); *PINK1* (-/-)) have also been developed but similarly exhibit no significant nigral degeneration [85, 86].

To date, the genetic models of PD that best replicate key features of the disease are ones based on α-synuclein, particularly virally-based expression models or fibril-based models. There continues to be research into improving models based on other PD-linked genes, typically through experimenting with different breed backgrounds, deletions of different exons, or conditional knockout methods. However, the genetic models as they stand today have the major disadvantage of lacking utility as a research and development tool for Parkinson's disease because of minimal observed specific degeneration of the nigrostriatal pathway.

## 1.2: PI3K/Akt Signaling

### 1.2.1 PI3K/Akt Overview and Activation

With the diverse genetic, environmental, and potentially other endogenous processes

involved in the progression of PD, a therapy that addresses one cause may not be efficacious in patient populations with other risk factors or underlying causes. However, regardless of the initiating causes of the disease, the diverse pathways eventually converge onto classic cell death pathways involved in neurodegeneration. Thus, a promising therapeutic strategy may be to target pathways modulating neuronal survival. In particular, the PI3K pathway has been shown to be necessary and sufficient for growth factor-dependent survival in a variety of neuronal cell types, thus suggesting its potential to prevent neurodegeneration [87-90]. The main mediator of this PI3K pathway, the serine- threonine-directed kinase Akt (also known as protein kinase B), has been extensively studied and provides a potential molecular target to control neuronal survival.

Akt was discovered through the initial isolation of a transforming murine T-cell lymphoma virus in 1977 from the AKR mouse strain, which was termed AKT8 as a shortened name for AKR Thymoma #8 [91]. This virus was found to encode an oncogene "v-Akt" in 1987 [92], and subsequently, the cellular homolog "c-Akt" was cloned along with the protein kinase Bα (PKBα) and Related to A- and C-Protein Kinase α (RAC-PKα), which were found to be encoded by the same gene, *Akt*, in 1991 [93-95]. As a landmark finding in the field of PI3K signaling, Akt was found to be activated by various growth factors in a PI3K-dependent manner, thus establishing Akt as a previously unknown downstream effector of PI3K [96-98].

The Akt kinase belongs to the AGC kinase family, named such because it includes AMP/GMP kinases and protein kinase C [99]. Since its discovery, three mammalian isoforms of Akt have been identified: Akt1 (PKBα), Akt2 (PKBβ), and Akt3 (PKBγ), all of which are highly homologous but have been found to have only partially overlapping functions, contributing to the diverse downstream functions of Akt discussed in the next section [100]. Additionally, although all three isoforms are generally ubiquitously expressed, there exists differential tissue expression

of the isoforms. Akt1 has been found to be most highly expressed in brain, thymus, and testis as well as slightly lower levels found in the heart, lung, spleen, pancreas, and fat [101]. Akt2 has been found to be most predominantly expressed in tissues involved in insulin regulation, such as brown fat, skeletal muscle and liver, while Akt3 is most highly expressed in the brain, testis, lung, mammary gland, and fat but almost absent in other tissues [99, 101].

Research has elucidated much regarding the structure and function of Akt. The structure of Akt is comprised of 3 major domains: an N-terminal pleckstrin homology (PH) domain, a catalytic (kinase) domain, and a hydrophobic C-terminal tail (Figure 1.1). The primary structure of Akt is highly conserved across the three isoforms with slight variations in the C-terminal tail [102]. The PH domain is ~80% identical across the Akt isoforms and 30% identical to PH domains in other proteins [103]. This domain is crucial for binding of Akt to the plasma membrane as well as mediating protein-protein interactions [102]. Additionally, the sequence of the catalytic domain across the three Akt isoforms has been shown to be ~90% identical and closely related to other members of the AGC kinase family [103]. Finally, the hydrophobic C-terminal tail is ~70% identical in sequence across Akt isoforms and most closely related to the PKC family [103].

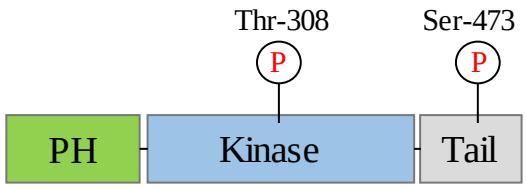


***Figure 1.1: Akt structure***
The protein has 3 main domains: N-terminal pleckstrin homology (PH) domain, catalytic kinase domain, and a C-terminal hydrophobic tail.

Canonical Akt activation begins when a trophic factor binds to receptor tyrosine kinases

and activates PI3K, which phosphorylates lipids at the plasma membrane to generate phosphatidylinositol 3,4 bisphosphate ($PI3,4P_2$) or phosphatidylinositol 3,4,5 triphosphate ($PIP_3$) [104]. These phosphorylated lipids exhibit high affinity for the PH domains of Akt as well as other relevant kinases such as phosphoinositide-dependent protein kinase 1 (PDK1), and thus lead to the recruitment of Akt to the inner surface of the membrane [96]. Membrane translocation of Akt and the binding of its PH domain to phospholipids leads to a conformational change in Akt from a "PH-in" to a "PH-out" conformation, allowing access to its kinase domain and its phosphorylation at two sites: Thr308 within the catalytic domain by PDK1 and Ser473 within the C-terminal hydrophobic domain by mammalian target of rapamycin complex 2 (mTORC2) [102, 105]. PDK1 is also recruited to the membrane via its own PH domain following PI3K activation, thus bringing it into phosphorylation proximity to Akt [106]. Recent reports have suggested that mTORC2 may also contain a PH domain within the SIN1 component, leading to disinhibition of its kinase activity, although its dependency on PI3K activation is unclear [107, 108]. Additionally, recent findings have suggested the existence of internal $PIP_3$ pools at the nuclear envelope and early endosomes, thus adding potential dimensionality to Akt activity and substrate specificity based on intracellular localization [109].

The two phosphorylation events at Thr308 and Ser473 are required for full catalytic activity of Akt, and phosphomimetic residues at the two sites lead to constant partial activation of Akt [102]. Whether the two canonical sites have distinct functions has not been fully parsed out; however, it has been discovered that phosphorylation of the Thr308 site will induce a conformational change in Akt that can enable substrate binding and stimulate enzymatic activity by an estimated 100-fold, whereas phosphorylation of the Ser473 site can induce activity levels by an additional 7 to 10-fold [106, 110-113]. In another sense, monophosphorylated Akt at the

Thr308 site has been estimated to be 10% as active as the fully phosphorylated kinase, meaning that only 10% of monophosphorylated Thr308 Akt molecules will adopt an active conformation [114]. However, it has also been suggested that the phosphorylation of Ser473 may be a prerequisite for, or enhance, the binding of PDK1 to Akt, as the phosphorylated Ser473 within the hydrophobic motif interacts with PDK1, bringing it into the proximity of the Thr308 site within Akt [110]. Additionally, the same phosphorylated hydrophobic motif is thought to double as a stimulator of kinase activity through stabilization of the active state and a docking site to mediate substrate interactions and allow for some level of substrate specificity [110, 114, 115].

Outside of the two canonical phosphorylation sites of Akt, there also exist numerous other sites for post-translational modification that may help fine-tune Akt activity, cellular localization, and substrate specificity. These include additional phosphorylation sites, mediated by cell cycle proteins and mTORC2 to enhance Akt activity and GSK3α to attenuate Akt activity, as well as hydroxylation sites that trigger interactions with von Hippel-Lindau tumor suppressor protein (pVHL), acetylation of the PH domain, and glycosylation of the catalytic domain for further functional tuning (reviewed in [105]).

Conversely, Akt inactivation was found to be mediated upstream by the tumor suppressor PTEN, a known $PIP_3$ phosphatase [116]. Thus, PTEN essentially works in opposition to PI3K, removing the membrane binding site for Akt and preventing its membrane recruitment, which therefore prevents its phosphorylation and activation by PDK1 and mTORC2. Direct dephosphorylation of Akt has been found to be mediated by protein phosphatase 2A (PP2A), specific to the Thr308 site, and PH domain leucine-rich repeat protein phosphatases 1 and 2 (PHLPP1 and 2), specific to the Ser473 site [105].

### 1.2.2 Physiological Effects of Akt and Associated Substrates

Once Akt has become catalytically activated through phosphorylation of Thr308 and/or Ser473, it can then in turn interact with over 100 reported substrates to induce various downstream physiological effects [117]. Since its initial discovery as an oncogene capable of inducing T cell lymphomas in mice through the retrovirus AKT8, much of Akt research has focused on its role in mediating cell growth, proliferation, and survival, particularly within the context of cancer [99]. However, many of these same physiological processes that are mediated by Akt in cancer are also relevant to neurodegenerative disease, particularly Parkinson's disease, as is discussed in the following section. In this section, we will explore the major Akt roles in cell growth, proliferation, and apoptosis and corresponding major substrates that help mediate these downstream effects.

The great number of downstream Akt substrates lend to the diversity of physiological effects caused by Akt activation, often through inhibition of substrate activity through the creation of a phosphorylated 14-3-3 binding motif [117]. Furthermore, many Akt substrates are involved in multiple cellular functions, which may be cell context-specific [117].

The most well-established function of Akt is its role in mediating cell survival. This role is often, but not always, dependent on its negative regulation of proteins involved in promoting apoptosis. This includes several proapoptotic Bcl-2 family members that only contain a single BH3 domain, such as BAD [118], as well as inhibition of transcription factors that promote the expression of BH3-only proteins, such as FoxO transcription factors FoxO1, FoxO3a, and FoxO4 [117, 119, 120]. In both cases, phosphorylation by Akt creates a binding site for cytosolic sequestration protein 14-3-3, and in the case of FoxO transcription factors, causes their exit from the nucleus, thus blocking induction of its target proapoptotic genes [119, 120]. Additionally, the

first Akt substrate discovered, glycogen synthase kinase 3β (GSK3β), is known to play a central role in insulin and Wnt signaling, but also is involved in promoting the degradation of cell survival proteins MCL-1 and c-Myc [105, 121-123]. GSK3β is inhibited through phosphorylation at the Ser9 site by Akt and therefore leads to stabilization of aforementioned pro-survival proteins and promotion of cell survival [105, 117].

A highly conserved function of Akt is its promotion of cell growth, or control of cell size [117]. This function is predominantly mediated through indirect activation of the mTOR complex 1 (mTORC1) pathway, which is known to regulate translation initiation and ribosome biogenesis [124]. Although Akt has been suggested to directly phosphorylate substrates downstream of mTORC1, such as S6K1 and eukaryotic initiation factor 4E-binding protein 1 (4E-BP1) [117], the major mechanism of mTORC1 pathway activation is more likely through inhibition of factors upstream of mTORC1. For instance, tuberous sclerosis complex 2 (TSC2), a tumor suppressor that is a known inhibitor of mTORC1 signaling, has been shown to be inhibited through direct phosphorylation by Akt at multiple sites, which then allows for activation of the Ras-related small G protein Rheb and subsequent activation of mTORC1 [125-127]. Additionally, proline-rich Akt substrate of 40 kDa (PRAS40), a negative regulator of mTORC1, was found to be directly phosphorylated and inhibited by Akt [128, 129].

Cell proliferation is another important downstream function of Akt, although less well understood than cell growth or survival, that relies on both direct and indirect actions on substrates important in the regulation of the cell cycle [117]. Several independent studies have demonstrated Akt phosphorylation of cell cycle inhibitor p27 within its nuclear localization signal, thus impairing its nuclear import and p27-mediated G1 arrest [130-132]. Additionally, Akt can indirectly regulate the expression of cell cycle proteins through inhibition of

transcription factors such as FoxO, as discussed above, or regulation of stability and synthesis of cell cycle proteins through inhibition of GSK3β, which plays a role in mediating proteasomal degradation of cyclin proteins [133, 134], as well as inhibition of the mTORC1 signaling pathway proteins TSC2 and PRAS40, which can mediate cap-dependent translation of cyclins [135].

A more recent potential function of Akt is its ability to induce sprouting or growth of axons. Earlier studies have implicated Akt as a mediator of both neurite outgrowth as well as growth in the thickness of processes [136, 137]. Importantly, recent studies by our collaborator, Dr. Robert Burke, have established a role for Akt activity in the significant increase of dopaminergic nigrostriatal projections within mice, even after degeneration induced by 6-OHDA lesions [138, 139]. This effect is believed to be mediated by the mTOR pathway, as overexpression of constitutively active Rheb, an mTOR regulator, has been found to recapitulate the protective and regenerative effects seen with overactive Akt [139, 140].

### 1.2.3 Akt in Parkinson's Disease and other Neurological Disorders

Although the initial research surrounding Akt was intensely focused on cancer, the last two decades of research have elucidated the crucial role of Akt for neuronal survival, as well as evidence for dysfunction within neurological and neurodegenerative disorders.

First, the importance of Akt in promoting survival within the context of a neuronal cell type under stress conditions has been clearly demonstrated in various studies (reviewed in [141]). Importantly, expression of dominant-negative Akt was shown to reduce the numbers of dopaminergic neurons in the substantia nigra (SN) of mice while expression of a constitutively active form of Akt significantly reduced developmental neuron death in the SN, thus highlighting

the important role that Akt plays in promoting survival in the neuronal population directly affected in PD [142].

The role of Akt has also been explored within the context of various neurological diseases. For instance, loss of activity of the isoforms Akt1 and Akt3 has been implicated in neuropsychiatric disorders such as schizophrenia [143, 144]. Furthermore, dysfunction of the signaling cascade involving PI3K-Akt-mTOR has been identified as a core cause of neurodevelopmental and neuropsychiatric disorders, including autism spectrum disorder, epilepsy, and developing brain malformations (reviewed in [145]).

Akt dysfunction specifically within the context of neurodegenerative disorders, including prion disease, Alzheimer's disease (AD), and PD, has been widely investigated, with various studies implicating dysregulation of the kinase as a critical "common core" event underlying the mechanism of degeneration. Recent research has demonstrated that the repressor element 1-silencing transcription factor (REST), a neuroprotective factor that is lost in AD [146] and prion disease models [147], is correlated with downregulation of Akt-mTOR signaling [148]. Other studies also provide evidence for impaired Akt signaling in AD; however, these studies suggest that aberrant, hyperactivation of Akt signaling may be an early feature of AD and is associated with Aβ and tau pathology [149-151].

Most relevant to the work presented here, PD research has demonstrated impaired or decreased levels of Akt signaling within the disease. Immunostaining of postmortem brains from patients with sporadic PD has shown significantly decreased levels of phosphorylated Akt in the SN compared to non-PD patients, providing direct evidence of dysfunctional Akt signaling in PD, [152, 153]. In addition, global gene expression analysis of isolated dopaminergic neurons from the SNpc of PD patients and age-matched controls revealed disrupted pathways of energy

metabolism and cell survival in diseased neurons, with PI3K/Akt/mTOR signaling being the central hub of these signaling networks [154]. A separate study exploring microRNA profiles of isolated dopaminergic neurons from PD brains identified miR-126 as a potentiator of vulnerability to neurotoxins, such as 6-OHDA, by dysregulating insulin-like growth factor/PI3K signaling [155]. As further supporting evidence, there have been studies demonstrating the specific involvement of apoptosis in the development of PD through diminished upstream signaling of the PI3K/Akt pathway. Studies of postmortem brains from PD patients demonstrate the presence of apoptosis in nigral neurons [156-158], as well as dramatically decreased levels of trophic factors BDNF, GDNF, and NGF within the SN of PD brains [159-161]. As Akt is a core mediator of apoptotic signaling, these studies implicitly suggest that dysfunction of Akt signaling is likely involved.

Outside of studies using human postmortem PD brains, deficiencies in Akt signaling have been found in genetic models of DJ-1, parkin, and PINK1 mutations [162, 163]. Furthermore, although the pathogenesis of PD remains to be fully elucidated, oxidative stress has been suggested to play a large role in the degeneration and progression of PD [164]. In relation to this mechanism, studies involving oxidative stressors and PD mimetic toxins, including hydrogen peroxide, 6-OHDA, $MPP^+$ *in vitro*, and MPTP in mice, found selective dephosphorylation of Akt [152, 165, 166]. Thus, a large array of evidence points to the crucial role of diminished Akt signaling in PD disease contexts, supporting the potential of Akt signaling as a therapeutic target. It is worth noting that the contrasting reports on the role of Akt in AD and PD highlight the complexity and potentially very distinct pathological mechanisms behind these two degenerative diseases, which may be related to the complex interplay between PI3K/Akt/mTOR signaling and autophagy in both AD and PD [167].

Importantly, various studies have successfully demonstrated that directly restoring or elevating Akt activity may be protective in various PD and cell death models. For instance, virally delivered myristoylated-Akt has been shown to protect SNpc dopaminergic neurons from death and promote sprouting in a 6-OHDA lesioned PD mouse model [138]. Overexpression of constitutively active Akt(E17K) in neuronal cultures was also found to be protective against PD toxin insults [152]. Further linking Akt signaling to PD genetics, a study in 2012 established that overexpression of PINK1 can rescue C2-ceramide induced cell death through maintenance of Akt phosphorylation and activity [168]. Similarly, a separate study investigating DJ-1 revealed that the neuroprotective effects of DJ-1 against hydrogen peroxide/$MPP^+$ *in vitro* and MPTP *in vivo* was dependent on Akt activity [169]. In this same study, myristoylated Akt was demonstrated to exhibit protective effects *in vitro* against hydrogen peroxide, regardless of DJ-1 genotype. There also have been various studies demonstrating that the protective roles of rapamycin, Rho-associated kinase inhibition, a squamosamide derivative, and insulin-like growth factor 1 are attributed to activation of Akt signaling pathways in both *in vitro* and *in vivo* PD models [170-173]. It is noteworthy that all of these studies citing the neuroprotective capacity of Akt restoration utilized toxin models of PD. To our knowledge, there have been no research studies demonstrating neuroprotective effects of Akt in non-toxin PD models.

Such lines of evidence support the importance of Akt signaling in neuronal survival and repair, particularly in the case of PD, and potentially with wider implications in neuropsychiatric and other neurodegenerative diseases.

### 1.2.4 Translational Approaches to Activate Akt Signaling in Parkinson's Disease

With mounting evidence to suggest deficiency in Akt signaling as a core component of

neurodegeneration in PD, translational approaches to treat PD could involve maintaining the phosphorylation status of Akt. Because membrane recruitment is not only a prerequisite, but also sufficient for the activation of Akt, controlling localization of Akt to the membrane is an effective method of controlling its activation. As such, myristoylated-Akt is commonly used as an equivalent to constitutively-active Akt due to its greatly increased phospholipid binding, which leads to increased levels of phosphorylated, and therefore active Akt [138, 139, 174]. Importantly, interventional approaches to activate Akt signaling are especially attractive due to evidence supporting not only its neuroprotective effects, but also potential neurorestorative effects in PD models. As mentioned previously, Akt activation has been observed to promote neurite outgrowth and axonal branching in a variety of models both *in vitro* and *in vivo* [136, 137, 142, 175]. More contextually relevant to PD, myristoylated-Akt was demonstrated to promote neurorestoration of axonal projections from the SNpc to the striatum post-6-OHDA insult in mouse models [138]. Similarly, the constitutively-active human Rheb (S16H), a downstream effector of Akt signaling, was found to induce regrowth of dopaminergic axons post-6-OHDA insult in mouse models [139, 140].

The activation of Akt signaling can be achieved by a few different approaches, which include pharmacological approaches, delivery of neurotrophic factors, and viral delivery of Akt overexpression constructs. Until recently, potential pharmacological activators of the Akt signaling pathway were limited to those targeting downstream effectors, such as rapamycin as an inhibitor of mTOR [176], or compounds that are reported to indirectly activate Akt, such as glucagon like peptide-1 (GLP-1) analogs [177] or rasagiline, a monoamine oxidase-B inhibitor that was reported to exhibit neuroprotective effects in preclinical studies but was not proven in clinical trials due to failure of dose responsiveness [178, 179]. More recently in 2012, a small

molecule activator of Akt (SC79) was identified to specifically bind to the PH domain of Akt, inducing a conformational change that allows for phosphorylation of Akt residues, similar to the conformational change that occurs when Akt binds to the membrane [180]. Regardless of the pharmacological method, however, these approaches have the distinct disadvantage of off-target or systemic activation of Akt, which may carry the risk of inducing cancer given the evidence of activating Akt mutations described in human cancers [181, 182].

Delivery of neurotrophic factors, such as glial cell line-derived neurotrophic factor (GDNF), brain-derived neurotrophic factor (BDNF), or neurturin, has long been a therapeutic approach of great potential, with strong data supporting their involvement in the pathogenesis of PD and potential neuroprotective effects in various PD models both *in vitro* and *in vivo* [159, 160, 183-185]. However, while GDNF showed initial promise in early clinical trials, a subsequent placebo-controlled trial showed no significant functional improvement in PD patients [186]. The failure of GDNF protein in clinical trials could potentially be due to the metabolism of the proteins by endogenous enzymes, patient selection for clinical trials, insufficient dosing, or poor diffusion of the neurotrophin from the delivery site. The use of viral vector-mediated delivery of neurotrophin genes can circumvent the dose or diffusion issues. Thus, GDNF as well as neurturin have entered clinical trials again, utilizing either adeno-associated virus (AAV)-mediated delivery or improved infusion protocols. However, the latest neurturin trials did not yield positive results [187], and GDNF trials are still ongoing [188].

Finally, the use of viral vectors to deliver gene constructs for activation of Akt signaling has been validated as a potential therapeutic approach *in vivo* through AAV1-mediated delivery of myristoylated-Akt or constitutively-active Rheb [138, 140]. Furthermore, the safety of gene therapy techniques has been validated in clinical trials involving the AAV-mediated delivery of

neurturin and human aromatic L-amino acid decarboxylase (hAADC) [187, 189], as well as the lentiviral-delivered ProSavin (combination of three genes: AADC, TH, and GTP-cyclohydrase 1) [190]. However, the use of a system where Akt is always activated would be disadvantageous as a therapy because overactivity of Akt has been clearly linked to diseases such as cancer and has the potential for extraneous sprouting of neurites [99, 138, 139]. Thus, there is a need for an inducible system in which the activation of Akt can be controlled, ideally under the control of a small molecule that is easily administered and has brain penetration.

## 1.3: Destabilizing Domain Inducible System

### 1.3.1 Development and Overview of the DD System

The ideal therapeutic approach to control Akt activity levels in PD would fulfill four general criteria: 1) dose-responsive control of the Akt levels, 2) sufficient and robust activation of Akt, 3) reversibility of activation, and 4) minimal off-target effects, through the utilization of a well-characterized, activator molecule that is specific to Akt. Although there are many inducible systems with the potential for conditional control of Akt expression levels, we chose a novel post-translational system with the potential to fulfill these criteria and that is based on control of protein stabilization: the Destabilizing Domain (DD) system [191]. Further fulfillment of the fourth criteria can be achieved through gene therapy approaches as outlined in the previous section, using viral vector-mediated delivery of the DD system to the local brain region of interest, the SNpc, in conjunction with a cell type-specific promoter to ensure that the control of Akt activity is constrained to dopaminergic neuronal populations.

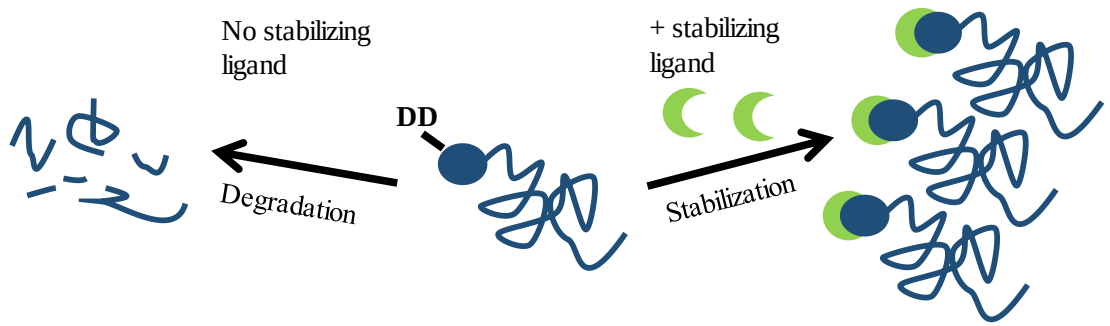


***Figure 1.2: DHFR-derived DD confers inducible stability***The DD domain confers instability to a fused protein and leads to proteasomal degradation. A stabilizing ligand with high specificity to the DD domain stabilizes the entire DD-fusion protein, allowing it to accumulate within the cell.

The DD system allows for the control of protein stability through the presence or absence of a cell-permeable compound (Figure 1.2). It was first developed by the Thomas Wandless group at Stanford when human FKBP12 mutants were engineered to be rapidly and constitutively degraded unless bound to a synthetic ligand, Shield-1 (Shld-1) [192]. Importantly, the mutants' instability was found to be transferred when the mutant FKBP12 proteins were fused to other proteins of interest [192]. The mutant FKBP12 proteins were screened to identify the most destabilizing mutations with the most efficient rescue upon addition of Shld-1. These mutants were further demonstrated to successfully confer Shld-1-dependent stabilization of various proteins when genetically fused to either their N- or C-terminus. This held true for a variety of proteins differing in size, folding, function, and cellular localization as follows: small GTPases Rac1, RhoA, Cdc42, Arf6, Arl7, kinases GSK3β and CDK1, cell cycle regulatory proteins securing and p21, transcription factor CREB, and even a transmembrane glycoprotein CD8α [192]. Since its discovery, the FKBP12-derived DD inducible system has been validated in a variety of organisms including mice [193] and various parasites [194-199], as well as in mammalian cell lines [200-204]. Additionally, CRISPR/Cas9 has been used to knock in the FKBP12-derived DD domain to the essential gene Treacher Collins-Franceschetti syndrome 1

(TCOF1) in human 293T cells as a proof of principle study to demonstrate that the DD inducible system can be used to confer small molecule-controlled regulation of an endogenous protein [205].

Alternative DD systems have since been developed based on other ligand-protein pairs, including *E. coli* dihydrofolate reductase (DHFR) [191], human estrogen receptor ligand binding domain [206], or degrons with light sensitivity for control of protein stability with light [207]. These multiple DD systems permit the orthogonal control of multiple proteins within the same cellular system [208]. Of these alternative DD systems, the DHFR-derived version of the DD system has additionally been validated in a variety of biological contexts, including parasites [209, 210], mammalian cell lines [191, 208, 211, 212], and rodents [191, 211-213].

The mechanism of destabilization and degradation has been further studied in the context of both the FKBP12-derived and DHFR-derived DD systems. Initial studies demonstrated that inhibition of the proteasome blocks the degradation of both FKBP-derived and DHFR-derived DD proteins in the absence of their stabilizing ligands, suggesting that the inducibility of the DD system relies on proteasomal degradation [191, 192]. A subsequent investigation of purified FKBP12-derived DD fusion proteins in a cell-free system revealed that the DD protein in the absence of Shld-1 adopts a misfolded state with the propensity to unfold, whereas the binding of Shld-1 stabilizes the DD protein by reversing the unfolded state and folding the protein into a more stable structure [214]. Furthermore, when expressed within cells, it was observed that unstable DD proteins are rapidly ubiquitinated and tagged for the ubiquitin-proteasome system, whereas the presence of Shld-1 was found to prevent the polyubiquitination of DD [214]. Interestingly, the data in this study show that the recognition of unstable DD proteins and their ubiquitination is rapid, observable within minutes, but that the degradation by the proteasome

occurs more slowly, thus suggesting that there will be a pool of ubiquitinated but undegraded proteins at steady state [214].

### 1.3.2 The DHFR-Derived DD System as a Gene Therapy Approach for PD

The DHFR-derived DD system controlled by the ligand Trimethoprim (TMP) is of particular interest as a potential therapeutic approach due to its use of an inexpensive, well-characterized, and commonly prescribed antibiotic as the stabilizing ligand [191]. Importantly, TMP is known to cross the blood brain barrier [215] and be safe for long-term prophylactic use [216-219], thus making this ligand particularly attractive as a therapeutic drug that can exert effects in the CNS even when administered orally. As such, the oral administration of TMP for 3 weeks to control protein stability in the CNS of rodent models has been validated by several groups [191, 211-213].

This DD inducible system shows great potential as a therapeutic approach to control the activity levels of Akt in the context of PD. To achieve control over Akt activity levels, the DHFR-based DD domain must be genetically fused with a constitutively active form of Akt such that any level of stabilization by TMP will lead to direct increase in Akt activity. One such active form of Akt is Akt(E40K), a mutant Akt with a glutamate to lysine substitution at E40 [220]. This mutant was first engineered in 1998 for use in studies elucidating the activation process of Akt and was found to enhance Akt's membrane binding affinity due to the removal of the negatively-charged glutamate from the phospholipid-binding pocket within the PH domain [220, 221]. With enhanced membrane binding affinity, Akt(E40K) was found to have higher basal activity that was sufficient to replicate physiological effects of Akt such as transformation of hematopoietic cells and inhibition of apoptosis induced by IL-3 withdrawal [222, 223].

Importantly, a similar form of Akt, Akt(E17K), was found to be neuroprotective against PD mimetic toxins *in vitro* [152].

### 1.4: Significance and Outline

Based on the above considerations, we created a DHFR-derived inducible Akt(E40K) system. Our rationale was that expression of this protein could be controlled by the ligand TMP and would potentially serve as a tool to selectively turn Akt activity on and off in cells as well as promote cell survival and neuroprotection in the context of PD. The following chapters report our investigation into the utility of DD-Akt(E40K) as a research and clinical tool for control of Akt activity and signaling across a variety of biological contexts. Our particular focus is on the application of this novel technology as a potential therapeutic approach in Parkinson's disease.

Chapter 2 outlines the experimental methods that were used over the course of this research. Chapter 3 describes the *in vitro* characterization of DD-Akt(E40K) and establishment of inducibility across diverse cellular contexts. Chapter 4 explores the biological consequences of DD-Akt(E40K) induction in various *in vitro* cell death paradigms. Chapter 5 expands the *in vitro* studies of DD-Akt(E40K) and investigates its inducible behavior as well as physiological effects in mice. Finally, Chapter 6 provides the major conclusions and future directions of this research.

In summary, this dissertation describes a novel technology that permits the control of Akt, a kinase that is crucial to survival signaling, and findings that provide insight into the technology's utility within a research and clinical setting as well as potential insights into PD pathogenesis.

# Chapter 2: Materials and Methods

## 2.1: Cell Culture

### 2.1.1 HEK293T/17

HEK293T/17 cells were grown in DMEM supplemented with 10% FBS and penicillin/streptomycin. Cell culture medium was changed every other day. Cells were passaged every 1 to 3 days. Cultures were transfected for experiments using Lipofectamine 2000 (ThermoFisher Scientific) according to manufacturer protocols, 10 µM TMP was added to cultures 24 h after transfection, and protein extraction or immunofluorescence staining was performed 24 h after TMP treatment.

### 2.1.2 PC12 Cells

PC12 cells were cultured as described previously (Greene and Tischler, 1976) [224]. Cells were cultured on plastic cell culture dishes coated with rat tail collagen (Roche). Undifferentiated PC12 cells were grown in RPMI 1640 cell culture medium supplemented with 10% heat inactivated horse serum (Sigma), 5% FBS, and penicillin/streptomycin. For neuronal differentiation, cells were grown in RPMI 1640 cell culture medium supplemented with 1% horse serum, penicillin/streptomycin, and 50 ng/ml final concentration of human recombinant NGF (kind gift of Genentech, Gemini Bio-Products #300-174P). Cell culture medium was changed every other day. Lentivirus was added to the cultures at an approximate MOI of 5-10 on day 1-2 *in vitro* of undifferentiated cultures and 4-5 *in vitro* of differentiated cultures, 10 µM TMP was added to cultures 4-5 days after infection, and protein extraction was performed 24 h after TMP treatment.

### 2.1.3 Primary Rat Cortical Neurons

Primary cortical cultures were prepared as previously described [225]. Briefly, cortices were isolated from E18 rat embryos, dissociated, and plated on poly-D-lysine (Sigma) coated plates at a density of 3 x $10^5$ cells/well. Cultures were maintained in Neurobasal medium (ThermoFisher Scientific) supplemented with 2% B-27 (ThermoFisher Scientific) and 0.5 mM glutamine (ThermoFisher Scientific). Half of the medium was changed every 3 days after plating. Lentivirus was added to the cultures at an approximate MOI of 5-10 on day 5-7 *in vitro* and protein extraction was performed 4-7 days after infection.

### 2.1.4 Primary Ventral Midbrain Dopaminergic Neurons

Ventral midbrain dopaminergic neurons from P0-P3 rats were dissected, dissociated, and plated on a confluent glial monolayer following the protocol kindly provided by Dr. David Sulzer (Columbia University) and as described previously (Rayport et al., 1992) [226]. Briefly, 1 $mm^3$ blocks were dissected from the substantia nigra of a coronal midbrain slice, according to anatomical landmarks, and enzymatically dissociated in a papain solution for 20-30 minutes. Digested tissue blocks were rinsed and triturated 10 times with large-bore tech tips, 10 times with medium-bore tech tips, and 10 times with small-bore tech tips. Cells were centrifuged, resuspended in SF1C medium, and plated at a density of 80,000 cells per dish on top of a glial monolayer. Cultures were treated with GDNF (10 ng/ml) and processed as needed for experiments. Lentivirus was added to the cultures at an approximate MOI of 10 on day 6-7 *in vitro*, 10 µM TMP was added to cultures 6-10 days after infection, and processed for immunofluorescence after 4 days of TMP treatment.

## 2.2: PI3K Inhibitor Experiments

HEK293 cells transfected with DD-Akt(E40K) or pWPI empty vector plasmids were pretreated with 10 µM TMP for 24 h and treated with 50 µM LY294002 (Cell Signaling Technology #9901). Protein extraction was performed at 24 h after LY294002 addition.

## 2.3: Cell Death Paradigms

### 2.3.1 Serum Deprivation

For serum deprivation of undifferentiated PC12 cells, cells were detached from wells with serum-free RPMI 1640 and pelleted at 1500 rpm for 5 min. Pellets were washed in serum-free RPMI 1640 and spun again at 1500 rpm for 5 min. Cells were resuspended in serum-free RPMI 1640 or RPMI 1640 medium supplemented with 10% heat inactivated horse serum (Sigma) and 5% FBS, corresponding to experimental conditions, and plated at a density of $5 \times 10^5$ cells/ml. Cells were analyzed for survival 24 h after serum deprivation.

### 2.3.2 PD Toxins

For neuronal PC12 cells, 10 mM stock solutions of 6-hydroxydopamine (Tocris) or 1-methyl-4-phenylpyridinium ($MPP^+$) (Sigma) diluted in water were freshly prepared just before each experiment. 6-OHDA was used at final concentrations ranging from 100 to 150 µM, and MPP+ was used at a final concentration of 0.25 mM, for 16-24 h.

## 2.4: Quantification of Cell Survival *In Vitro*

For PC12 cells infected with lentiviral particles (typically achieving a 50% transduction rate in undifferentiated PC12 cells and 75% transduction rate in differentiated PC12 cells) and treated

with PD toxins or deprived of serum, cell survival was assessed on the total cell population level by incubating the cell cultures with a detergent solution that lyses the plasma membrane and leaves the nuclei intact (10x counting lysis buffer: 5 g of cetyldimethyl-ethanolammonium bromide, 0.165 g of NaCl, 2.8 ml of glacial acetic acid, 50 ml of 10% Triton-X, 2 ml of 1 M $MgCl_2$, 10 ml of 10 × PBS, 35.2 ml of $H_2O$); 150 µl of 1x counting lysis buffer was added per $cm^2$ of culture dish area, and the suspended nuclei were counted in a hemacytometer.

## 2.5: Cloning

### 2.5.1 DD-Akt(E40K)

The DHFR-derived DD-YFP gene insert in a pBMN vector was obtained from Addgene (Plasmid #29325). The HA-tagged mouse Akt1(E40K) plasmid was provided by our collaborator, Dr. Thomas Franke. The HA-Akt1(E40K) gene insert (from here on called Akt(E40K)) was amplified using PCR and primers as follows: Fwd 5'-gcgcatgcTACCCATACGATGTTCCAGATT-3' and Rev 5'-atccgcggTCAGGCTGTGCCACTGG-3'. The amplified Akt(E40K) gene was inserted 3’ of the DD domain, replacing YFP, in a pBMN vector using restriction sites Sph1 and SacII to create pBMN-DD-Akt(E40K). The entire DD-Akt(E40K) gene was then inserted using restriction sites BamHI and SacII and blunt-end ligation into the overexpression vector pWPI (Addgene, Plasmid #12254), a bicistronic lentiviral vector allowing the simultaneous expression of the transgene and EGFP under the control of the EF1-α promoter.

### 2.5.2 DD-Akt(WT)

Akt(WT) was amplified from mouse cDNA using primers as follows: Fwd 5'-

tctagcgcatgcATGAACGACGTAGCCATTGTGAA-3' and Rev 5'-cattatccgcggTCAGGCTGTGCCACTGGCTGA-3'. The amplicon was inserted 3' of the DD domain, replacing YFP, in a pBMN vector using restriction sites Sph1 and SacII to create pBMN-DD-Akt(WT).

### 2.5.3 Double DD-Akt(E40K)

All double DD-domain constructs were generated using the In-Fusion Cloning kit from Clontech. Primers were designed using the online tool provided by Clontech specifically for this cloning technique. Glycine linkers (Gly-Gly-Gly-Gly-Ser) were generated using GenScript Codon Usage Frequency Table Tool (http://www.genscript.com/tools/codon-frequency-table) to determine most common codons within the human and rat species. Linkers were inserted in between the two DD domains and in between the DD domains and Akt gene as indicated in Figure 3.13. A Kozak sequence (5'-TCCGCCACC-3') was inserted 5' of the ATG start site. The complete insert was concurrently cloned into a pWPI expression vector.

## 2.6: Biochemistry

### 2.6.1 Western Immunoblotting

Cells and brain tissue were homogenized in 1x cell lysis buffer (Cell Signaling Technology, #9803) with LDS-sample buffer (Invitrogen) supplemented with 50mM dithiothreitol and complete mini protease inhibitor mixture (Roche, #11836170001), or in 1x sample buffer (5x sample buffer: 250 mM Tris-HCl pH 6.8, 10% SDS, 0.5% bromophenol blue, 50% glycerol, 5% 2-hydroxy-1-ethanethiol). Lysates were boiled at 100°C for 10-20 min prior to running. A total

of 20 μg of proteins was loaded per well of 10% or 4-12% Bis-Tris polyacrylamide gels (Invitrogen) and separated by electrophoresis for 1.5 h at 100 V. Proteins were then transferred onto a nitrocellulose membrane (Bio-Rad) for 1 h 30 min at 40 V. Membranes were blocked with 5% powdered milk in TBS containing 0.1% of Tween 20 (TBST) and incubated overnight at 4°C with primary antibodies. The following primary antibodies were used for Western blotting: rabbit anti-phospho-Akt (Thr308) (Cell Signaling Technology #13038, #2965), mouse anti-phospho-Akt (Thr308) (Cell Signaling Technology #5106), rabbit anti-phospho-Akt (Ser473) (Cell Signaling Technology #4060), rabbit anti-pan-Akt (Cell Signaling Technology #4685), rabbit anti-phospho-FoxO4 (Cell Signaling Technology #9471), rabbit anti-total FoxO4 (Cell Signaling Technology #2499), mouse anti-actin (Sigma #A3853), GAPDH (Abcam), and rabbit anti-Erk1/2 (Santa Cruz Biotechnology, #sc-93). Membranes were washed 3 times with TBST and incubated with HRP-conjugated secondary antibodies or IRDye secondary antibodies (Li-Cor, goat anti mouse #680LT, goat anti rabbit #800CW). After 3 final washes with TBST, blots were incubated with ECL reagents (GE Healthcare), and chemiluminescent signals were detected by exposure to autoradiography film, or blots were imaged using a Li-Cor Odyssey CLX imaging system. Films were scanned using a desktop scanner, and band intensities were determined using ImageJ, or Odyssey images were analyzed using Image Studio Lite Ver 4.0.

### 2.6.2 Immunofluorescence

Cells were fixed for 12–15 min in 4% PFA and washed 3 times with 1x PBS. Cells were blocked with Superblock (Thermo Scientific) supplemented with 0.3% Triton-X for 1 h at room temperature and incubated overnight at 4°C with primary antibodies. The following primary antibodies were used for immunofluorescence: mouse anti-tyrosine hydroxylase (Millipore,

#MAB318), rabbit anti-tyrosine hydroxylase (Millipore, #AB152), rabbit anti-GFP (Invitrogen, #A11122), chicken anti-GFP (Invitrogen, #A10262), mouse anti-HA (Cell Signaling Technology, #2367), and rabbit anti-phospho-Akt (Thr308) (Cell Signaling Technology, #13038). Cells were washed 3 times with PBS and incubated with fluorescent secondary antibodies for 1-2 h at room temperature: AlexaFluor-568 anti-mouse, or anti-rabbit, AlexaFluor-488 anti-chicken, anti-mouse, or anti-rabbit, and AlexaFluor-350 anti-mouse or anti-rabbit (Invitrogen). For HEK293 cells grown in multiwell dishes, Hoechst 33328 was added to the first PBS wash, cells were washed 2 additional times in PBS, and cultures were observed with an inverted fluorescence microscope. For ventral midbrain dopaminergic neurons grown on glass coverslips, after 3 final washes with PBS, coverslips were mounted on slides with Vectashield mounting medium containing DAPI for nuclear staining (Vector Laboratories). Images were acquired using an Olympus inverted or upright fluorescent microscope equipped with a digital camera and Cellsens software.

### 2.7: Rodent Husbandry and Handling

All rodent procedures were approved by the Columbia University Institutional Animal Care and Use Committee.

### 2.8: Preparation and Injection of Viral Vectors

#### 2.8.1 Lentivirus

All viral plasmids were obtained from Addgene. The transfer plasmid for overexpression was pWPI, which encodes transgene-IRES-GFP under the control of the EF1-alpha promoter. Viruses were prepared in HEK293T cells using second-generation packaging plasmids pMD2G

and psPAX2 (obtained through Addgene) through calcium phosphate transfection. Lentiviral supernatants were collected twice (48 h and 72 h after transfection) and concentrated using Lenti-X concentrator (Clontech, #631231) according to manufacturer protocols, resuspended in PBS, and stored at -80°C.

For transduction of neuronal cultures, 5-10 MOI were added directly in the medium of neuronal PC12 cells, primary cortical neurons, or ventral midbrain dopaminergic neurons. Transduced neurons were analyzed by western blot or immunofluorescence after 5-7 days.

### 2.8.2 Adeno-Associated Virus

All vectors used for these studies were AAV1 serotype. For AAV vector generation, the DD-HA-Akt(E40K) gene was modified to incorporate a Flag-encoding sequence (5'-GACTACAAAGACGATGACGACAAA-3') (denoted as DD-Akt(E40K)-Flag in Chapter 5) and inserted into an AAV packaging construct that utilizes the chicken β-actin promoter and contains a 3′ WPRE (pBL) as previously described (Ries et al, 2006) [138]. Similarly, an Akt(E40K) insert with no DD domain was modified to incorporate a Flag-encoding sequence and inserted into an AAV packaging construct (pBL). All nucleotide sequences in the AAV packaging constructs were confirmed before AAV production. AAVs were produced by the University of North Carolina Vector Core. The viral titer of AAV-DD-Akt(E40K)-Flag was 2.3 x $10^{11}$ viral molecules/ml and those of AAV-Akt(E40K) was 4.9 x $10^{12}$ viral molecules/ml.

For AAV injections, adult (8 week) male C57BL/6 mice were obtained from Charles River Laboratories, Wilmington, MA. Mice were anesthetized with ketamine/xylazine solution and

placed in a stereotaxic frame (Kopf Instruments, Tujunga, CA) with a mouse adapter. For intranigral injections, the tip of a 5.0 µl syringe needle (26S) was inserted to stereotaxic coordinates AP: −0.35 cm; ML: +0.11 cm; DV: −0.37 cm, relative to bregma. For intrastriatal injections, the tip of a 5.0 µl syringe needle (26S) was inserted to stereotaxic coordinates AP: +0.09 cm; ML: +0.22 cm; DV: -0.25 cm relative to bregma. Viral vector suspension in a volume of 2.0 µl was injected at 0.1 µl/minute over 20 minutes.

### 2.9: Oral Trimethoprim (TMP) Administration

Six out of 13 mice injected with intranigral DD-HA-Akt(E40K)-Flag injections and 8 out of 13 mice with intrastriatal DD-HA-Akt(E40K)-Flag injections were given freshly 1.31 mg/ml TMP-lactate, which is an equivalent of 1 mg/ml TMP, in their drinking water. TMP solutions were covered with aluminum foil to protect from light exposure and changed every 2-4 days for 3 weeks.

### 2.10: Immunohistochemical Processing

#### 2.10.1 Tyrosine Hydroxylase (TH) Immunostaining

For TH immunostaining, mice were perfused with 0.9% NaCl for 5 min followed by 4% paraformaldehyde in 0.1 M phosphate buffer for 10 min. The brain was postfixed for 1 week, cryoprotected in 20% sucrose overnight, and then rapidly frozen by immersion in isopentane on dry ice. A complete set of serial sections was then cut through the SN at 30 µm. Beginning with a random section between 1 and 4, every fourth section was processed free-floating. Primary antibodies used were rabbit anti-TH (Calbiochem #657012) at 1:750. Sections were treated with biotinylated protein A and avidin-biotinylated horseradish peroxidase complexes (ABC; Vector

Labs, Burlingame, CA). After immunoperoxidase staining, sections were mounted, dehydrated, and analyzed for neuronal cell size quantification.

### 2.10.2 Flag Immunostaining

For immunostaining of the FLAG epitope, perfused mouse brains were postfixed for 24 h, cryoprotected in 20% sucrose overnight, and then rapidly frozen by immersion in isopentane on dry ice. A complete set of serial sections was then cut through the SN or striatum at 30 µm. Nigral sections from a complete set were chosen as for TH immunostaining (described above). For striatal sections, beginning with a random section between 1 and 6, every sixth section was chosen for immunostaining. Chosen sections were treated with Mouse-on-Mouse Blocking Reagent (Vector Labs) and processed free-floating with a mouse monoclonal anti-Flag antibody (Sigma, St Louis, MO) at 1:1000. Sections were incubated with biotinylated anti-mouse IgG (Vector Labs), followed by ABC (Vector Labs). After immunoperoxidase staining, sections were mounted, dehydrated, and analyzed for neuronal counts using stereological analysis or thionin-counterstained for neuronal cell size analysis.

## 2.11: Quantitative Analysis of Neurons In Vivo

### 2.11.1 Stereological Analysis

To determine the number of Flag-positive neurons in the SN, the entire SN was identified as the region of interest within the StereoInvestigator program (MicroBrightField, Williston, VT). A fractionator probe was established for each section. The number of Flag-positive neurons in each counting frame was determined by focusing down through the section, using x100 objective under oil, as required by the optical dissector method. Our criterion for counting an individual

TH-positive neuron was the presence of its nucleus either within the counting frame, or touching the right or top frame lines (green), but not touching the left or bottom lines (red). The total number of Flag-positive neurons for each brain was then determined by the StereoInvestigator program.

### 2.11.2 Neuronal Size Analysis

To determine the size of injected SN neurons, the StereoInvestigator program was used. For each brain hemisphere, five representative sections (one caudal, two middle, two rostral) were chosen, and five neurons from each section were selected at random sites within the SN to provide a total of 25 neurons per brain per condition (uninjected vs. injected). The area of each neuron cell body was determined under x100 objective under oil. The contralateral, uninjected hemisphere for each mouse brain was used for control neuron sizes.

## 2.12: Statistical Analysis

All statistical analyses were performed with GraphPad Prism software. Simple comparisons of two experimental groups were performed using t-tests. Multiple comparisons of more than two experimental groups were performed using two-way ANOVA and Tukey's multiple comparisons test. The threshold of significance was set at $\alpha = 0.05$ for all experiments.

## 2.13: Materials

### 2.13.1 Antibodies

| Target | Species | Dilution | Company | Catalog # |
|---|---|---|---|---|
| HA | Mouse | 1:1000 (western blot) | Cell Signaling Technology | 2367 |

| | | | | |
|---|---|---|---|---|
| | | 1:100 (IF) | | |
| pAkt308 | Mouse | 1:1000 (western blot) | Cell Signaling Technology | 5106 |
| pAkt308 | Rabbit | 1:1000 (western blot)<br>1:1600 (IF) | Cell Signaling Technology | 13038 |
| pAkt308 | Rabbit | 1:1000 (western blot) | Cell Signaling Technology | 2965 |
| pAkt473 | Rabbit | 1:1000 (western blot) | Cell Signaling Technology | 4060 |
| Total Akt | Rabbit | 1:1000 (western blot) | Cell Signaling Technology | 4685 |
| pFoxO4 | Rabbit | 1:1000 (western blot) | Cell Signaling Technology | 9471 |
| Total FoxO4 | Rabbit | 1:400 (western blot) | Cell Signaling Technology | 2499 |
| GFP | Rabbit | 1:1000 (IF) | Invitrogen | A11122 |
| GFP | Chicken | 1:1000 (IF) | Invitrogen | A10262 |
| Actin | Mouse | 1:3000 (western blot) | Sigma | A3853 |
| GAPDH | Mouse | 1:5000 (western blot) | Abcam | ab9484 |
| ERK1/2 | Rabbit | 1:5000 (western blot) | Santa Cruz | SC-93 |
| TH | Mouse | 1:1000 (IF) | Millipore | MAB318 |
| TH | Rabbit | 1:1000 (IF) | Millipore | AB152 |
| TH | Rabbit | 1:750 (IHC) | Calbiochem | 657012 |
| Flag | Mouse | 1:1000 (IHC) | Sigma | F3165 |

### 2.13.2 Other Reagents

| Name | Description | Company | Catalog # |
|---|---|---|---|
| LY294002 | PI3K inhibitor | Cell Signaling Technology | 9901 |

| | | | |
|---|---|---|---|
| Trimethoprim | DD stabilizing ligand | Sigma | 92131 |
| Trimethoprim-lactate | DD stabilizing ligand | ChemImpex International | 03552 |
| Vectastain ABC HRB kit | Peroxidase staining | Vector Laboratories | PK-400 |
| Mouse on Mouse kit | Immunohistochemistry for mouse antibodies | Vector Laboratories | BMK-2202 |

## Chapter 3: Creation and Validation of DD-Akt(E40K)

### 3.1: Introduction

The destabilizing domain (DD) system was developed as a means for inducible protein control. It was first created by Thomas Wandless in which human FKBP12 protein was engineered to confer instability to other proteins when fused to the DD domain, and this instability was reversible by the addition of a synthetic FKBP12 ligand, Shield-1 (Shld1) [192]. The engineered destabilizing domain has the propensity to become misfolded or partially unfolded and rapidly promotes the ubiquitination of the protein, marking it for proteasomal degradation [214]. When the Shld1 is added, it binds the FKBP12-derived DD domain within a cavity formed by an F36V mutation, inducing the stable and folded conformation of the DD domain and preventing its degradation [214].

Through further engineering of the DD domain, the Wandless group discovered that Shld1-dependent stabilization can be conferred to a variety of proteins of different sizes, folding, function, and cellular localization [192]. Furthermore, this DD system was demonstrated to confer inducible regulation of secreted proteins in a dose-dependent manner in mice [193].

The Wandless group subsequently engineered a second destabilizing domain based on *E. coli* dihydrofolate reductase (DHFR), which can be stabilized by the antibiotic Trimethoprim (TMP) [191]. Similar to the FKBP12-derived DD system, DHFR-derived DD can confer instability if fused to a protein of interest, leading to its degradation via the proteasome [191]. The addition of TMP will stabilize the DD-fusion protein, allowing it to then accumulate within the cell. This version of the DD system was demonstrated to be effective at control of protein stability when placed at the N-terminus or C-terminus, thus providing flexibility of DD domain placement within the protein of interest [191]. Furthermore, the DHFR-derived DD system has

the significant advantage of utilizing TMP, an FDA-approved antibiotic commonly used for treatment of urinary tract infections, as the stabilizing ligand. TMP has been demonstrated to be safe for long-term prophylactic use and can cross the blood brain barrier effectively [215-219]. Importantly, the DHFR-derived DD system has been demonstrated by several groups to be inducible in the rodent striatum with oral administration of TMP [191, 211-213]. These characteristics of the DHFR-derived DD system suggest that it can be utilized as a therapeutic strategy in Parkinson's disease to regulate protein levels within the CNS with systemic administration of TMP.

To fulfill our objective to create an inducibly active Akt system, we have chosen to genetically fuse DHFR-derived DD to the N-terminus of our protein of interest, the constitutively active Akt(E40K), which was provided by our collaborator, Dr. Thomas Franke. Specifically, this construct was chosen for its constitutively high activity, which would allow for accumulation of active Akt when fused to the DD domain and treated with the stabilizing ligand, TMP (Figure 3.1). High constitutive activity of Akt is especially critical for a therapeutic approach in PD, as reports of disrupted PI3K/Akt signaling in the disease imply that simply increasing wild type Akt levels may not sufficiently increase Akt-mediated survival signaling if upstream signaling pathways are suppressed in the disease [154, 155].

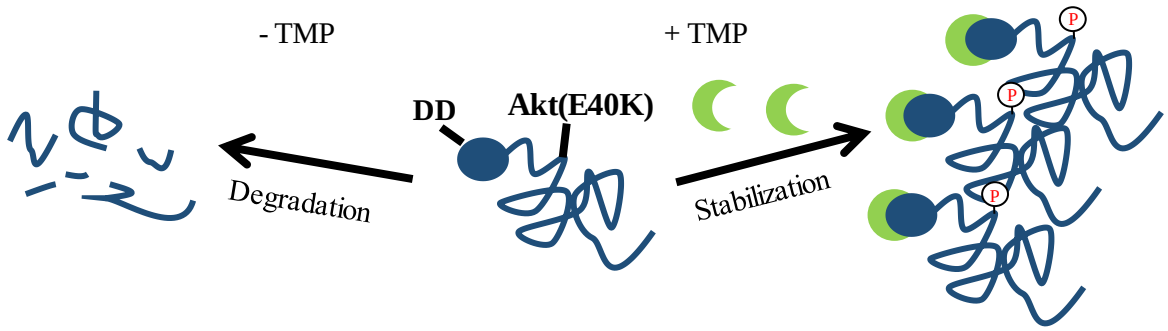


***Figure 3.1: DD-Akt(E40K) is inducibly stabilized by TMP***
The DD-Akt(E40K) protein is unstable and degraded through the proteasome. Trimethoprim (TMP) stabilizes the fusion protein through binding of the DD domain, allowing active Akt to accumulate within the cell.

The Akt(E40K) construct used here consists of the mouse Akt1 isoform with a glutamate to lysine substitution at E40, which is predicted to lie within the phospholipid binding pocket of the PH domain [221]. This mutant was first engineered for use in studies elucidating the activation process of Akt [220]. The substitution mutation at E40 was found to enhance the binding affinity of Akt to phospholipids at the plasma membrane due to the removal of the negatively charged glutamic acid within the phospholipid binding pocket. The enhanced membrane translocation led to higher basal activity of Akt(E40K), which was sufficient to replicate biological effects of Akt activity, including transformation of hematopoietic cells and inhibition of apoptosis induced by IL-3 withdrawal [222, 223]. Overexpression of Akt(E40K) has been shown to protect against growth factor-induced apoptosis *in vitro* [227] as well as increase angiogenesis and reduce apoptosis *in vivo* in a pressure overload-induced heart failure mouse model [228]. Another mutant form of Akt with a similar mutation in the PH domain, Akt(E17K), has been demonstrated *in vitro* to protect against PD mimetic toxins, further supporting the hypothesis that Akt(E40K) can potentially exhibit neuroprotective effects [152].

There also exist phosphomimetic mutants of Akt wherein the canonical phosphorylation sites Thr308 and Ser473 are substituted with an aspartate residue to mimic a phosphorylated

residue [229]. However, these mutants have been found to have low oncogenicity and signaling activity compared to myristoylated Akt or Akt(E40K), suggesting that phosphomimetic Akt mutants do not recapitulate all biological effects of active Akt, [229, 230].

High constitutive activity of Akt may also be achieved through the addition of a myristoylation sequence to the N-terminus of the kinase [231]. However, we chose not to use this form of Akt for two different reasons: better fine-tune control of Akt activity and simpler construct generation. To the first point, myristoylated Akt (myr-Akt) has been suggested to have higher activity levels than that of PH domain mutants, as is implied by much larger increases in heart size with overexpression of myr-Akt compared to Akt(E40K) in rats [232, 233]. Thus, fusion of the DD domain to a constitutively active Akt with lower activity levels, such as Akt(E40K), would potentially allow for better tunability of Akt activity and a wider dose-responsive window. To the second point, generating a myr-DD-Akt construct would require the combination of three elements (a myristoylation sequence, DD domain, and Akt kinase) compared to the two in a DD-Akt(E40K) construct, which would require a more complicated cloning strategy for unclear added benefit.

Although the DHFR-derived DD system provides the flexibility of being placed at the C- or N-terminus of the protein of interest, the C-terminus of Akt contains a highly conserved hydrophobic region that has been shown to be critical for stimulating kinase activity by stabilizing the active state of Akt and serving as a docking site to mediate substrate interactions [110, 115, 234]. Thus, to avoid the possibility of a C-terminal DD domain hindering Akt function, we chose to place the N-terminal DHFR-derived DD domain (from Addgene plasmid #29325) at the 5’ end of the Akt(E40K) expression construct, which also includes an HA tag for ease of identification in biochemistry experiments (Figure 3.2). The fusion gene was

subsequently cloned into a pWPI lentiviral overexpression plasmid and confirmed through Sanger sequencing. The resulting DD-Akt(E40K) fusion protein would be expected to be tunable through TMP treatment and have rapid and reversible induction. Specifically, with the addition of TMP to the extracellular milieu, TMP would bind to the DHFR-DD domain, stabilizing the fusion protein and allowing DD-Akt(E40K) to become activated and accumulate within the cell.

In this chapter, we introduce the *in vitro* characterization of the regulation of DD-Akt(E40K). An inducibly active Akt that utilizes a system based on protein stabilization and under the control of a widely-used antibiotic has not previously been demonstrated. With the importance of Akt signaling in normal cell function and in a wide variety of degenerative diseases as well as cancer, a robust inducible Akt system would have potentially wide implications as a research tool to further elucidate Akt signaling in disease states as well as provide a potential means to develop targeted therapies.

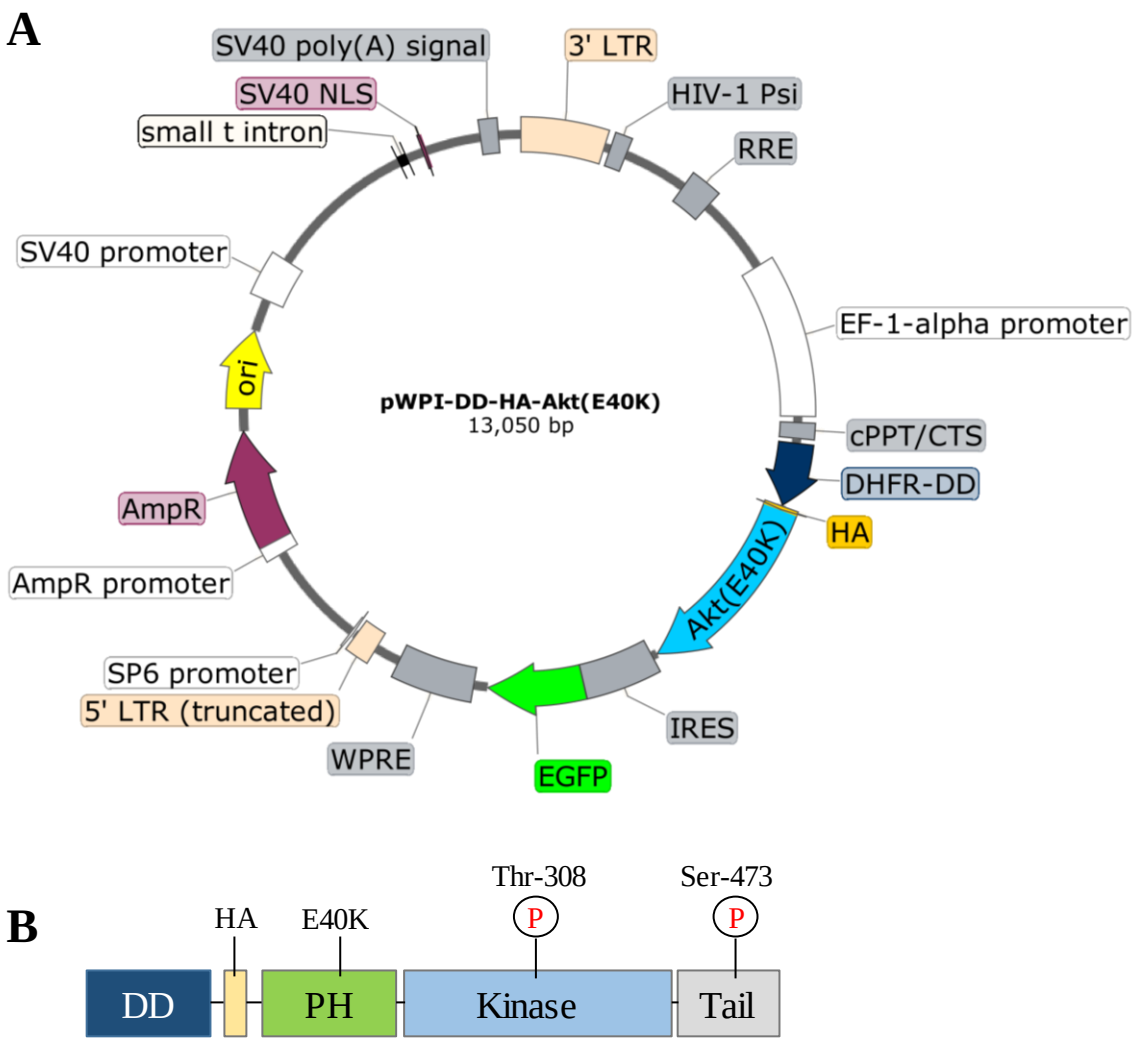


***Figure 3.2: DD-Akt(E40K) construct and protein***
(A) The HA-tagged DD-Akt(E40K) construct was cloned into a pWPI vector.
(B) The DD-Akt(E40K) fusion protein contains a DD domain for inducible stability, an E40K mutation in the PH domain for enhanced membrane binding, and canonical Akt phosphorylation sites.

## 3.2: Results

### 3.2.1 Validation of DD-Akt(E40K) Inducibility

The DD inducible system has not previously been applied to create a tunable form of the kinase Akt. To first validate the inducibility of the DHFR-derived DD construct that we obtained through Addgene (Plasmid #29325), the expression construct was transiently transfected into

HEK293T cells in the form of the fusion gene, DHFR(DD)-YFP. TMP at the dose of 10 µM was added to the cell culture medium at 24 hours post-transfection in order to allow for protein expression of transfected constructs to reach steady state. A 10 µM dose of TMP was chosen based on previous *in vitro* studies of the DHFR-DD system demonstrating efficient control of DD-YFP with 10 µM TMP [191]. Cells were treated for 24 hours to allow for stabilization and accumulation of the DD-YFP fusion protein, after which the cells were imaged with an epifluorescence microscope to assess levels of YFP across conditions (Figure 3.3). The results demonstrate clear induction in levels of YFP fluorescence with TMP treatment in cells that were successfully transfected, while there was no YFP fluorescence observed in untreated cells. This thus confirmed that the DHFR-derived DD system can control the stabilization of YFP as reported in the literature.

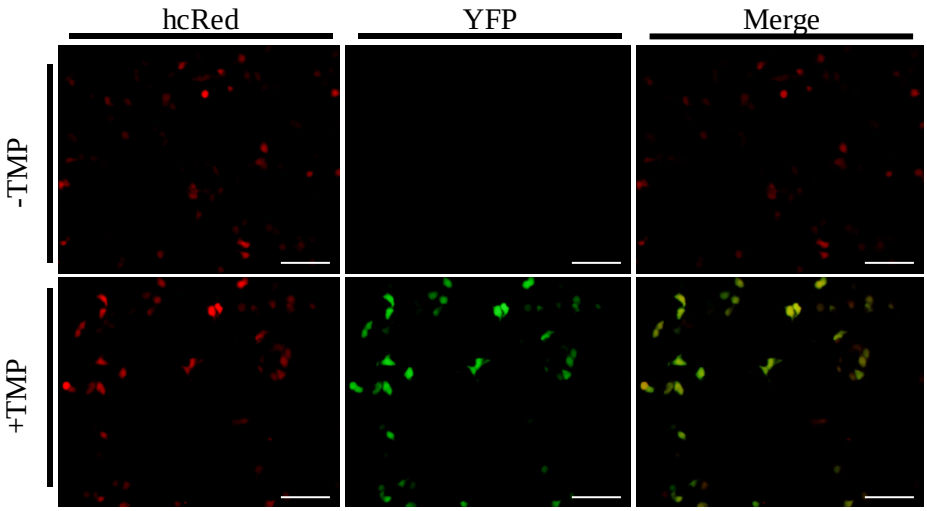


***Figure 3.3: DD-YFP is inducible in HEK293 cells***
HEK293T cells were transfected with a bicistronic IRES expression vector containing a DHFR(DD)-YFP fusion gene and an hcRed gene under the same promoter (Plasmid #29325, Addgene). Cells were treated with 10 µM TMP for 24 hours and imaged with an epifluorescence microscope. Red fluorescence indicates cells expressing the vector and green fluorescence indicates levels of YFP within the cells. Scale bar indicates 100 µm.

To validate the inducibility of the DD-Akt(E40K) fusion protein, the expression vector was transiently transfected into HEK293T cells. The expression vector contains an IRES to allow for bicistronic expression of both DD-Akt(E40K) as well as GFP as a readout for successful transfection (Figure 3.2A). To allow for protein expression of transfected constructs to reach steady state, 10 µM TMP was added to the cell culture medium 24 hours after transfection to start stabilizing the fusion protein. After 24 hours of TMP treatment, the cells were then processed for immunofluorescence staining of GFP to identify transfected cells and HA to identify expression levels of the HA-tagged DD-Akt(E40K) protein. We observed that treatment with TMP led to increased levels of HA staining within the cultures that were transfected with pWPI-DD-Akt(E40K), demonstrating that the TMP treatment indeed leads to stabilization and accumulation of DD-Akt(E40K) *in vitro* in HEK293T cells as was anticipated (Figure 3.4). There was a slight level of HA staining in cultures transfected with DD-Akt(E40K) but untreated with TMP compared to cultures transfected with an empty vector (pWPI), indicating that there is a detectable basal level of DD-Akt(E40K) protein present even without the presence of TMP.

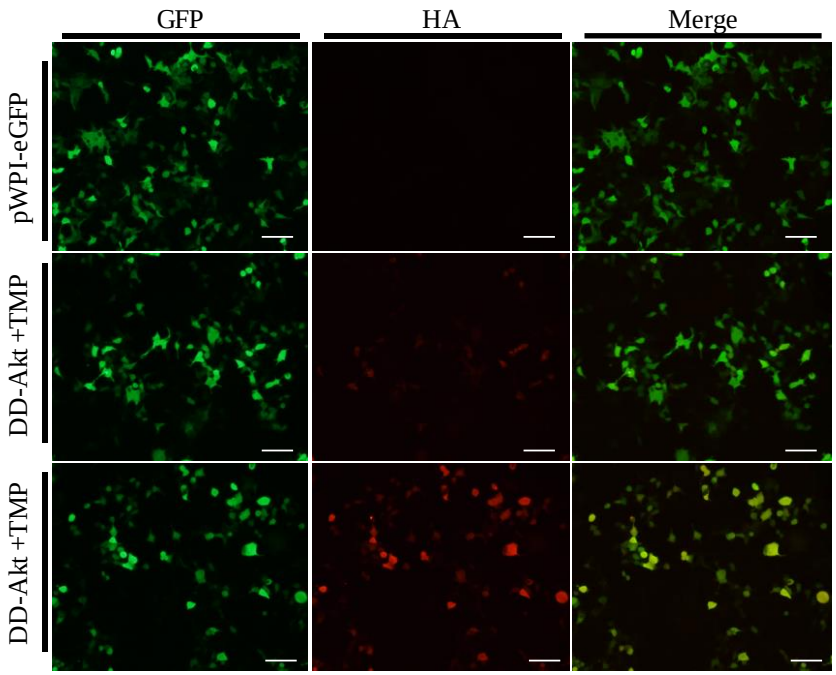


***Figure 3.4: DD-Akt(E40K) is inducible in HEK293 cells*** HEK293T cells were transfected with a bicistronic IRES expression vector (pWPI) containing the DD-Akt(E40K) fusion gene and an eGFP gene. Cells were treated with 10 µM TMP for 24 hours and then fixed for immunofluorescence staining. GFP staining indicates cells expressing the vector and HA indicates levels of DD-Akt(E40K) protein. Scale bar indicates 100 µm.

As discussed above, Akt(E40K) has enhanced membrane binding affinity, which promotes its activation. To determine whether treatment with TMP would also lead to enhanced levels of phosphorylated Akt due to induction of total DD-Akt(E40K) protein levels, HEK293T cells were transfected with the DD-Akt(E40K) construct, treated with 10 µM TMP for 24 hours, and processed for immunofluorescence staining of pAkt308 to identify the levels of phosphorylated, and therefore active, Akt present within the cells (Figure 3.5). We observed robust induction of active Akt within transfected cells with TMP treatment, thus paralleling the increased expression of stabilized DD-Akt(E40K) (Figure 3.4). There was a low background level of active Akt detected in certain cells within cultures that were not treated with the stabilizing ligand, which may reflect a combination of background staining, endogenous pAkt308 presence, and basal levels of DD-Akt(E40K) as observed in Figure 3.4.

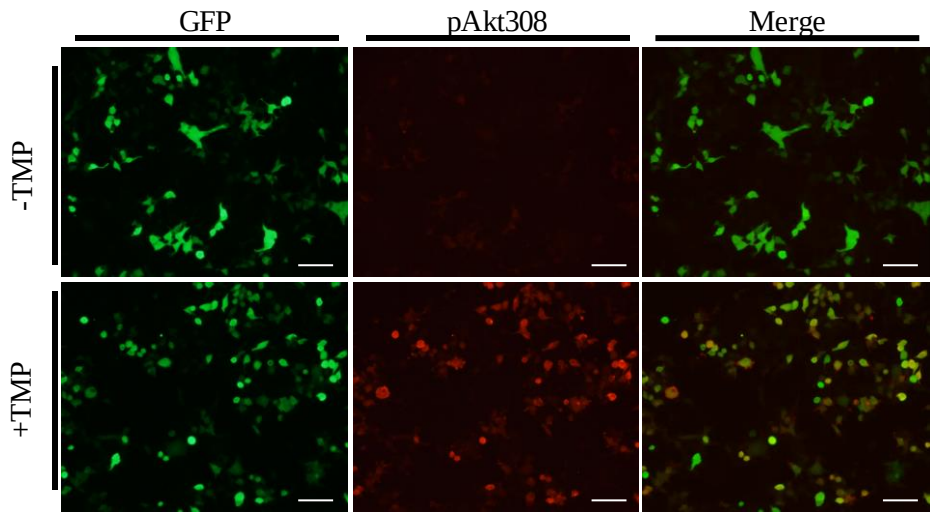


***Figure 3.5: TMP treatment induces active DD-Akt(E40K) in HEK293 cells***
HEK293T cells were transfected with a bicistronic IRES expression vector (pWPI) containing the DD-Akt(E40K) fusion gene and an eGFP gene. Cells were treated with 10 µM TMP for 24 hours and then fixed for immunofluorescence staining. GFP staining indicates cells expressing the vector and pAkt308 indicates levels of active Akt. Scale bar indicates 100 µm.

The induction in activated Akt was also apparent when cells were processed for western immunoblotting (Figure 3.6). With the addition of the DHFR-derived DD domain, DD-Akt(E40K) can be easily distinguished from endogenous Akt due its higher molecular weight and therefore lower electrophoretic mobility. The average fold induction levels across 8-9 experiments was found to be 2.6-fold ± 0.2 for total Akt levels ($p < 0.001$ vs. -TMP), 2.7-fold ± 0.4 for phosphorylated Akt at the S473 site ($p < 0.01$ vs. -TMP), and 4.9-fold ± 1.0 for phosphorylated Akt at the T308 site ($p < 0.01$ vs. -TMP). It should be noted that fold-induction was variable across experiments primarily due to variability in the detectable background levels of DD-Akt(E40K) when not treated with TMP. This variability was particularly apparent for the pAkt308 site where fold inductions ranged from 1.6-fold to 10.8-fold across independent experiments. Across independent experiments, the induction of pAkt473 ranged from 1.7-fold to 4.5-fold and total Akt ranged from 1.9-fold to 3.7-fold.

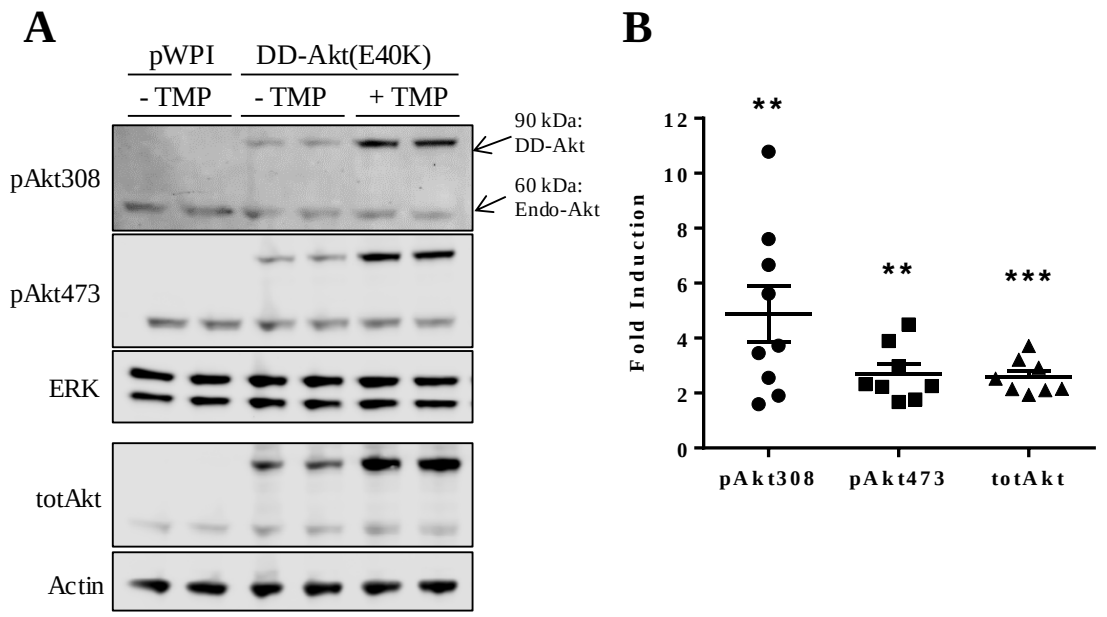


***Figure 3.6: DD-Akt(E40K) is consistently inducible in HEK293 cells***
HEK293T cells were transfected with either an empty expression vector (pWPI) or an expression vector containing the DD-Akt(E40K) fusion gene. Cells were treated with 10 µM TMP for 24 hours and then lysed for western blotting. (A) A representative blot of the expression levels of phosphorylated and total DD-Akt(E40K). "DD-Akt" indicates DD-Akt(E40K) protein bands and "Endo-Akt" indicates endogenous Akt protein. (B) Average fold induction with TMP treatment. N = 8-9 experiments each, with duplicate or triplicate wells per condition. Graph shows means with SEM. **$p < 0.01$, ***$p < 0.001$, paired t-test +TMP vs. –TMP levels.

The inducibility of DD-Akt(E40K) was further tested to assess its utility and consistent inducibility across different cell types, such as neuronal cell types, with higher relevance to potential applications in PD. Because neuronal cell types tend to be difficult to transfect using traditional methods, DD-Akt(E40K) was packaged into a lentiviral vector for transduction and overexpression.

The first neuronal cell type in which DD-Akt(E40K) inducibility was test was neuronal PC12 cells. PC12 cells were differentiated as described in Chapter 2 for 4-5 days and subsequently infected with either an empty lentiviral vector or a DD-Akt(E40K)-containing

lentiviral vector. The cells were treated with 10 µM TMP for 24 hours at 3-4 days post-transduction to allow for full expression of DD-Akt(E40K). Cultures were subsequently processed and analyzed by immunoblotting to determine levels of DD-Akt(E40K) induction with TMP treatment (Figure 3.7). Mean levels of induction in neuronal PC12 cells across 4-6 independent experiments were comparable to those found in HEK293 cells with 2.6-fold ± 0.3 induction for pAkt308 ($p < 0.05$ vs. -TMP), 3.6-fold ± 0.7 induction for pAkt473 ($p < 0.05$ vs. -TMP), and 11.9-fold ± 2.7-fold induction for total Akt ($p < 0.05$ vs. -TMP). Additionally, to understand how phosphorylated DD-Akt(E40K) induction relates to endogenous pAkt signaling, the levels of phosphorylated DD-Akt(E40K) were quantified and compared to endogenous pAkt levels (Figure 3.8). When the phosphorylated DD-Akt(E40K) levels with TMP treatment were calculated as a percentage of endogenous pAkt, phosphorylated DD-Akt(E40K) at the pAkt308 site was found to reach 131.3% ± 27.6% and the pAkt473 site was found to reach 109.0% ± 22.9%. Although transduction efficiency was not assessed in all experiments, efficiency was approximately 75% for these experimental conditions, as measured by the proportion of GFP-expressing cells in a culture.

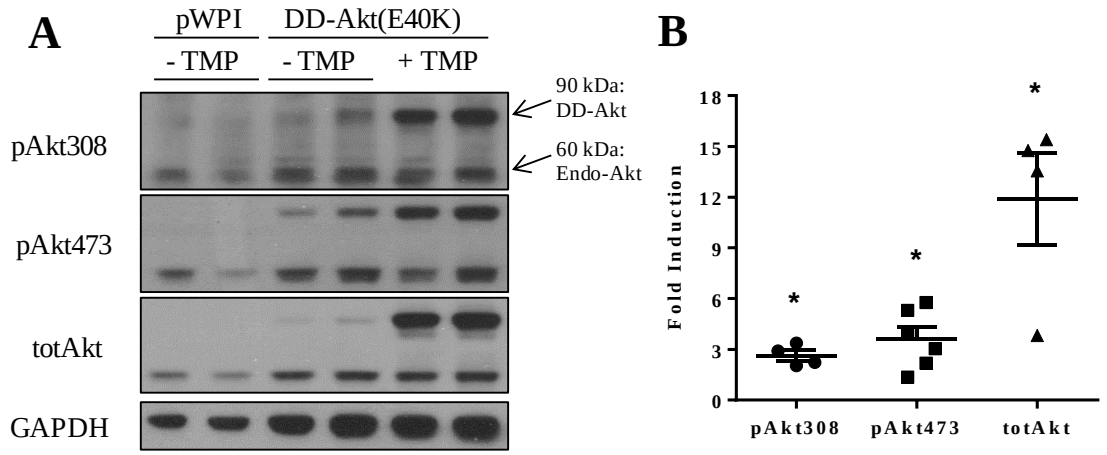


***Figure 3.7: DD-Akt(E40K) is inducible in neuronal PC12 cells***
Neuronal PC12 cells were transduced with a lentiviral vector containing either an empty expression vector (pWPI) or an expression vector containing the DD-Akt(E40K) fusion gene. 4-5 days post-transduction, cells were treated with 10 µM TMP for 24 hours and then lysed for western blotting. (A) A representative blot of the expression levels of phosphorylated DD-Akt(E40K) (indicated by "DD-Akt") and endogenous Akt (indicated by "Endo-Akt"). (B) Average fold induction with TMP treatment. N = 4-6 experiments, with duplicate or triplicate wells per condition. Graph shows means with SEM. *$p \leq 0.05$, paired t-test, +TMP vs. –TMP levels. Transduction efficiency estimated to be 75%.

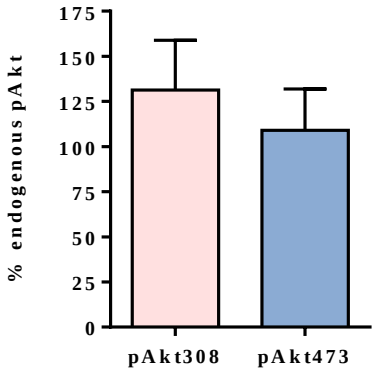


***Figure 3.8: DD-Akt(E40K) reaches control endogenous pAkt levels in neuronal PC12 cells***
Neuronal PC12 cells were transduced with DD-Akt(E40K) lentiviral overexpression constructs and treated with 10 µM TMP for 24 hours and then lysed for western immunoblotting. The percentage of phosphorylated DD-Akt(E40K) to endogenous pAkt levels was quantified and calculated as a percent ratio. N=4-6 independent experiments. Graphs are means with SEM. Transduction efficiency estimated to be 75%.

DD-Akt(E40K) was additionally tested in primary neuronal cultures (Figure 3.9). The induction levels were measured in primary rat cortical cultures with similar methods as in neuronal PC12 cells and as described in Chapter 2. The mean induction levels in one independent experiment with duplicate cultures were measured to be 2.0-fold ± 0.1 ($p < 0.05$ vs. -TMP) at the phosphorylated serine site, and 3.7-fold ± 0.07 ($p < 0.01$ vs. -TMP) of total Akt,

with a transduction efficiency of 50.4% (Figure 3.9). If transduction efficiency is considered, the actual fold induction on a per cell basis may be higher, up to a maximum of double what is quantified in this experiment (4-fold increase at S473 and 6.4-fold increase of total Akt). However, it is probable that increased transduction rates would also increase the detected basal levels proportionally, which may lead to minimal changes in fold-induction. Overall, the induction levels in primary cortical neurons were found to be comparable to induction levels observed in HEK293 and neuronal PC12 cell cultures, thus demonstrating successful TMP-mediated DD-Akt(E40K) inducibility in these cultures.

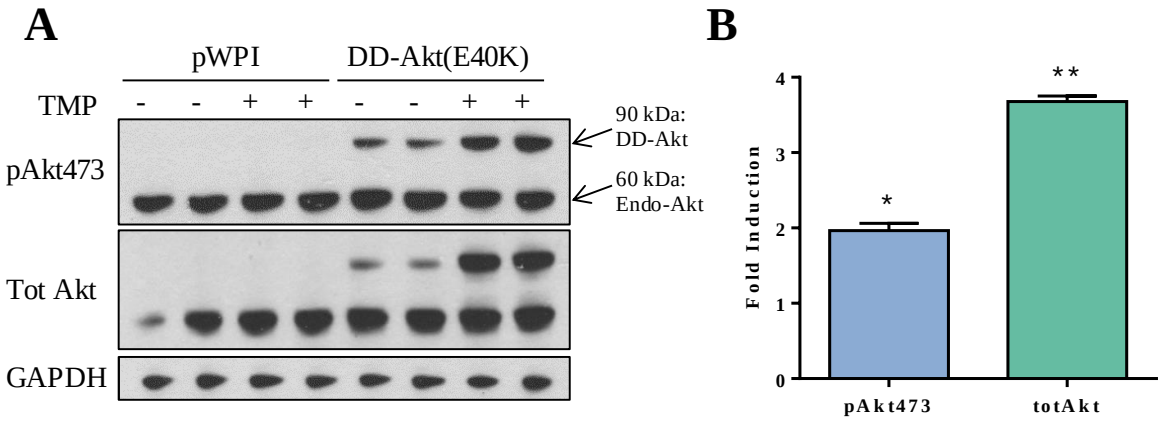


***Figure 3.9: DD-Akt(E40K) is inducible in primary cortical neurons***
Primary cortical neurons (rat E18) were isolated and transduced with a lentiviral vector containing an empty expression vector (pWPI) or an expression vector containing the DD-Akt(E40K) fusion gene. 4 days post-transduction, cells were treated with 10 µM TMP for 24 hours and then lysed for western blotting. (A) A representative blot of the expression levels of phosphorylated and total DD-Akt(E40K). (B) Average fold induction with TMP treatment. N=2 samples per condition. Graphs shows means with SEM. *$p < 0.05$, **$p < 0.01$, unpaired t-test, +TMP vs. –TMP. Transduction efficiency was quantified to be 50.4%.

Finally, the DD-Akt(E40K) system was tested in primary dopaminergic neuron cultures to determine its utility as an inducible system in a cell type that is most relevant to Parkinson's disease. Ventral midbrain dopaminergic neurons were isolated from P0-P3 rats and plated on a confluent glial monolayer as per the protocol utilized in Dr. David Sulzer's laboratory [226]. Due

to the heterogeneity of the cultures, levels of induction could not be measured through western immunoblotting and instead were measured through intensity of immunofluorescence staining through ImageJ. The cultures were processed for immunofluorescence staining after 13-15 days *in vitro*, triple-stained for tyrosine hydroxylase (TH) to identify dopaminergic neurons, GFP to identify transduced cells, and HA to identify levels of DD-Akt(E40K). Cultures were then imaged using an upright fluorescence microscope. Resulting fluorescent images exhibit a visible increase in HA fluorescence intensity (Figure 3.10). Dopaminergic neurons exhibiting dual fluorescence signals for both GFP and TH were chosen for quantification of HA fluorescence levels using ImageJ. Quantification of one experiment with 8 -TMP neurons and 7 +TMP neurons exhibiting GFP and TH fluorescence as described above were measured showed a significant increase of 1.85-fold ± 0.23 ($p < 0.005$ vs.-TMP) in HA fluorescence intensity within neurons treated with TMP (Figure 3.11), thus demonstrating that the levels of DD-Akt(E40K) can be successfully controlled by TMP in primary dopaminergic neurons.

Due to the heterogeneous nature of the dopaminergic cultures, it was possible to determine the levels of DD-Akt(E40K) in non-dopaminergic cells within the same cultures. The HA fluorescence intensity in randomly chosen, neighboring non-TH stained neurons that exhibited GFP expression was quantified through ImageJ (Figure 3.12). Interestingly, the level of HA fluorescence intensity observed in non-dopaminergic cells in the absence of TMP was on average 3.5-fold lower than in dopaminergic neurons at 8.5 ± 1.4 A.U. in non-dopaminergic cells compared to 30.3 ± 4.4 A.U. in dopaminergic neurons (N=12 non-TH neurons, N=8 TH+ neurons, one independent experiment). This was in spite of the observation that the absolute HA fluorescence intensity reached with TMP remained the same across neuronal type at 51.7 ± 5.9 A.U. in non-dopaminergic cells and 56.1 ± 5.6 A.U. in dopaminergic neurons. As a result, the

fold-induction of DD-Akt(E40K) in non-dopaminergic cells was found to be higher at 6.1-fold compared to 1.9-fold in dopaminergic neurons. These results indicate that basal levels of DD-Akt(E40K) are higher in dopaminergic neurons than neighboring non-dopaminergic cells within the same cultures, even though the absolute levels of DD-Akt(E40K) expression reached with TMP treatment were comparable regardless of cell type.

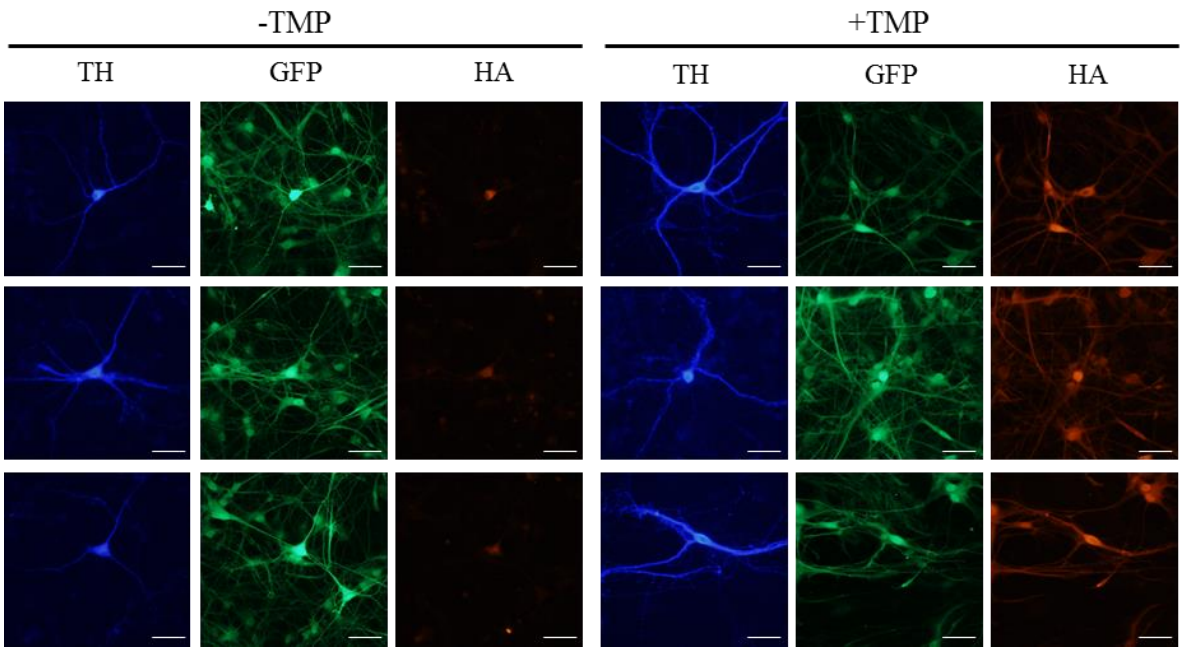


***Figure 3.10: TMP increases DD-Akt(E40K) protein levels in primary dopaminergic neurons***

Primary ventral midbrain cultures were isolated from rat pups P0-3 and seeded on a glial layer. Neurons were transduced with a lentiviral vector containing an expression vector with the DD-Akt(E40K) fusion gene. 6-10 days post-transduction, cultures were treated with 10 µM TMP for 4 days and then processed for immunofluorescence. Cultures were stained for TH to identify dopaminergic neurons, GFP to identify transduced cells, and HA to determine the presence of DD-Akt(E40K). Scale bar indicates 50 µm.

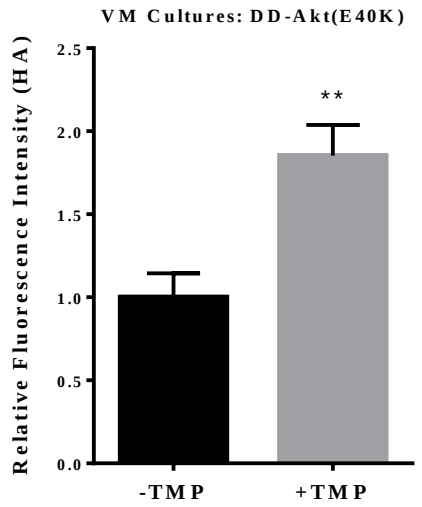


***Figure 3.11: DD-Akt(E40K) is inducible in primary dopaminergic neurons***
HA fluorescence intensity was measured in identified transduced dopaminergic neurons using ImageJ. The relative fluorescence intensity was then quantified. **p < 0.005, unpaired t-test +TMP vs. -TMP conditions. Graph shows means with SEM. N = 8 neurons in -TMP conditions, 7 neurons in +TMP conditions.

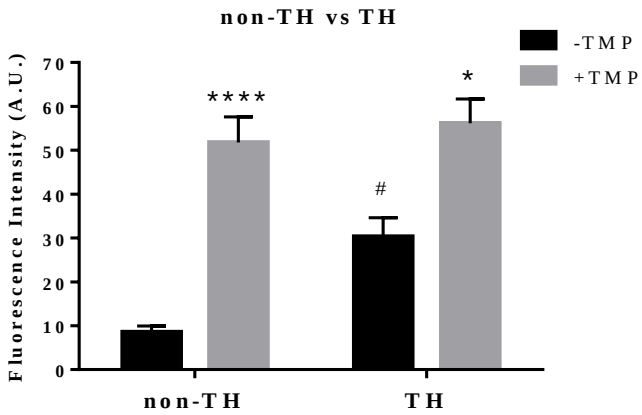


***Figure 3.12: DD-Akt(E40K) has higher basal levels in dopaminergic neurons***
HA fluorescence intensity was measured in transduced (GFP+) neurons using ImageJ. Dopaminergic vs. non-dopaminergic neurons were identified via TH staining. Graph is mean with SEM. N = 7-8 neurons measured for TH+ conditions, 12-14 neurons measured for non-TH conditions. *p < 0.05: TH, -TMP vs. + TMP; ****p < 0.0001: non-TH, -TMP vs. + TMP; #p < 0.05: TH, -TMP vs. non-TH, -TMP, 2-way ANOVA.

### 3.2.2 Potential Strategies to Reduce Basal Levels of the DD-Akt(E40K) System

To address the potential issues of basal DD-Akt(E40K) activity in absence of TMP, we pursued several different strategies. One of our colleagues, Dr. Roger Lefort, acquired preliminary data suggesting that adding a second DD domain to a different protein of interest further reduced basal levels of the protein in absence of TMP (personal communication). Additionally, because DD-YFP had been demonstrated to have much higher fold induction than DD-Akt(E40K), reaching approximately 65-fold [191], and the Akt protein is much larger at 60 kDa compared to YFP at 26.4 kDa, we considered the possibility that the DD domain is not able

to become fully unstable in the absence of TMP due to close proximity and hindrance by the Akt protein. Although the DD-Akt(E40K) protein contains a 3-amino acid linker (Arg-Ala-Cys) between the DD domain and HA-tagged Akt(E40K), it is possible that this linker is not flexible enough to permit full destabilizing function of the DD domain. It is interesting to note that the Wandless group did utilize glycine linker chains to separate the DD domain and YFP domains when spliced internally to the YFP protein ($YFP_N$-DD-$YFP_C$) [191]. The inclusion of a glycine linker appeared to improve inducibility to about 10-fold induction compared to 7-fold induction without a glycine linker, thus suggesting that flexibility of linker chains may improve the destabilizing function of the DD domain [191].

Thus, to determine whether 1) a second DD domain, and 2) a flexible linker could reduce basal levels of DD-Akt(E40K), we created constructs with an additional DD domain at the N-terminus of DD-Akt(E40K) using glycine linker sequences (Gly-Gly-Gly-Gly-Ser) of various lengths (Figure 3.13).

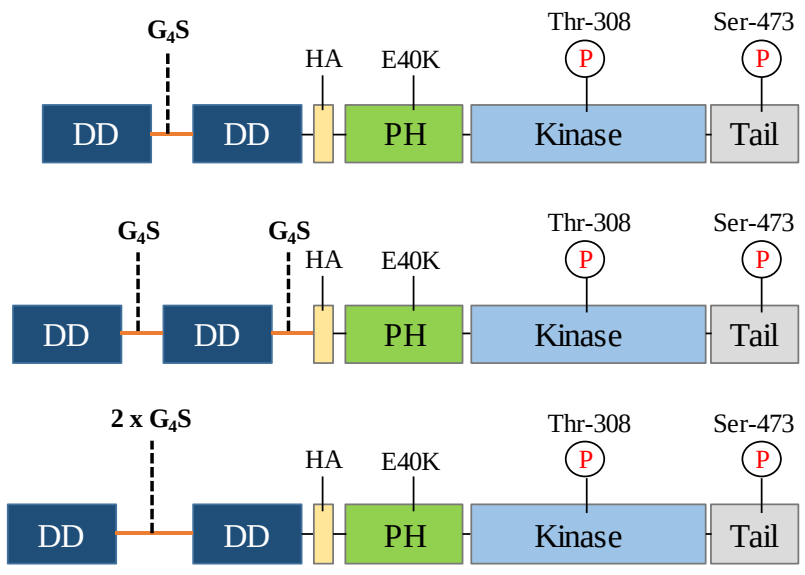


***Figure 3.13: Double DD-Akt(E40K) fusion proteins***

It was important that the addition of the second DD domain did not change the absolute

levels of Akt(E40K) reached when treated with TMP because levels of active Akt with TMP-mediated stabilization would need to remain high for potential pro-survival effects. In other words, we wanted to ensure that any strategy to lower basal levels did not also lower induction levels that were reached with TMP treatment. Thus, we measured the fold-induction achieved by the double DD domain constructs in HEK293 cells (Figure 3.14). If the basal levels were reduced with the second DD domain and the "on" levels of Akt(E40K) with TMP treatment remained the same, the fold induction should increase. Interestingly, the fold induction levels did not appear to change with the addition of the second DD domain, with the exception of (DD-$G_4S$)x2-Akt(E40K) vs. DD-Akt(E40K) at the pAkt308 site (2-way ANOVA with multiple comparison). These data indicate that the second DD domain was not able to achieve both lower basal levels and maintenance of induced levels across both Akt phosphorylation sites.

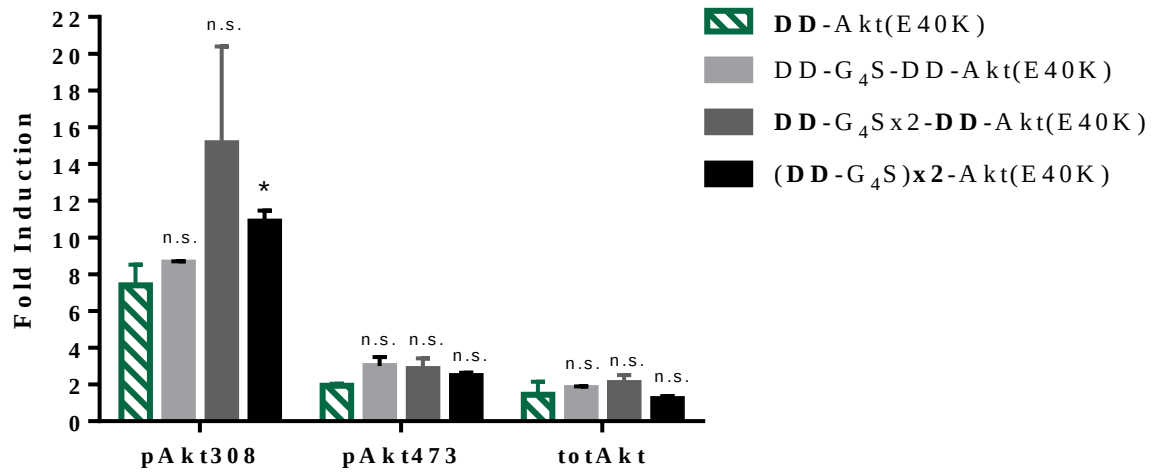


***Figure 3.14: Adding a second DD domain does not improve fold induction or basal activity*** HEK293 cells were transfected with constructs to overexpress single DD domain Akt(E40K) or double DD domain Akt(E40K) with various linker combinations. Cells were treated with 10 µM TMP for 24 hours and then lysed for western blotting. Protein expression levels were quantified and normalized to ERK as a loading control. Fold induction was calculated as a ratio of protein levels with TMP treatment divided by protein levels without TMP treatment. Graph shows means with SEM. N = 2 independent experiments. *$p < 0.05$ vs. DD-Akt(E40K), n.s. determined through 2-way ANOVA with multiple comparisons.

Another consideration to optimize basal levels of the DD-Akt(E40K) system is the membrane binding of the mutant Akt. As discussed in Section 3.1, the E40K mutation within the PH domain of Akt increases its membrane affinity, thus increasing membrane binding and phosphorylation of Akt. Although the FKBP12-derived DD system had been validated to inducibly stabilize transmembrane proteins [192], the DHFR-derived DD system has only been applied to non-membrane bound proteins in the literature. Thus, it is conceivable that the increased membrane binding of Akt(E40K) may impede its degradation when not treated with TMP and increase the basal levels of the protein. To determine whether the PH domain mutation interferes with DD-mediated degradation, a construct with no PH mutation, DD-Akt(WT), was created. HEK293 cells were transfected with the WT and E40K constructs and treated with TMP for 24 hours to compare and determine any differences in basal protein levels or induction that may be caused by the mutation (Figure 3.15). There was no difference detected in either total levels of Akt or phosphorylated Akt between WT or the E40K proteins when untreated with TMP (n.s., 2-way ANOVA with multiple comparisons), indicating that increased membrane affinity does not impede DD-mediated degradation. As expected, the levels of phosphorylated Akt were induced with TMP but to a lesser extent in the WT Akt compared to the E40K mutant.

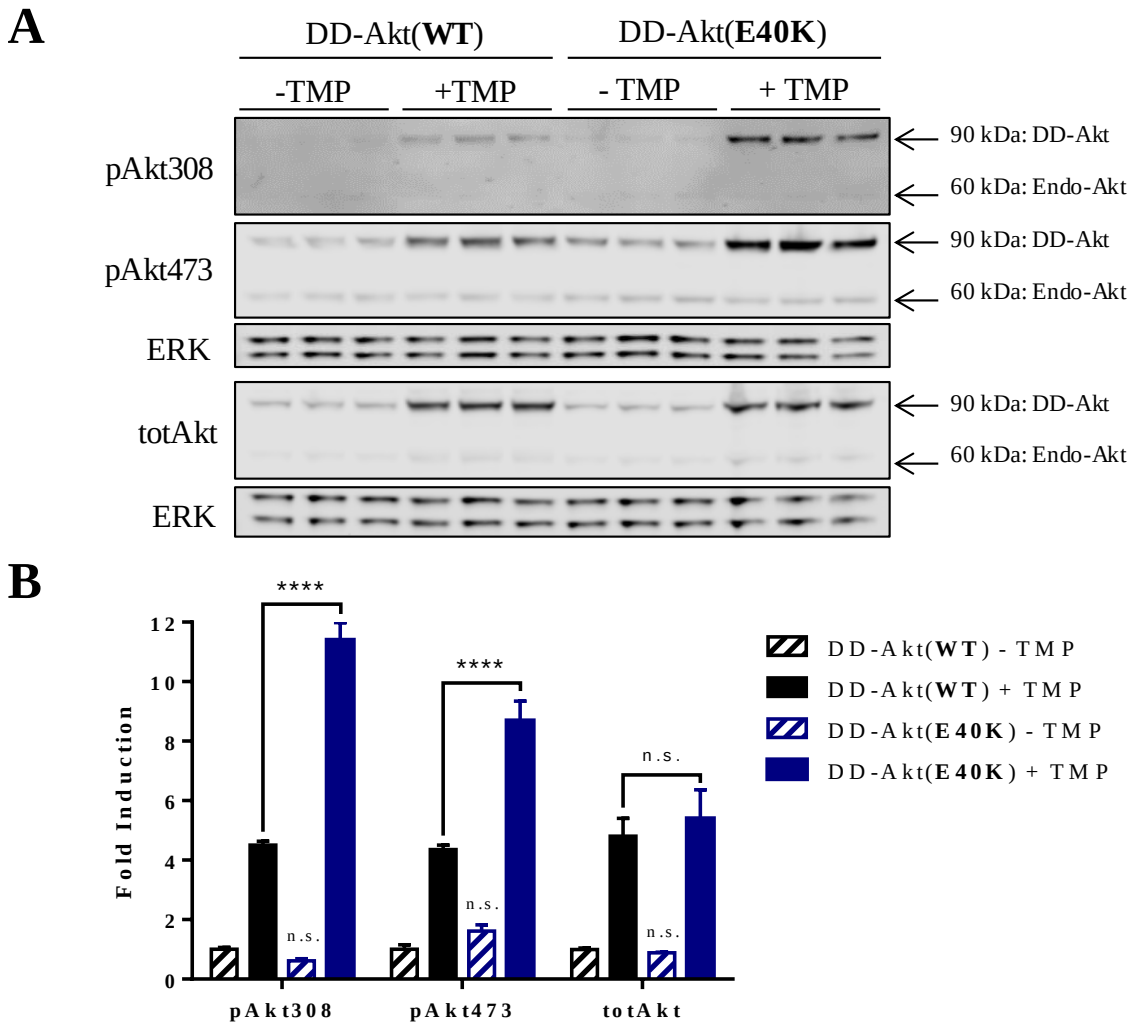


***Figure 3.15: Increased membrane affinity does not affect DD-mediated destabilization***
HEK293 cells were transfected with DD constructs with WT Akt or Akt(E40K). Cells were treated with 10 µM TMP for 24 hours and then lysed for western blotting. Protein expression levels were quantified and normalized to ERK as a loading control. Fold induction was calculated as a ratio of protein levels with TMP treatment divided by Akt(WT) protein levels without TMP treatment. Graph shows means with SEM. N = 3 replicate samples per condition. ****$p < 0.0001$; n.s. vs. DD-Akt(WT) –TMP unless otherwise indicated, 2-way ANOVA with multiple comparisons.

### 3.2.3 Characterization of DD-Akt(E40K) Regulation

Once TMP-mediated DD-Akt(E40K) inducibility was established in multiple cell systems, and optimization strategies of basal levels was attempted, the next important step to test this system's full applicability as a tool to control Akt levels was to further characterize the

regulation of DD-Akt(E40K) by TMP.

One of the potential advantages of the DD system is its dose-responsive inducibility that is mediated by the stabilizing ligand. As such, the levels of stabilized protein should depend on the levels of TMP available to bind and stabilize the DD-fusion protein. Thus, we investigated whether the DD-Akt(E40K) fusion protein exhibited dose-responsive behavior to TMP treatment. HEK293 cells were transiently transfected with DD-Akt(E40K) expression vectors and subsequently treated with different doses of TMP, ranging from 10 nM to 100 µM for 24 hours. Cells were then lysed for protein extraction and Akt protein levels were quantified through immunoblotting. The DD-Akt(E40K) protein was found to be dose-responsive to TMP, reaching half-maximal induction by 50-100 nM and maximal induction by 500 nM (Figure 3.16).

An additional advantage of the DD system is its ability to rapidly permit elevation of protein levels, due to constitutive expression and degradation of the protein as well as the reversibility of the induction. To better determine the kinetics of induction, HEK293 cells were transiently transfected with DD-Akt(E40K) and treated with 10 µM TMP for different lengths of time. Induction of DD-Akt(E40K) by TMP was found to steadily increase across a period of 24 hours (Figure 3.17A). Additionally, transfected cells were treated with 10 µM TMP for 24 hours and then washed with 1X PBS 3 times at different time points to determine the length of time required for reversal of induction. When the total levels of DD-Akt(E40K) protein were quantified, reversal of induction was found to happen as a steady decrease of DD-Akt(E40K) protein levels, with an estimated 30 hours required for half reversal. At least 48 hours were required for DD-Akt(E40K) protein levels to return close to baseline (Figure 3.17B). These results clearly demonstrate that levels of DD-Akt(E40K) can be induced by TMP and reversed with removal of TMP to baseline *in vitro*, a potentially important characteristic for the utility of

the system if used for signaling studies and therapeutic approaches.

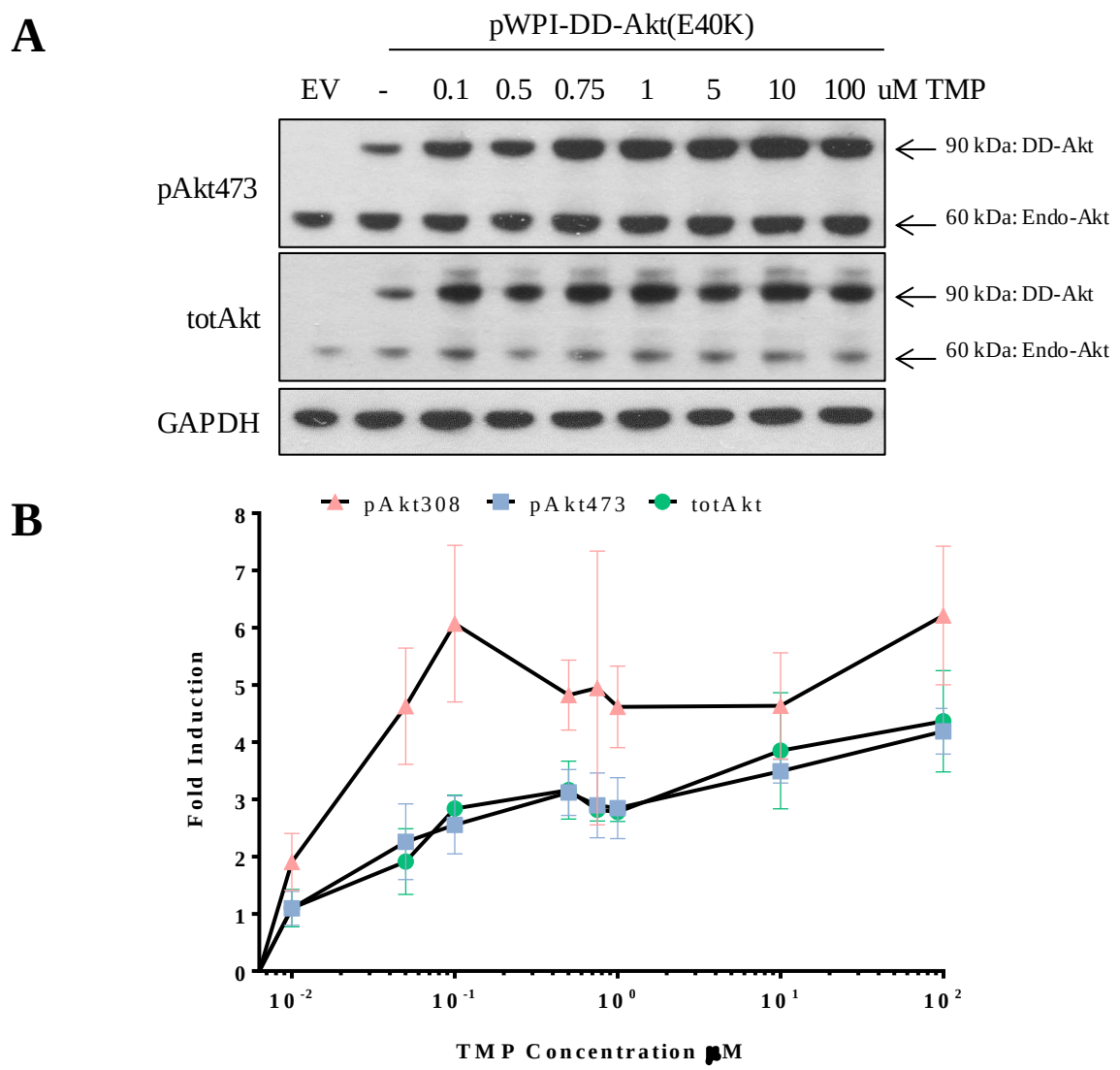


***Figure 3.16: DD-Akt(E40K) is dose-responsive to TMP treatment***
HEK293 cells were transfected with DD-Akt(E40K) and treated with differing doses of TMP for 24 hours. Cells were then lysed and processed for immunoblotting. (A) This representative blot shows a clear increase in levels of DD-Akt(E40K), both phosphorylated and total, with increasing doses of TMP. The top band represents DD-Akt(E40K) and the bottom represents endogenous Akt, as indicated. (B) DD-Akt(E40K) levels were quantified and normalized to a loading control. The dose responsive range of DD-Akt(E40K) was found to be between 10 nM and 500 nM. Graph shows means with SEM. N=3-4 independent experiments.

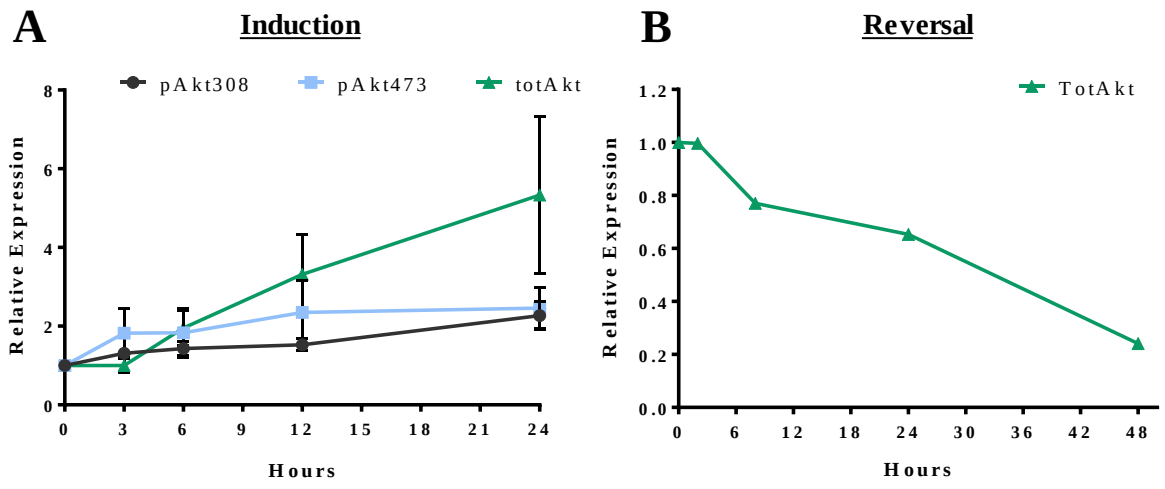


***Figure 3.17: DD-Akt(E40K) is steadily induced across 24 hours and is reversible***
(A) HEK293 cells were transfected with DD-Akt(E40K) and treated with 10 μM TMP for different time points. Graph shows means with SEM. N = 2-4 independent experiments. (B) Cells treated with 10 μM TMP for 24 hours were washed to remove TMP in the medium at different time points. Protein levels of phosphorylated and total DD-Akt(E40K) were analyzed to determine time course reversal. Data shown are from one independent experiment.

### 3.2.4 DD-Akt(E40K) Regulation Under Conditions of Reduced PI3K Signaling

As various studies have suggested that PI3K signaling is impaired or dysfunctional in PD [154, 155], we strove to understand the induction of the DD-Akt(E40K) system under conditions in which PI3K has been inhibited.

HEK293 cells were transiently transfected with DD-Akt(E40K) and pre-treated with 10 μM TMP for 24 hours before adding 50 μM PI3K inhibitor LY294002 for 24 hours. Importantly, although the overall levels of active DD-Akt(E40K) were suppressed by about 5-fold when PI3K was inhibited, the overall fold-induction by TMP treatment was maintained, indicating that the inducibility of the system is not compromised under conditions with little to no PI3K signaling (Figure 3.18). Furthermore, the addition of the inhibitor was enough to eliminate detectable endogenous active Akt, as measured by pAkt308 and pAkt473 (Figure 3.19). However, the

activity of DD-Akt(E40K) was maintained to an average of 67% of endogenous pAkt308 levels under normal (with no PI3K inhibition) conditions and 45% of endogenous pAkt473 levels under normal (with no PI3K inhibition) conditions (Figure 3.19). These results demonstrate that DD-Akt(E40K) can maintain inducibility under conditions involving very low PI3K signaling, which is again important for applications as a therapeutic strategy in PD.

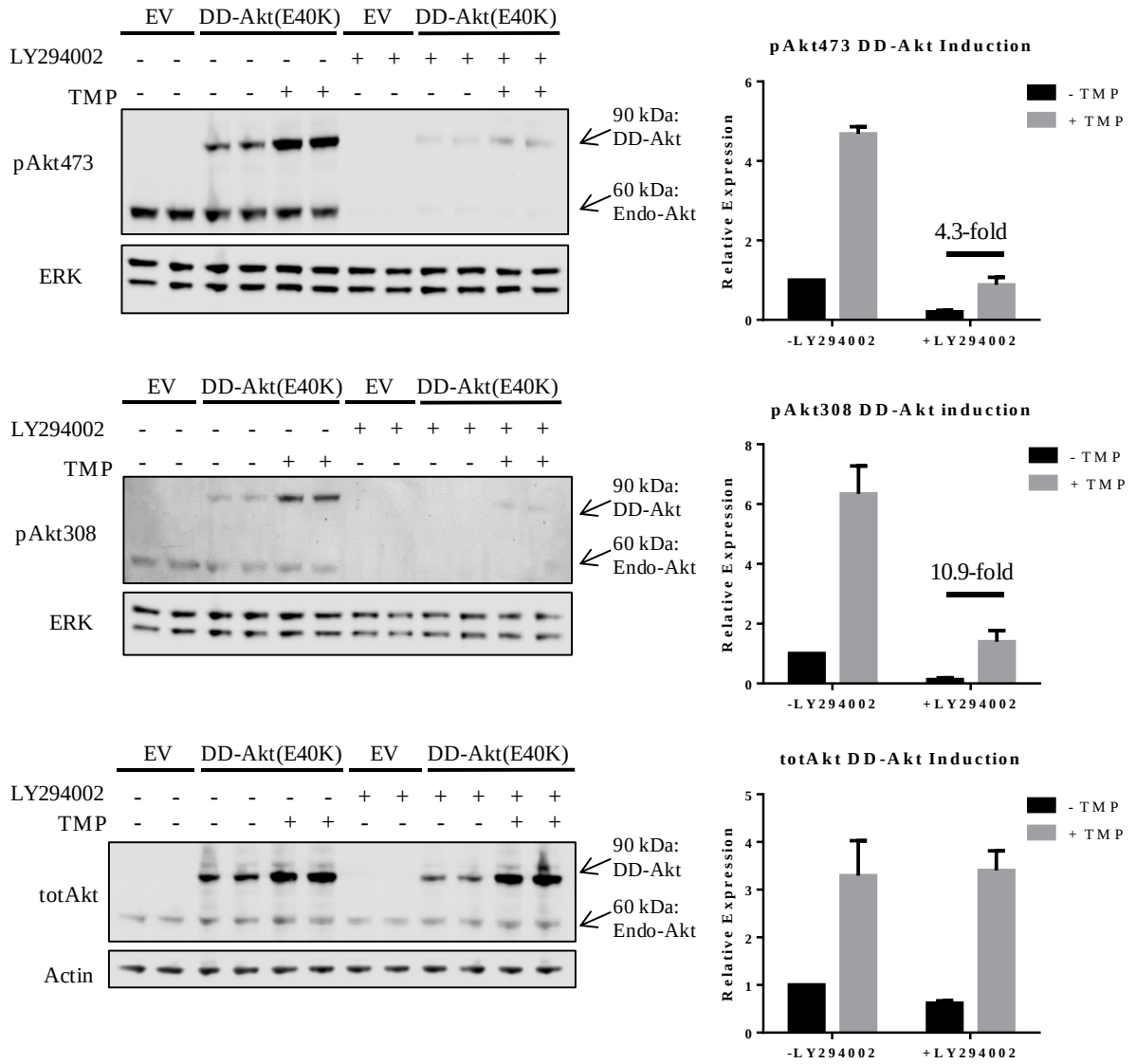


***Figure 3.18: DD-Akt(E40K) inducibility persists with inhibited PI3K signaling***
HEK293 cells were transfected with DD-Akt(E40K) and pre-treated with 10 μM TMP for 24 hours before adding 50 μM LY294002. Protein levels of phosphorylated and total Akt were analyzed through immunoblotting. Graphs are means with SEM. N=3 independent experiments.

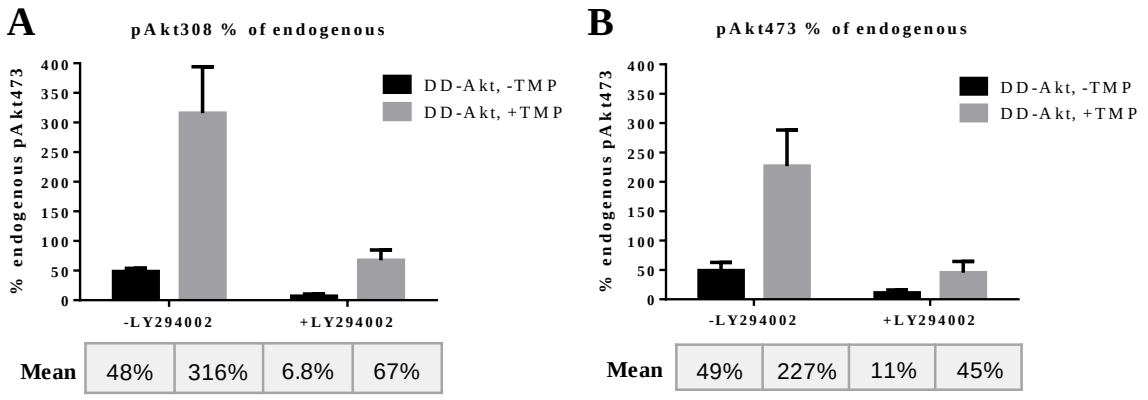


***Figure 3.19: DD-Akt(E40K) activity persists despite suppressed PI3K activity***
HEK293 cells were transfected with DD-Akt(E40K) and pre-treated with 10µM TMP for 24 hours before adding 50µM of LY294002. Protein levels of phosphorylated Akt were analyzed through immunoblotting. The protein band intensity levels were calculated as a percent of endogenous pAkt signaling under control conditions. The mean of expression levels in each condition is indicated below each bar. Graphs are means with SEM. N=3 independent experiments.

## 3.3: Discussion

In this chapter, we report the creation of an innovative method for post-translational control of Akt levels using a DHFR-derived destabilizing domain. The addition of this destabilizing domain to a mutant Akt with high activity levels (Akt(E40K)) gives rise to a fusion protein that is constitutively expressed and degraded. This technique has the unique advantage of permitting control of DD fusion protein levels via a commonly used antibiotic, Trimethoprim (TMP), that is inexpensive and membrane permeable. Here we show successful TMP-mediated inducibility in a variety of cell types, including human embryonic kidney cells, neuronal PC12 cells, rat primary cortical neurons, and dopaminergic neuronal cultures (Section 3.2.1). This induction was demonstrated to be dose-responsive to TMP and reversible (Section 3.2.3), as well as able to maintain inducibility and activity in conditions with suppressed PI3K signaling

(Section 3.2.4).

Our data reveal an interesting finding regarding the levels of DD-Akt(E40K) induction across cell types. In HEK293 cells, fold-induction levels of the phosphorylated form of DD-Akt(E40K) at Ser473 and total DD-Akt(E40K) were found to be roughly equivalent, while phosphorylated DD-Akt(E40K) at Thr308 was slightly higher (Figure 3.6). However, in a neuronal cellular context (neuronal PC12 cells and primary cortical neurons), the fold-induction levels of phosphorylated DD-Akt(E40K) appeared to be much lower than fold-induction levels of total DD-Akt(E40K) (Figures 3.7 and 3.9). This phenomenon directly implies that there exists some difference in the proportion of total Akt available that is phosphorylated across the different cell types tested. Potential reasons for this distinction are two-fold: first, there may be lower efficiency of the Akt phosphorylation machinery in neuronal PC12 cells and cortical neurons than in HEK293 cells such that with a certain increase in total Akt, a smaller proportion is phosphorylated in the cell; second, the levels of phosphorylated Akt within the cell may be so tightly regulated that there is a cap on the level of increase a cell will permit, perhaps based on upstream phosphatase activity, and beyond that cap, there will be no further increase in phosphorylated Akt regardless of further increases in total Akt. Our data suggests that the second explanation may be more plausible because the overall fold-increases of total DD-Akt(E40K) were drastically increased from 2.6-fold in HEK293 cells to 11.9-fold in neuronal PC12 cells, but the increases in phosphorylated DD-Akt(E40K) were different in inconsistent directions between HEK293 cells and neuronal PC12 cells. However, it is difficult to conclusively deny the former explanation for the observed distinctions in fold-induction across cell types with the data observed, because the fold-induction for phosphorylated DD-Akt(E40K) at the serine site were highest in neuronal PC12 cells than in HEK293 cells or primary cortical neurons – this may

indicate that increases in total DD-Akt(E40K) did lead to some increase in phosphorylated DD-Akt(E40K), though we cannot be sure if this increase was equally or less proportional with total Akt increases up to the aforementioned "cap". Furthermore, our data cannot distinguish whether this difference could be attributed to either a difference in cell type (i.e., neuronal versus kidney) or in species of animal that the cell line is sourced from (i.e., rat versus human). Further investigation into this phenomenon may lead to insights about differences in endogenous Akt activation levels dependent on cell type.

One of the potential weaknesses of our DD-Akt(E40K) system lies in the basal levels of the protein present even without TMP treatment. We believe this may be due to the nature of the degradation domain-based inducible system, wherein the protein of interest is constitutively expressed and degraded by the proteasome such that there must exist a steady state basal level of the protein even without the stabilizing ligand. In investigating levels of basal DD-Akt(E40K) across dopaminergic neurons and non-dopaminergic cells, we came across an intriguing finding of greater than 250% higher basal DD-Akt(E40K) levels detected in dopaminergic neurons than non-dopaminergic neurons (Figure 3.12). This finding leads to the interesting question of whether protein degradation activity is different depending on cell type. Given the literature supporting dysfunction of the ubiquitin-proteasome system as a contributing factor in Parkinson's disease [235, 236] and reports of lower proteasome activity in the substantia nigra compared to other brain regions even in non-disease contexts [237, 238], it is very likely that the observed higher basal levels of DD-Akt(E40K) in dopaminergic neurons are due to impaired or lower proteasomal activity in dopaminergic neurons, which would impact the proteasome-dependent degradation of DD-fusion proteins [191]. Although the observed differences in basal DD-Akt(E40K) levels in these cultures is statistically significant, this intriguing result may merit

further investigation with larger numbers of neurons. Results could potentially lead to insights into selective vulnerability of dopaminergic neurons in Parkinson's disease.

Finally, our data on DD-Akt(E40K) signaling in the context of impaired PI3K activity demonstrates the maintenance of inducible control with TMP in these conditions, enough to reach 45-67% of control endogenous pAkt levels (under PI3K non-inhibited conditions) (Figure 3.19). This finding is important because it establishes that the DD-Akt(E40K) inducible system will remain reliably regulatable, even within Parkinson's disease contexts where PI3K signaling is reported to be decreased [154, 155]. The question remains whether 45-67% of endogenous Akt signaling is sufficient to promote Akt-mediated survival of cells. We will explore this question in detail in Chapter 4.

## Chapter 4: Physiological Activity of DD-Akt(E40K) in vitro

### 4.1: Introduction

The previous chapter established DD-Akt(E40K) as a reliably inducible Akt construct in multiple cellular contexts that can partially maintain its activity under conditions with low or absent PI3K signaling. The next step in our work was to determine whether DD-Akt(E40K) can show inducible physiological functions. Our data in this chapter demonstrate that DD-Akt(E40K) can reliably and inducibly phosphorylate a known downstream substrate of Akt, FoxO4 [117] in 293 cells, and can promote survival in a neuronal cell line against various cellular insults.

FoxO4 is a member of the FoxO family of transcription factors, which have been widely studied for their effects on cell cycle regulation, metabolism, and survival [239]. The FoxO family has also been implicated as tumor suppressors, as chromosomal translocations involving the genes encoding FoxOs have been found to occur in acute myeloid leukemia and rhabdomyosarcomas [240]. Additionally, FoxO4 has specifically been shown to mediate cell cycle and apoptosis through upregulation of cell cycle protein p27 Kip1 and proapoptotic gene Bim [241-243]. As mentioned above, FoxO4 is a direct substrate of Akt, with PI3K-Akt signaling demonstrated to negatively regulate FoxOs, through phosphorylation by Akt, which sequesters the transcription factors with 14-3-3, thus impairing its nuclear translocation and upregulation of proapoptotic genes [120, 244, 245]. This relationship is evolutionarily conserved, thus implying its importance as a general regulatory mechanism in cells [239].

As discussed in detail in Chapter 1, Akt signaling is regarded to be a critical signaling pathway with a variety of downstream physiological effects ranging from cell growth and metabolism to survival [117]. With the reported involvement of suppressed Akt signaling in a variety of Parkinson's disease (PD) models, we sought to verify the physiological effects of DD-

Akt(E40K) in various models of suppressed Akt signaling including growth factor removal (serum deprivation) and PD toxin models.

To carry out our physiological studies in a relevant neuronal context, we employed the PC12 cell line. The PC12 cell line was derived from a transplantable rat adrenal pheochromocytoma and has been used extensively as a cellular model for pathological conditions including neurodegeneration [224, 246]. While in the naïve state, PC12 cells depend on serum-supplemented medium, and removal of serum from the medium leads to apoptotic death. PC12 cells can be differentiated into nondividing sympathetic-neuron like cells with the addition of nerve growth factor (NGF). Differentiated PC12 cells exhibit morphologies consistent with neuronal cells, including extension of axonal processes [224]. Importantly, differentiated PC12 cells are sensitive to PD mimetic toxins such as 6-hydroxydopamine (6-OHDA) and 1-methyl-4-phenylpyridinium ($MPP^+$), among others [247, 248]. Both 6-OHDA and $MPP^+$ are mitochondrial toxins that can induce cellular degeneration within 24-48 hours of exposure.

In this chapter, we explore the ability of DD-Akt(E40K) to inducibly phosphorylate a known downstream substrate involved in survival signaling and its ability to promote cellular survival in various cellular stress models, including serum deprivation and toxin-based PD models. The research presented here demonstrates that the expression of DD-Akt(E40K) can protect cellular models against stress conditions that induce apoptosis. Importantly, the results also demonstrate that the physiological effects on survival can be controlled by the presence of the stabilizing ligand and antibiotic, trimethoprim (TMP).

## 4.2: Results

### 4.2.1 Downstream Signaling of DD-Akt(E40K)

To better understand the signaling of DD-Akt(E40K) and validate that the fusion protein maintains its function as a kinase, we investigated the effect of DD-Akt(E40K) induction on a known Akt substrate, FoxO4 [117]. As mentioned in Section 4.1, FoxO4 is a transcription factor of the FoxO family of proteins that is known to be a mediator of apoptosis through upregulation of proapoptotic gene targets such as BH3-only protein BIM [243]. Akt blocks FoxO-mediated transcription of proapoptotic genes through phosphorylation of the FoxO protein, which leads to nuclear exit and sequestration of FoxO in the cytosol [117].

HEK293T cells were transfected with DD-Akt(E40K) expression vector and then treated with 10 μM TMP for 24 hours. Cells were then lysed to isolate protein and the levels of phosphorylated FoxO4 (pFoxO4) at the Akt phosphorylated site, S193, were analyzed through immunoblotting. Results demonstrate a 2.2-fold ± 0.95 elevation of pFoxO4 ($p \leq 0.01$ vs -TMP, 1-way ANOVA) with the induction of DD-Akt(E40K), indicating that TMP can stabilize the fusion protein and permit accumulation of active Akt within the cell, which subsequently phosphorylates an Akt substrate important for cell survival (Figure 4.1). Importantly, there was no significant elevation of pFoxO4 in conditions with DD-Akt(E40K) transfection but without TMP treatment, thus indicating that basal expression levels of DD-Akt(E40K) were not sufficient to significantly elevate phosphorylated downstream substrates. Additionally, there was no elevation of total FoxO4 observed. This is an important result that shows that the addition of the DD domain to Akt does not interfere with its ability to bind and phosphorylate known substrates.

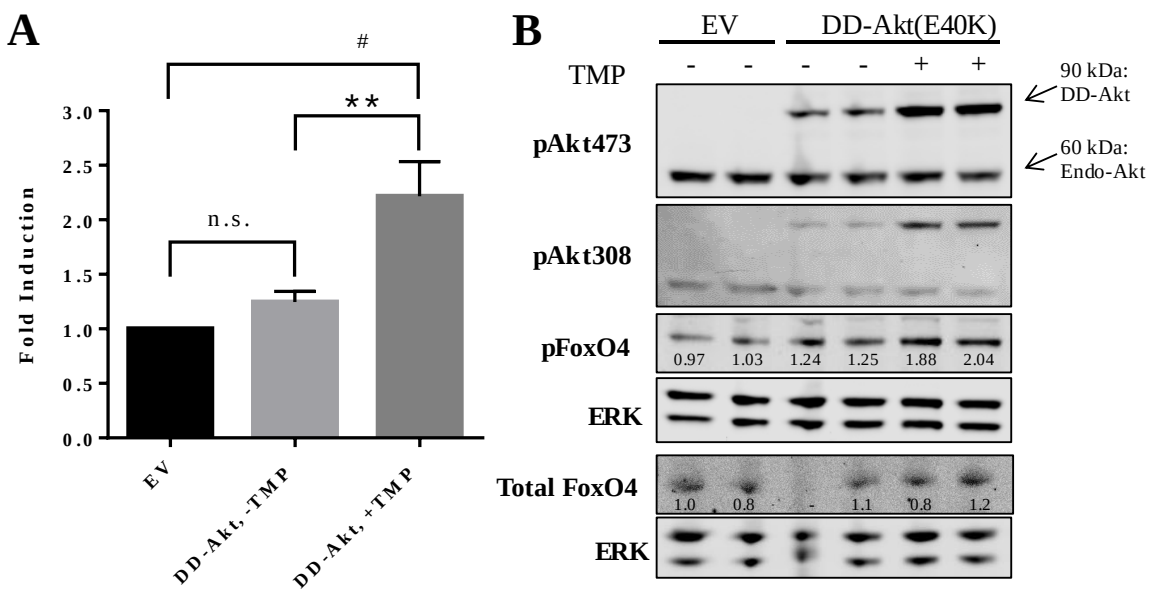


***Figure 4.1: DD-Akt(E40K) phosphorylates downstream substrate pFoxO4***
HEK293 cells were transfected with DD-Akt(E40K) and treated with 10μM TMP for 24 hours. (A) Protein levels of phosphorylated FoxO4 S193 were analyzed to determine any induction of pFoxO4 with increase in active DD-Akt(E40K). Graph is mean with SEM. N = 9 independent experiments (7 experiments with no serum, 2 experiments with serum). **$p<0.01$ compared with DD-Akt(E40K) - TMP condition, #$p<0.05$ compared with empty vector (EV) condition, one-way ANOVA. (B) A representative blot is shown on the right.

### 4.2.2 DD-Akt(E40K) Inducibly Protects Naïve PC12 Cells Against Serum Deprivation

As mentioned above, naïve, undifferentiated PC12 cells rely on the presence of serum in the medium for survival. When serum is removed from the medium, PC12 cells begin to undergo apoptosis due to the removal of growth factor signaling. Thus, we used this model to investigate potential physiological effects of inducible DD-Akt(E40K) on promoting survival. Because Akt signaling has been well-characterized, particularly with regards to its crucial role as a mediator of growth factor signaling and cellular survival, we anticipated that DD-Akt(E40K) would have similar pro-survival effects in this model when induced with TMP, but not in the absence of TMP.

Naïve PC12 cells were seeded onto collagen-coated dishes and transduced with a

lentiviral vector containing an IRES-overexpression construct to co-express DD-Akt(E40K) and GFP. After 4 days, the cultures were treated with 10 μM TMP, or NGF as a positive control, for 24 hours to induce DD-Akt(E40K) expression. Subsequently the cells were washed off the dishes, washed with serum-free medium, centrifuged to remove all medium, and replated with serum-free medium. After 16-24 hours of serum deprivation when approximately 50% of the cells have undergone apoptosis, the cells were then lysed to analyze survival through quantification of viable nuclei. Quantifications were normalized to cells treated with NGF as a positive control.

The results reveal a statistically significant protection effect of TMP-induced DD-Akt(E40K) with 92.4% ± 13.4% survival compared to 56.7% ± 1.8% survival in cultures transduced with an empty vector control and not treated with NGF or 60.7% ± 8.0% survival in cultures transduced by DD-Akt(E40K) but not induced by TMP treatment (Figure 4.2). Importantly, the level of protection by induced DD-Akt(E40K) was almost to equivalent to protection found with NGF-treated cells, indicating that DD-Akt(E40K) with TMP treatment is capable of protection against serum deprivation-induced apoptosis at levels comparable to a growth factor (Figure 4.2). The transduction efficiency across independent experiments was found to be approximately 60%, as determined through immunofluorescence staining of GFP-positive cells. Thus, if transduction efficiency had been 100%, one could potentially observe a survival rate even higher than that found with NGF treatment. Importantly, there was no additional protective effect found in cells expressing DD-Akt(E40K) but not treated with TMP, indicating that basal expression levels of the protein were not enough to promote survival in this model.

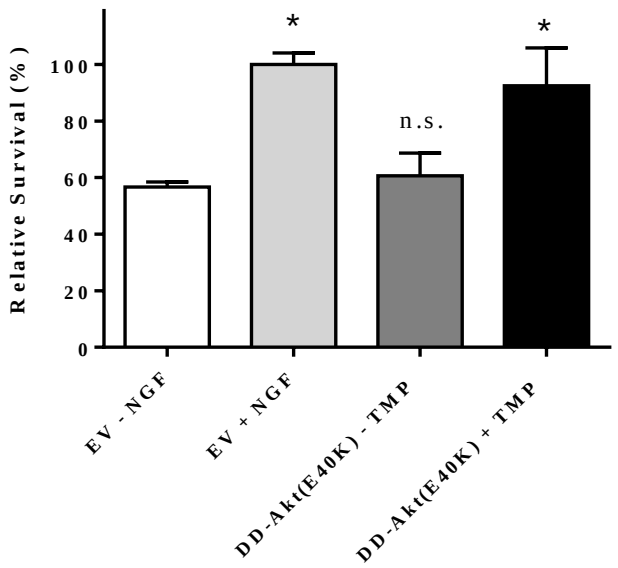


***Figure 4.2: DD-Akt(E40K) protects against serum deprivation***
Naïve PC12 cells were transduced with a lentiviral vector for overexpression of DD-Akt(E40K). Cultures were pre-treated with 10 μM TMP for 24 hours and then washed and replated with serum-free medium. After 16-24 hours of serum deprivation, cells were lysed for quantification of viable nuclei to measure survival. Average transduction efficiency was 60%. Graph shows means with SEM. *$p < 0.05$, n.s. vs. EV-NGF; 2-way ANOVA. N = 2-3 independent experiments.

### 4.2.3 DD-Akt(E40K) Inducibly Protects Neuronal PC12 Cells in PD Toxin Models

1-methyl-4-phenyl-1,2,3,6-tetrahydropyridine (MPTP) and 6-OHDA are neurotoxins that can cause selective degeneration of dopaminergic neurons when administered *in vivo*. MPTP itself is not toxic, but its lipophilic properties allow it to cross the blood brain barrier where it can subsequently be metabolized by glial cells into the toxic cation, 1-methyl-4-phenylpyridinium ($MPP^+$). Although the precise mechanism of action has been debated, both $MPP^+$ and 6-OHDA have been shown to be inhibitors of mitochondrial complex I and promote the formation of reactive oxygen species that lead to degeneration of catecholaminergic neurons [68]. The selectivity of the $MPP^+$ and 6-OHDA as well as the resulting mitochondrial dysfunction and oxidative stress that potentially mimic features of PD thus make these toxins useful in *in vivo* models that replicate certain features of classic Parkinsonism including degeneration of the nigrostriatal pathway and motor impairment [68]. Additionally, $MPP^+$ and 6-OHDA can induce degeneration of neuronal PC12 cells in culture, providing an *in vitro* model that is relevant to PD

[247, 248].

To determine whether DD-Akt(E40K) can inducibly protect neuronal PC12 cells against these PD mimetic toxin insults, we used a lentiviral vector to transduce cultures with an overexpression vector containing the DD-Akt(E40K) gene. Cultures were then pretreated with 10 μM TMP for 24 hours before adding varying concentrations of $MPP^+$ or 6-OHDA.

TMP-mediated induction of DD-Akt(E40K) was found to significantly protect neuronal PC12 cells against $MPP^+$ toxin insult with 87% ± 6.8% survival observed in TMP-treated cells compared to 62% ± 2.9% survival in cells expressing an empty vector control ($p \leq 0.01$, 2-way ANOVA) or 60% ± 2.1% in cells expressing DD-Akt(E40K) but not treated with TMP ($p \leq 0.01$, 2-way ANOVA) (Figure 4.3). No protection was observed when cultures were not treated with TMP, indicating that any basal expression of DD-Akt(E40K) was not enough to impact survival rates. The transduction efficiency for these cultures was found to be approximately 75%, as determined through immunofluorescence staining of GFP-positive cells. Thus, had transduction efficiency been 100%, the expected survival with TMP-induced DD-Akt(E40K) observed in the $MPP^+$ toxin model could potentially be 95%, an almost full rescue of toxin-induced death.

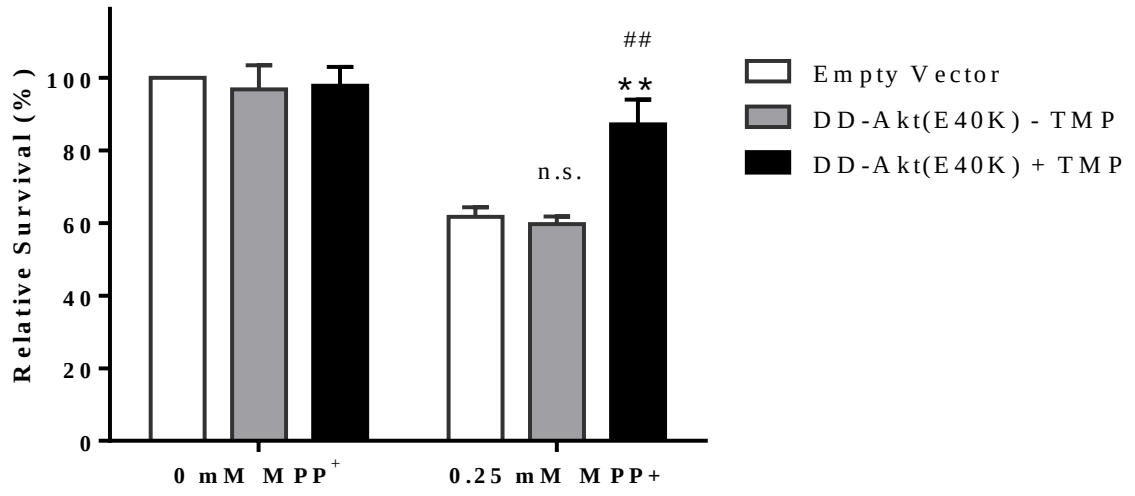


***Figure 4.3: DD-Akt(E40K) protects against MPP+***
Neuronal PC12 cells were transduced with a lentiviral vector for overexpression of DD-Akt(E40K). Cultures were pre-treated with 10 μM of TMP for 24 hours before the addition of 0.25 mM of $MPP^+$. After 18-24 hours of MPP+ treatment, cells were lysed for quantification of viable nuclei to measure survival. Graph shows means with SEM. **$p < 0.01$ vs. –TMP; ##$p < 0.01$ vs. EV; n.s. vs. EV; 2-way ANOVA. N = 3 independent experiments.

DD-Akt(E40K) was found to inducibly protect neuronal PC12 cells against 6-OHDA toxin as well (Figure 4.4). This protective effect was present even at higher (150 μM) doses of 6-OHDA with 74% ± 1.8% survival observed with TMP-induced DD-Akt(E40K) compared to 54% ± 4.7% in cultures with an empty vector control ($p \leq 0.001$, 2-way ANOVA) or 61% ± 4.9% in cultures expressing DD-Akt(E40K) but not stabilized with TMP ($p \leq 0.05$, 2-way ANOVA). The magnitude of protection was slightly lower than was observed at 100 μM 6-OHDA with 88% ± 5.4% survival in cells with induced DD-Akt(E40K) compared to 65% ± 3.1% in cells with an empty vector control ($p \leq 0.001$, 2-way ANOVA) or 66% ± 1.1% in cells with uninduced DD-Akt(E40K) ($p \leq 0.001$, 2-way ANOVA), but the proportional increase in survival with TMP-mediated induction of DD-Akt(E40K) was comparable at 35-37%. Again, it is important to note that our findings did not show any protective effect in conditions with DD-

Akt(E40K) expression but no TMP treatment, indicating that any basal expression that may be present in the cells was not enough to induce a physiological effect on survival. Although the transduction efficiency for these experiments was not directly determined, if we assume a similar efficiency of 75% as that observed in the $MPP^+$ experiments with the same culture type, the corrected survival with TMP-induced DD-Akt(E40K) becomes 96% at the lower dose of 6-OHDA and 81% at the higher dose of 6-OHDA.

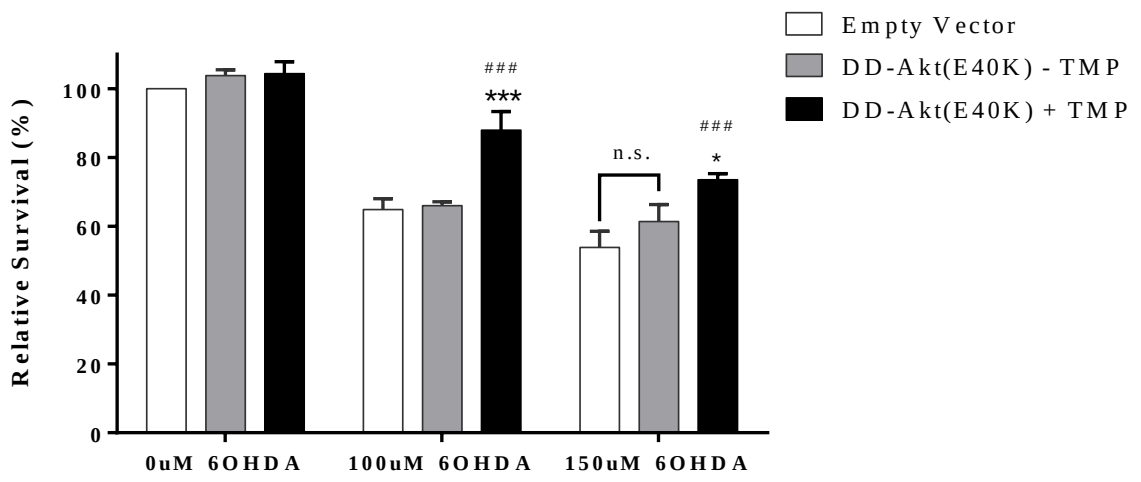


***Figure 4.4: DD-Akt(E40K) protects against 6-OHDA***
Neuronal PC12 cells were transduced with a lentiviral vector for overexpression of DD-Akt(E40K). Cultures were pre-treated with 10 μM TMP for 24 hours before the addition of 100 μM or 150 μM 6-OHDA. After 18-24 hours of 6-OHDA treatment, cells were lysed for quantification of viable nuclei to measure survival. Graph shows means with SEM. ***$p < 0.001$ vs. –TMP; *$p < 0.05$ vs. –TMP; ### $p < 0.001$ vs. Empty Vector; n.s. vs. Empty Vector; 2-way ANOVA. N = 3 independent experiments.

Importantly, treatment with TMP by itself was found to be insufficient for protection against 6-OHDA toxin insult (Figure 4.5). This finding confirms that any protective effect observed with DD-Akt(E40K) and TMP treatment is not due to any off-target effects of TMP, but rather the induction of active DD-Akt(E40K) within the cells.

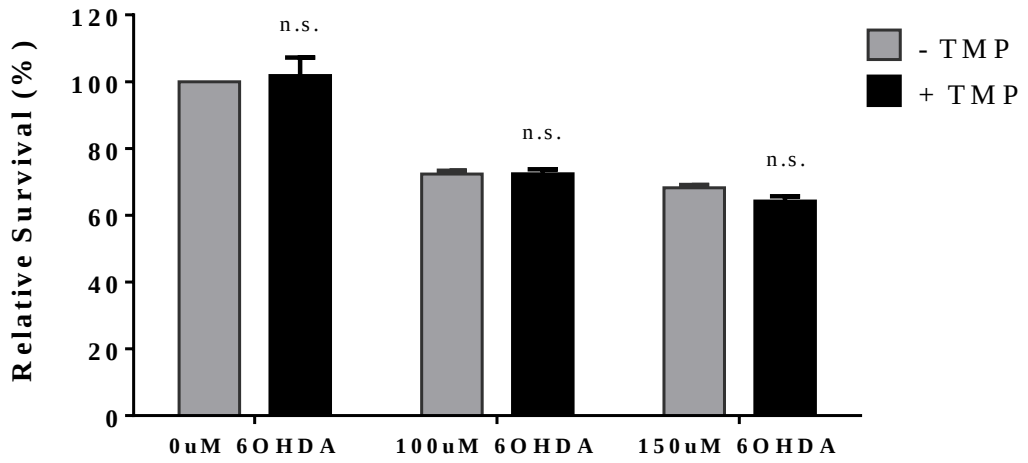


***Figure 4.5: TMP by itself is not protective against 6-OHDA***
Neuronal PC12 cells were pre-treated with 10 μM TMP for 24 hours before the addition of 100 μM or 150 μM 6-OHDA. After 18-24 hours of 6-OHDA treatment, cells were lysed for quantification of viable nuclei to measure survival. Graph is mean with SEM. No significance was found in comparison of any conditions, 2-way ANOVA. N = 2 independent experiments.

### 4.2.4 DD-Akt(E40K) Induction Persists With 6-OHDA Toxin Treatment

Suppression of Akt has been shown in various models of *in vitro* and *in vivo* PD as well as in the disease itself [138, 152, 162-164, 166]. Thus, it was important to determine whether DD-Akt(E40K) activation can persist in such PD models known to have dysfunctional Akt signaling. Neuronal PC12 cells were analyzed in a pilot experiment for protein expression of phosphorylated and total Akt under conditions of 6-OHDA treatment with DD-Akt(E40K) present (Figure 4.6). The protein levels indicate that DD-Akt(E40K) induction can indeed persist with the addition of 6-OHDA toxin, even at higher doses that can suppress endogenous Akt signaling. Furthermore, when compared to the average endogenous pAkt levels under control (no toxin) conditions, the levels of phosphorylated DD-Akt(E40K) at the threonine site (T308) when induced with TMP exceeded endogenous pAkt308 levels in control conditions (no toxin) by approximately 95% and remained approximately 35% higher than endogenous pAkt308 levels

even when treated with the higher dose of 6-OHDA (Figure 4.7). This result is consistent with the protective effects observed in the survival assays (Figure 4.4). The levels of phosphorylated DD-Akt(E40K) at the serine site (S473) appeared to be more suppressed by 100 µM 6-OHDA toxin treatment and reached approximately 55% of control endogenous pAkt473 expression levels with induction by TMP in toxin conditions, although there was clear induction of active DD-Akt(E40K).

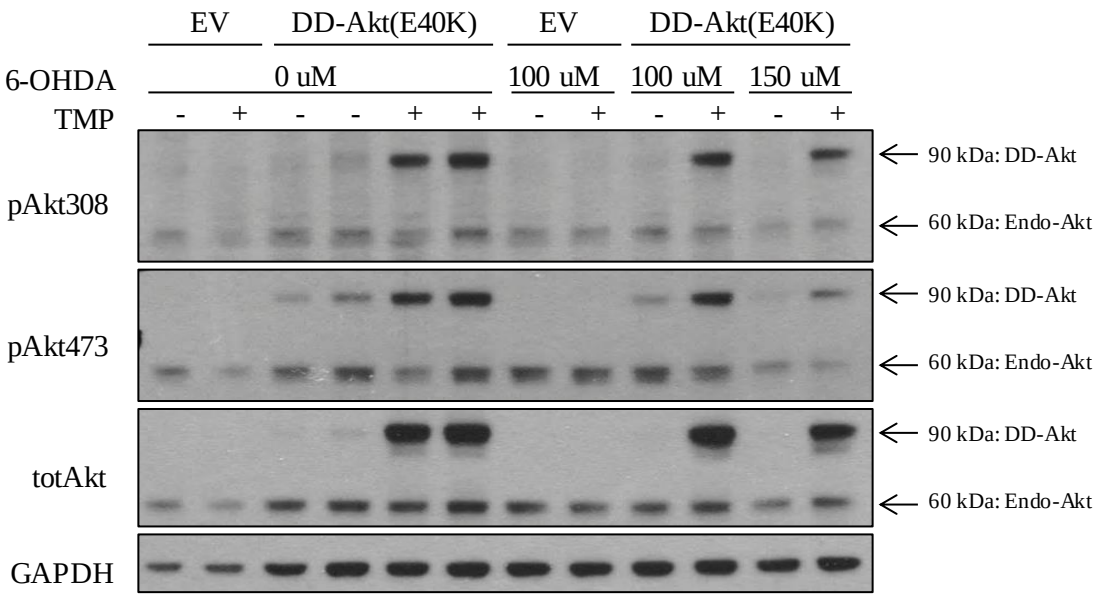


***Figure 4.6: DD-Akt(E40K) signaling persists in the presence of 6-OHDA***
Neuronal PC12 cells were transduced with a lentiviral vector for overexpression of DD-Akt(E40K). Cultures were pre-treated with 10 µM TMP for 24 hours before the addition of 100 µM or 150 µM 6-OHDA. After 8 hours of 6-OHDA treatment, cells were lysed for protein immunoblotting analysis. "DD-Akt" indicates protein bands for DD-Akt(E40K) and "Endo-Akt" indicates protein bands for endogenous Akt.

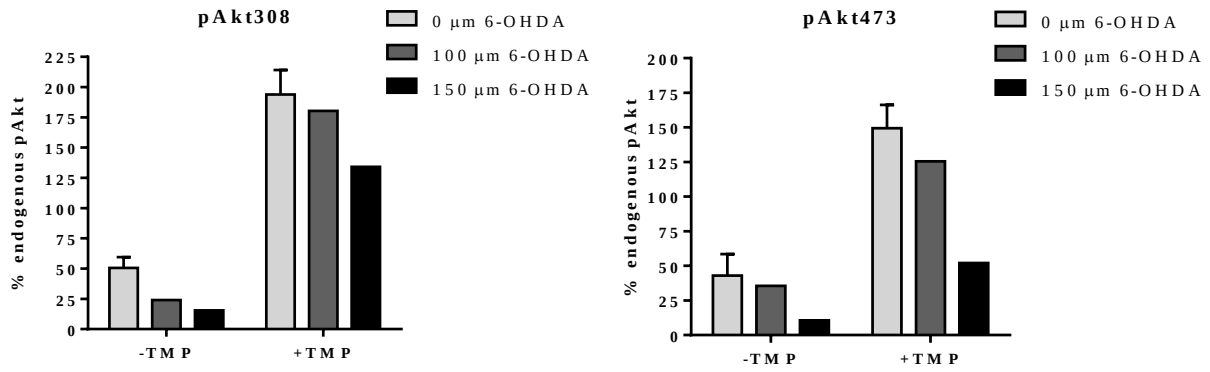


***Figure 4.7: DD-Akt(E40K) retains activity in the presence of 6-OHDA***
Neuronal PC12 cells were transduced with a lentiviral vector for overexpression of DD-Akt(E40K). Cultures were pre-treated with 10 µM of TMP for 24 hours before the addition of 100 µM or 150 µM 6-OHDA. After 8 hours of 6-OHDA treatment, cells were lysed for protein immunoblotting analysis. Densitometry analysis of the blot from Figure 4.6 is shown here. (A) pAkt308 protein levels and (B) pAkt473 protein levels were normalized to GAPDH as a loading control and calculated as a proportion to average endogenous pAkt levels under control (no toxin) conditions.

## 4.3: Discussion

Previous studies have established Akt signaling as a potential therapeutic target for Parkinson's disease due to its neuroprotective and neurorestorative features [138, 139]. However, precisely due to Akt's promotion of cell growth, survival, and proliferation, a constitutively active form of Akt is not a viable therapeutic tool because it can promote cancer and potentially promote extraneous sprouting of neuronal projections. Therefore, Akt as a therapeutic intervention must be one in which the activity can be controlled, ideally with a drug. We have for the first time to our knowledge, demonstrated that an inducible form of Akt can exhibit neuroprotective effects that are controllable through a commonly used antibiotic, TMP, within Akt-deficient models and *in vitro* PD models.

Importantly, our findings demonstrate that DD-Akt(E40K) is indeed catalytically active and able to phosphorylate a known Akt substrate, FoxO4, as a potential mediator of the

neuroprotective effects observed with DD-Akt(E40K) induction. As always, one must keep in mind the less than 100% transfection efficiency achieved, which implies that increases in phosphorylated FoxO4 we observed may be even higher. Importantly, our results demonstrate that there was no significant enhancement of phosphorylated FoxO4 without TMP (Figure 4.1). With the observed maintenance of active DD-Akt(E40K) levels in the cell during insult with a PD mimetic toxin, as shown in Figure 4.6, and the findings that phosphorylation of FoxO4 increase with induction of DD-Akt(E40K) in Figure 4.1, we believe that phosphorylation and subsequent cytosolic sequestration of FoxO4 may be involved as an effector of the protective effect observed in the cell death models presented in this chapter. It is also likely that other known Akt substrates may be involved, particularly those known to be part of the apoptotic pathway, such as BAD, BIM, and other FoxO proteins including FoxO3A. However, perhaps due to lack of 100% transfection efficiency, we were not able to detect reliable increases in phosphorylation of other signaling proteins downstream of Akt, including GSK3β, PRAS40, FoxO1, FoxO3a, and p70S6K (data not shown).

The serum deprivation model is a relatively straightforward model of apoptosis induced by removal of growth factor and therefore deficient PI3K/Akt signaling. Thus, it was anticipated that the induction of DD-Akt(E40K) would result in full protection against cell death in this model. Importantly, the degree of protection observed with induced DD-Akt(E40K) was similar to that of protection by NGF. In other words, the protective effect by active DD-Akt(E40K) is approximately equivalent to the protective effect by trophic factors, which would presumably constitute the “best” potential result in rescue of survival in a serum deprivation model. If one were to take the incomplete transduction efficiency into consideration, it is possible that induction of DD-Akt(E40K) could potentially protect cells to a higher degree than NGF.

However, due to right endogenous regulation of the PI3K/Akt signaling pathway activity, there may potentially be a cap on the level of protection observed with Akt overactivity.

Our findings further demonstrate that DD-Akt(E40K) can inducibly protect neuronal PC12 cells in PD toxin models of $MPP^+$ and 6-OHDA, with lower levels of surviving cells observed with increases doses of toxin, as demonstrated with 6-OHDA (Figure 4.3, Figure 4.4). In addition, we found that the proportional increase in survival against 6-OHDA with TMP-induced DD-Akt(E40K) was comparable at approximately 35-37% regardless of the dose of the toxin insult. Importantly, we have demonstrated that the increase in survival is not due to non-specific effects of TMP treatment (Figure 4.5), strengthening our conclusion that survival effects are dependent on DD-Akt(E40K) activity within cultures. For future work, it would be interesting to see whether this neuroprotective effect can be corroborated in non-toxin PD models, such as models of α-synuclein fibrils [32].

As mentioned previously, in all survival experiments presented here, the cultures were not transduced completely, which introduces the potential increased survival rates if corrected for transduction efficiency. This increase in survival rate can be estimated if one calculates the difference in survival between empty vector control (non-toxin) conditions and DD-Akt(E40K) + TMP conditions as a proportion of "available survival" and corrects based on known transduction efficiencies. By these corrections, 100% transduction efficiencies in neuronal PC12 cells would translate to almost full protection at approximately 95% total survival achieved by TMP-induced DD-Akt(E40K) against $MPP^+$-induced cell death as well as against the lower dose of 6-OHDA. It is also important to note that this estimate does not take into account the differences in level of protein expression within each cell, which is not reflected in the measurement of transduction efficiency. Thus, it is conceivable that full protection with

induction of DD-Akt(E40K) is possible in these cell death models with a higher viral titer that allows for increase in both proportion of cells transduced as well as protein load per cell.

Previous investigation has demonstrated the dephosphorylation of Akt following treatment with 6-OHDA [152]. Our findings corroborate the previous results and additionally show that DD-Akt(E40K) activity can persist despite the suppression of endogenous Akt phosphorylation by 6-OHDA (Figure 4.6). Further observation suggests that the Ser473 phosphorylation site may be more affected by the toxin than the Thr308 site, as the increasing dose of 6-OHDA leads to more dephosphorylation of the Ser473 site than Thr308 site. This is consistent with and reflective of the PI3K inhibitor experiments in Chapter 3 in which we observed that PI3K inhibition suppressed DD-Akt(E40K) phosphorylation with TMP treatment to 45% that of endogenous control levels at the Ser473 site, in contrast to 67% at the Thr308 site. Although the general mechanisms of activation of Akt by PDK1 and mTORC2 are well established, the detailed interplay between the two activators and phosphorylation sites is still poorly understood. Our findings indicate that there is a distinction in the behavior of the canonical Akt phosphorylation sites in response to cellular stressors. However, the significance of this observation is unclear and may merit further study and discussion.

Finally, our data presented in this chapter reveal that basal levels of DD-Akt(E40K) without TMP, which were observed in the findings described in Chapter 3, are not enough to increase phosphorylation of a known substrate (FoxO4), and as a result do not enhance the biological effects of Akt activity on survival. This is an important finding that supports the potential of this inducible system for clinical usage as its basal activity is not enough to induce any physiological outcomes of Akt signaling.

The findings presented in this chapter demonstrate the utility of this inducible Akt system

for signaling studies and as a proof of principle for Akt-based therapeutic strategies in pathological conditions, specifically within PD. Although the toxin models of PD do not perfectly replicate all characteristics of the disease, suppression of endogenous Akt signaling has been observed in various PD genetic models as well as post-mortem sporadic PD human brains [152]. Our results replicate this suppressive effect of Akt signaling using the PD-mimetic toxin 6-OHDA (Figure 4.6) and further demonstrate that the induction of DD-Akt(E40K) can reverse the total levels of active Akt enough to promote survival in PD toxin models. An interesting next step would be to test the protective effect of DD-Akt(E40K) in non-toxin models of PD. One model in particular that has come into the field as potentially relevant to disease pathology and progression is the α-synuclein fibril model [32-34]. This method would provide a robust non-toxin PD model to test the use of inducible Akt as a protective agent in Parkinson's disease.

# Chapter 5: DD-Akt(E40K) *In Vivo*

## 5.1: Introduction

As discussed in Chapter 1, PD is a neurodegenerative disease that is characterized by motor deficits associated with degeneration of dopaminergic neurons in a very specific subregion of the basal ganglia, called the substantia nigra pars compacta (SNpc). Thus, an ideal therapeutic strategy to treat PD would be targeted towards this subset of neurons. In Chapter 3, we demonstrated the trimethoprim (TMP)-mediated inducibility of DD-Akt(E40K) in various cell culture systems, including dopaminergic neurons. The regulation of DD-Akt(E40K) was found to be dose responsive to the administration of TMP and reversible with the removal of TMP from the medium. In Chapter 4, we demonstrated the physiological relevance and applicability of the DD-Akt(E40K) system as an inducible neuroprotective strategy in PD. Our findings established the capability of DD-Akt(E40K) to inducibly protect neuronal PC12 cells against PD mimetic toxin insults in culture and potentially achieves this through phosphorylation of the substrate, FoxO4. To further validate the DD-Akt(E40K) as a controllable protein expression system with potential applications as a PD therapy, we sought to test the regulatable expression of DD-Akt(E40K) *in vivo.*

We chose the adeno-associated virus (AAV) serotype 1 to deliver the DD-Akt(E40K) expression vector to the SNpc of mice for a variety of reasons. First, AAV vectors exhibit a strong preference for neuronal transduction with AAV1 in particular exhibiting significantly more efficient transduction of the primate SN compared to other serotypes [249, 250]. Second, AAV vectors support long-lasting transgene expression with even a single delivery [249]. Third, AAV vectors show no pathogenicity and have been used to safely deliver genetic material in clinical trials of neurturin and human aromatic L-amino acid decarboxylase (hAADC) [187, 189,

251]. Finally, Dr. Robert Burke, with whom we collaborated to perform these *in vivo* experiments, has extensive experience in utilizing AAV1 to deliver myristoylated Akt or constitutively-active Rheb to the SNpc of mouse models, often in the context of Parkinson's disease [138-140, 142, 174, 252, 253].

Our choice of TMP dosing and treatment paradigm was based on previously published literature utilizing the DHFR-derived DD system with TMP to inducibly express various proteins (YFP, GDNF) in the rat striatum. In all cases, TMP was administered orally, within the drinking water of the animals, for a 3-week period before beginning experimental procedures [191, 211, 212]. Additionally, these groups demonstrated successful induction of DD-fusion proteins within the rat striatum with TMP doses ranging from 0.1-0.5 mg/ml. We chose a 1.0 mg/ml dose of TMP that exceeded the doses used by these groups to better ensure that TMP would be present in high enough concentrations to regulate DD-Akt(E40K), as supported by the literature.

In this chapter, we investigate the inducibility and behavior of DD-Akt(E40K) *in vivo* within the mouse SNpc. With the supporting literature of DHFR-derived DD systems within rodent brains, we anticipated that oral TMP administration would induce expression of DD-Akt(E40K) within the mouse SNpc. Furthermore, we anticipated similar physiological effects to that observed with overexpression of myristoylated-Akt, including trophic effects on cell size and protection of dopaminergic neurons and axonal projections against PD mimetic toxin insults [138]. The findings presented here demonstrate a surprising lack of DD-Akt(E40K) inducibility in the SNpc, but significant TMP-mediated induction within the striatum, suggesting regional variability of the DD system efficacy. Additionally, our data corroborate reported trophic effects of active Akt within dopaminergic neurons of the mouse SNpc.

## 5.2: Results

### 5.2.1 Validating DD-Akt(E40K)-Flag *In Vitro*

The construct we created for packaging into an AAV vector was additionally Flag-tagged at the 3' end of the expression construct to allow for easy detection of the fusion protein if expressed within the SNpc of mice. Although DD-Akt(E40K) already contained an HA tag, the protocol for detecting Flag through immunohistochemistry had previously been validated and established by our collaborator, Dr. Robert Burke [138]. Thus, we chose to utilize a Flag-tagged version of DD-Akt(E40K) for our *in vivo* experiments.

To verify that the addition of the Flag tag does not interfere with the inducibility of DD-Akt(E40K), we tested the TMP-mediated induction of Flag-tagged DD-Akt(E40K), denoted as "DD-Akt(E40K)-Flag", along with non-Flag-tagged DD-Akt(E40K) *in vitro* in HEK293 cells. The two constructs were tested concurrently following the same experimental protocol as described for induction experiments in Chapter 3. Briefly, HEK293 cells were transiently transfected and treated with 10 µM TMP for 24 hours before isolating protein samples for immunoblotting. Samples were analyzed for pAkt473 expression, normalized to ERK for loading, and compared across conditions to identify any potential differences in induction with the addition of a C-terminal Flag tag (Figure 5.1). The results indicate no statistically significant difference with Flag addition in the basal levels of DD-Akt(E40K) when untreated with TMP or induced levels when treated with TMP. This finding thus demonstrates that the addition of a Flag tag did not affect the fusion protein behavior with regards to its inducibility or basal expression levels.

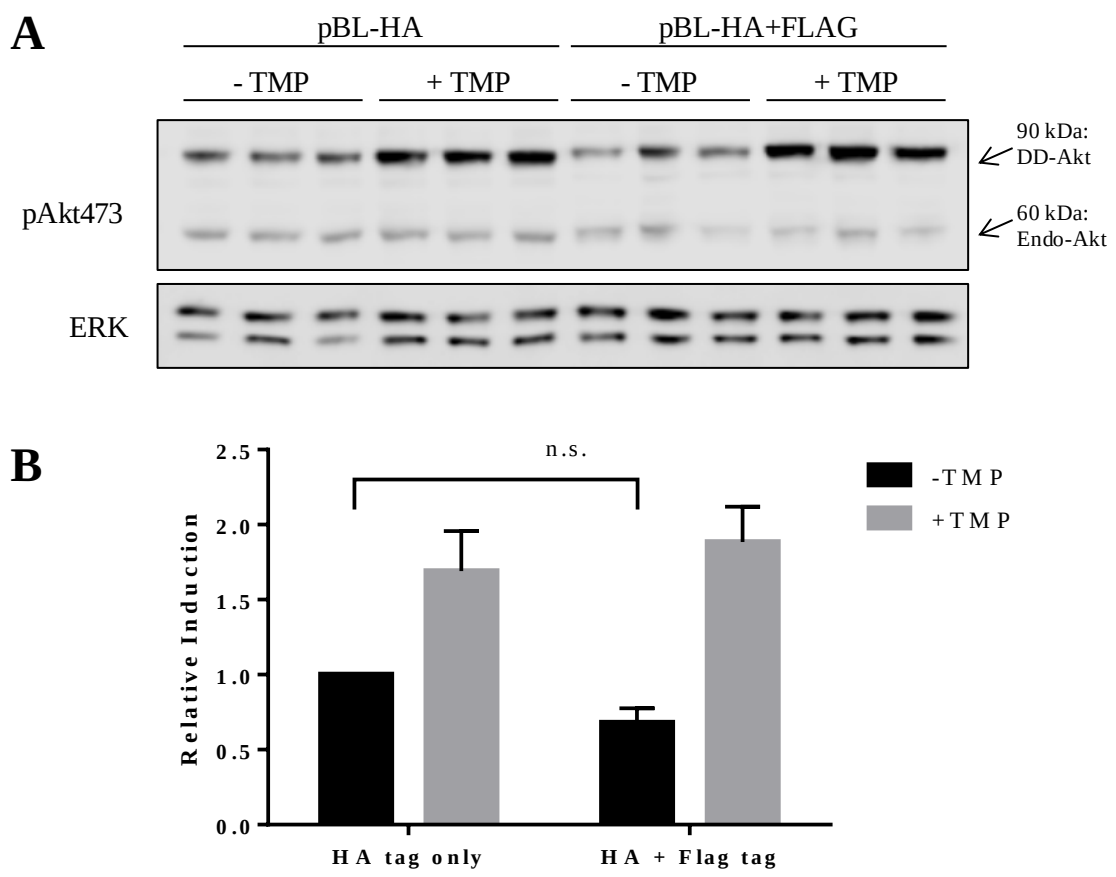


***Figure 5.1: Addition of Flag tag does not affect inducibility of DD-Akt(E40K)***
DD-Akt(E40K) with only an HA tag (as used in all *in vitro* experiments) and with an additional Flag tag at the 3' end of the expression construct was cloned into a pBL vector. Constructs were transiently transfected into HEK293 cells and treated with 10 µM TMP for 24 hours. Protein samples were processed for immunoblotting and levels of pAkt473 were quantified, normalized to ERK for loading, and normalized to levels in cells transfected with the HA only-tagged DD-Akt(E40K) – TMP. Graph shows means with SEM. N=3 independent experiments, each with 2-3 replicates per condition. N.s. vs HA only-tagged DD-Akt(E40K) – TMP determined by 2-way ANOVA with multiple comparisons.

### 5.2.2 Measuring DD-Akt(E40K)-Flag Induction *In Vivo*

Once we validated that the addition of the Flag tag at the C-terminus of DD-Akt(E40K) did not affect its inducibility, we wanted to determine whether DD-Akt(E40K)-Flag can be controlled in the mouse SNpc by oral TMP administration.

Because the treatment protocol requires TMP to be delivered through the drinking water

of mice, solubility in water was an important criterion for the antibiotic. However, the TMP compound used in our *in vitro* studies has low solubility in water. Therefore, we chose to use a TMP-lactate salt form of the antibiotic (purchased from ChemImpex International, Inc, catalog # CI-03552-5G), which is soluble in water up to 20 mg/ml. Before beginning the *in vivo* studies, we aimed to verify that TMP-lactate works as intended and induces DD-Akt(E40K) as TMP does. To test this compound, HEK293 cells were transiently transfected DD-Akt(E40K) and treated with either TMP or TMP-lactate, both at an equivalent dose of 10 µM TMP, for 24 hours. When levels of pAkt473 were quantified, the data showed that TMP-lactate was able to induce DD-Akt(E40K) to comparable levels as TMP used in previous *in vitro* studies as described in Chapter 3 and 4 (Figure 5.2).

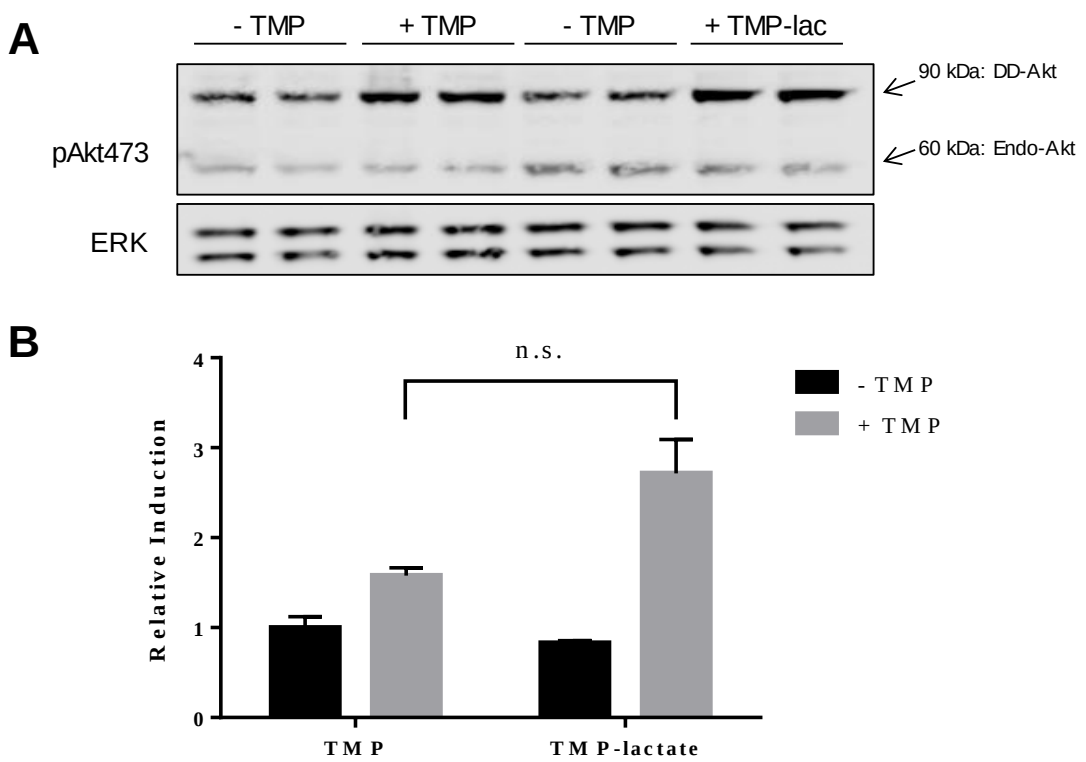


***Figure 5.2: TMP-lactate induces DD-Akt(E40K)***
HEK293 cells were transfected with DD-Akt(E40K) and treated with 10 µM TMP or TMP-lactate for 24 hours. Protein samples were collected for immunoblot analysis and quantified for pAkt473, normalized to ERK for loading. Graph shows means with SEM, N=2 samples per condition. N.s. determined by 2-way ANOVA.

Once TMP-lactate was verified to work in an equivalent manner to TMP, we sought to test the construct *in vivo*, in the SNpc of mice. To do this, AAV1-DD-Akt(E40K)-Flag was delivered unilaterally to the substantia nigra of adult (8 week) male C57BL/6 mice. TMP treatment began at 3 weeks post-injection to allow for expression of the transgene delivered by AAV. The injected mice were given 1 mg/ml TMP in the drinking water, or maintained on untreated water as a control, for 3 weeks and then processed for staining of Flag-tagged proteins (Figure 5.3). As mentioned in Section 5.1, the length and dosing of TMP was based previous literature describing the control of DD-fusion proteins in the striatum of rats using a dose range of 0.1-0.5 mg/ml TMP for 3 weeks, administered through the drinking water [191, 211, 212].

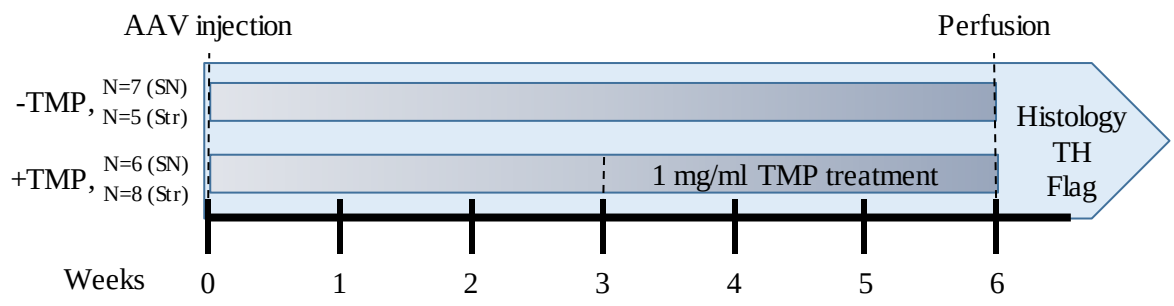


***Figure 5.3: Treatment timeline for in vivo induction experiments***

Nigral sections of injected mice were stained for Flag expression as a direct readout of DD-Akt(E40K)-Flag expression. A complete set of serial sections was cut through the substantia nigra and every fourth section was processed for staining of Flag. Stained sections were subsequently analyzed stereologically in a blinded manner to determine the number of total Flag-positive neurons within the SNpc as a measure of DD-Akt(E40K)-Flag expression. Surprisingly, there was no visibly observable difference in numbers of Flag-stained neurons or intensity of staining in the substantia nigra of mice with or without TMP treatment through visible

observation (Figure 5.4). However, though visible observation, we suspected that there might be a distinction in localization of staining between the treatment groups. Thus, we quantified the number of SNpc neurons with nuclear, cytoplasmic, or both nuclear and cytoplasmic localization of Flag staining as a readout of DD-Akt(E40K)-Flag induction using stereological methods (see Figure 5.4 for examples of each). Counts were done in a blinded manner, such that the treatment group of the mouse was not known until after counts had been completed.

When the nigral sections were quantified in this manner, there was no statistically significant difference in the quantity of Flag-positive neurons between the treatment groups, regardless of staining localization (Figure 5.5). As a result, when total counts were compiled, there was again no statistically significant difference in number of Flag-positive neurons between treatment groups (Figure 5.6). These results indicate that DD-Akt(E40K)-Flag is not controllable by oral administration of TMP in the SNpc of mice, which is discussed further in Section 5.3.

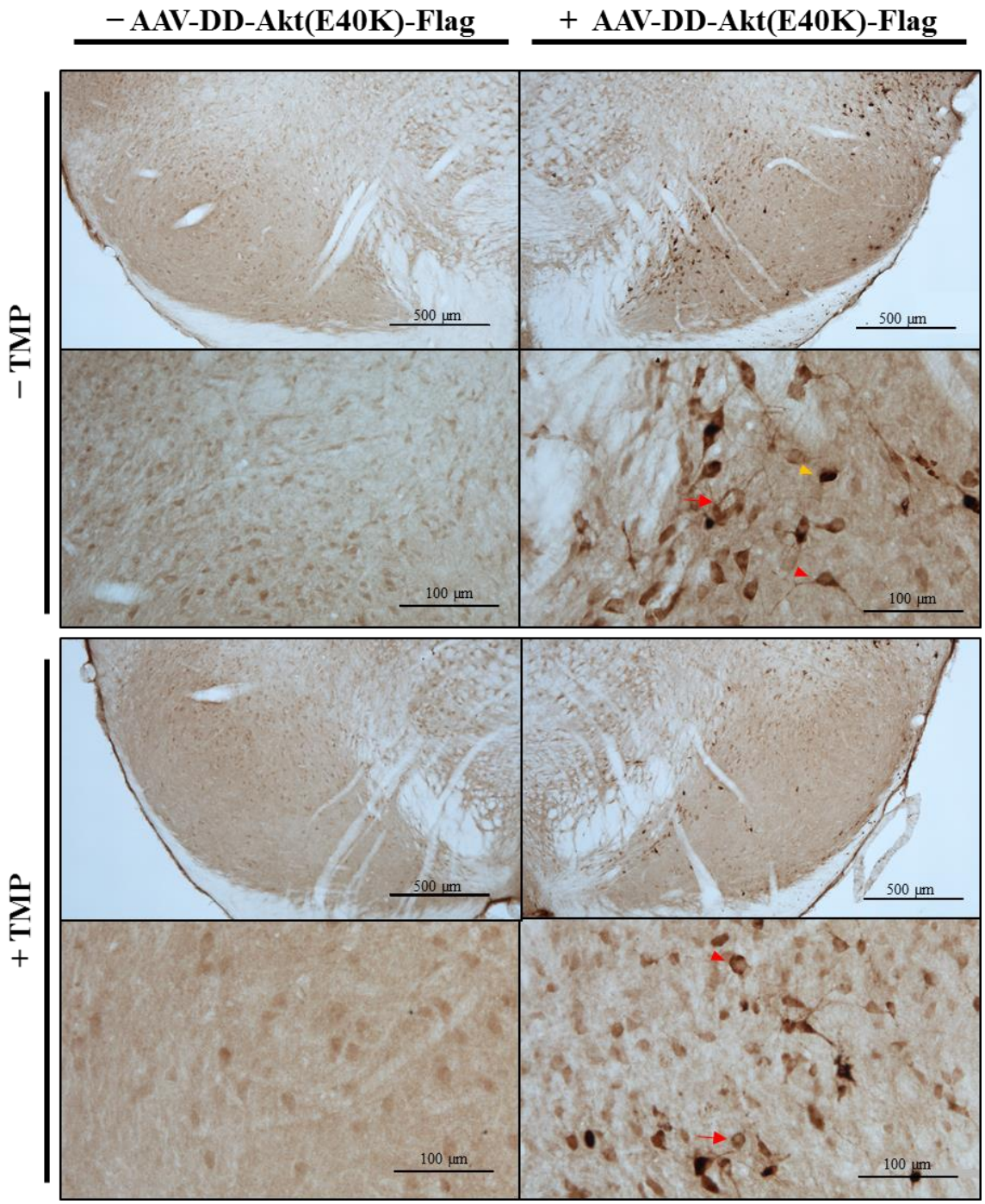


***Figure 5.4: DD-Akt(E40K)-Flag is expressed in SNpc of mice***

Adult C57BL/6 mice were treated with a unilateral AAV-DD-Akt(E40K)-Flag injection into the SNpc. At 3 weeks post-viral injection, mice were treated with 1 mg/ml TMP in their drinking water for 3 weeks and processed for staining of Flag. Representative images of Flag stained neurons in the SNpc of both non TMP-treated and TMP-treated mice are shown above. Red arrows indicate examples of cytoplasmic staining; red arrowheads indicate examples of both cytoplasmic and nuclear staining; orange arrowhead indicates nuclear staining.

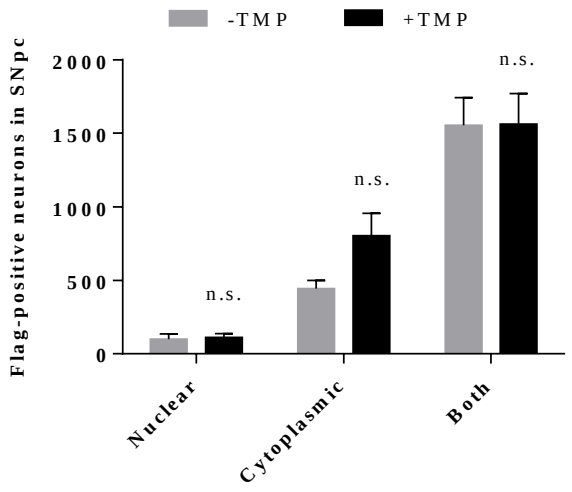


***Figure 5.5: Flag-positive neurons in the SNpc of non TMP-treated and TMP-treated mice***
AAV-DD-Akt(E40K)-Flag injected mice were divided into control and experimental groups, with the control group being given normal drinking water and the experimental group being given TMP-treated drinking water for 3 weeks. The SNpc was then sectioned and processed for stereological quantification of Flag-stained neurons, categorizing staining pattern by nuclear, cytoplasmic, or both. Graph is mean with SEM. N=7 mice for -TMP, N=6 mice for +TMP. N.s. vs. –TMP; 2-way ANOVA with multiple comparisons.

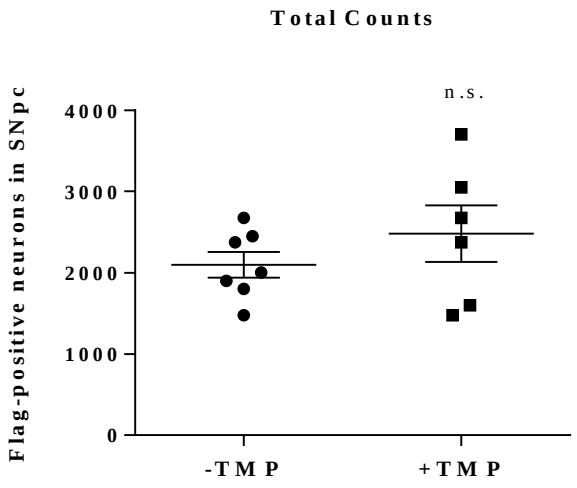


***Figure 5.6: DD-Akt(E40K)-Flag shows no induction by TMP in the SNpc of mice***
AAV-DD-Akt(E40K)-Flag injected mice were divided into control and experimental groups, with the control group being given normal drinking water and the experimental group being given TMP-treated drinking water for 3 weeks. The SNpc was then sectioned and processed for stereological quantification of Flag-stained neurons. The data represents total Flag-positive neurons in the SNpc per mouse. Graph is mean with SEM. N=7 mice for -TMP, N=6 mice for +TMP. N.s. determined by unpaired t-test.

This unexpected result contrasted with previous published studies demonstrating efficient control of the DD fusion protein in rodent brain by oral TMP administration [191, 211-213]. However, all of these studies involved expression of a DD fusion protein within the striatum rather than the substantia nigra, thus introducing the possibility of a region-dependent effect on the efficient degradation and induction of DD fusion proteins. To explore this possibility further,

we performed unilateral injections of AAV1-DD-Akt(E40K)-Flag into the striatum of adult (8 week) male C57BL/6 mice, following the same TMP treatment protocol of 1 mg/ml administered in the drinking water for 3 weeks (Figure 5.3). After 3 weeks of TMP-supplemented water, or non-treated water for the control group, the striatum was processed for Flag staining by collecting a complete set of serial sections and staining every sixth section for Flag.

Interestingly, the striatal sections of these mice appeared to have differences in Flag staining pattern that correlated with TMP treatment (Figure 5.7). Although both treatment groups exhibited Flag-positive neurons, indicating that DD-Akt(E40K)-Flag was expressed, the staining in non TMP-treated mice appeared to be limited to the needle tract and along the external capsule of the striatum. In contrast, Flag staining in TMP-treated mice appeared to be more diffuse along the needle tract in all mice and show a distinct area of staining in the medial striatum in four out of seven mice, neither of which was present in non TMP-treated mice (Figure 5.7). The peculiar staining pattern closer to the external capsule may be a result of viral diffusion through less dense tissue along the white matter fiber tracts. The staining within the medial striatum that only appears with TMP treatment may be a reflection of a lower concentration of virus farther away from the injection site, leading to less intense expression of DD-Akt(E40K)-Flag and decreased basal levels of protein off-TMP enough such that it is below detection threshold.

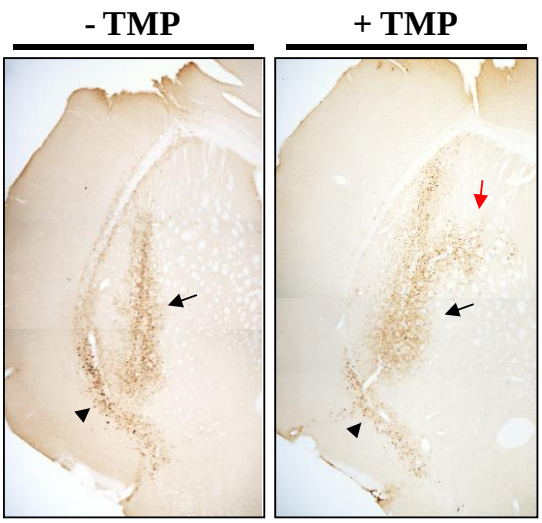


***Figure 5.7: DD-Akt(E40K)-Flag staining in the striatum of mice***
Adult C57BL/6 mice were treated with a unilateral AAV-DD-Akt(E40K)-Flag injection into the striatum. At 3 weeks post-viral injection, mice were treated with 1 mg/ml TMP in their drinking water for 3 weeks and processed for staining of Flag. Representative images of Flag staining in the striatum of both non TMP-treated and TMP-treated mice are shown to the left. Red arrows indicate staining in the medial striatum; black arrowheads indicate external capsule staining; black arrows indicate staining proximal to the needle track.

To determine the number of total Flag-positive neurons within the striatum. A complete set of serial sections was cut through the striatum and processed for Flag staining at every sixth section. These sections were subsequently analyzed stereologically in a blinded manner to determine the number of total Flag-positive cells within the striatum across non-TMP treated and TMP treated groups (Figure 5.8). We found a statistically significant difference between treatment groups with non-TMP treated mice exhibiting an average of 13,238 ± 2602 Flag-stained neurons and TMP-treated mice exhibiting an average of 24,009 ± 2984 Flag-stained neurons (*$p = 0.03$, Figure 5.8), indicating that DD-Akt(E40K)-Flag is controllable by oral TMP administration in the striatum of mice. The average induction of DD-Akt(E40K)-Flag, as measured by the proportional increase in number of Flag-stained neurons in TMP-treated mice compared to non TMP-treated mice, was 80%, or 1.8-fold. These results suggest a number of important points: 1) Oral TMP administration, as used in our protocol, is capable of inducing DD-Akt(E40K)-Flag, as has been demonstrated by other groups using other DD-fusion proteins, 2) There is a region-specific sensitivity in the inducibility of DD-Akt(E40K)-Flag, as indicated

by the contrasting results from DD-Akt(E40K)-Flag induction in the SNpc compared to the striatum, 3) The efficient control of DD-Akt(E40K)-Flag in the SNpc is lacking either due to high background expression off TMP treatment, small induction of stability with TMP treatment, or some combination of the two. These points will be explored further in the discussion in Section 5.3.

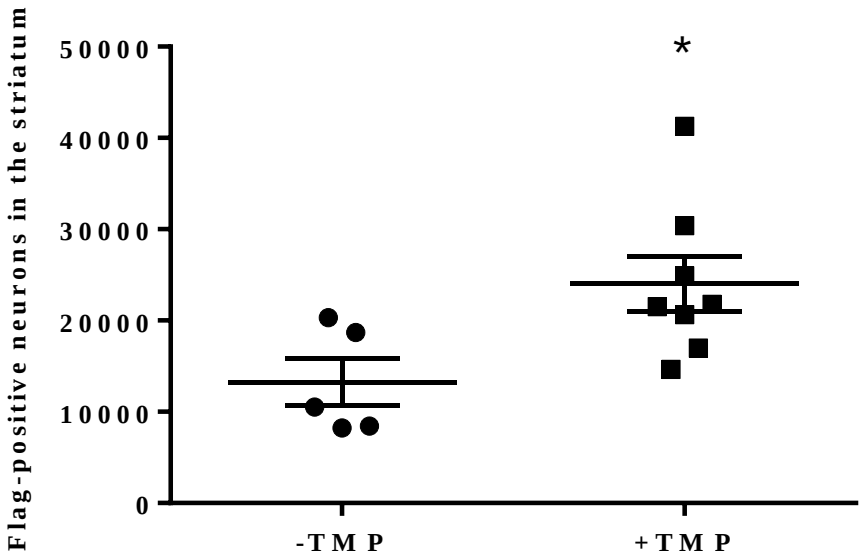


| | | | |
|---|---|---|---|
| **Mean** | 13,238 | 24,009 | **Induction** |
| **SEM** | 2602 | 2984 | 1.8 |

***Figure 5.8: DD-Akt(E40K)-Flag is induced by TMP treatment in the striatum of mice*** AAV-DD-Akt(E40K)-Flag was injected unilaterally into the striatum of adult C57BL/6 mice and given non-treated water or 1 mg/ml TMP-treated water for 3 weeks. Every sixth section of a complete set were stained for Flag and analyzed stereologically to determine the total number of Flag-stained cells within the whole striatum per mouse. Graph shows means with SEM. N=5 mice for –TMP, N=8 mice for +TMP. *p = 0.03, unpaired t-test.

### 5.2.3 DD-Akt(E40K)-Flag has Trophic Effects *In Vivo*

Previous work from the Burke laboratory has demonstrated a clear trophic effect of virally expressed myristoylated Akt on neurons of the SNpc [138]. This is in accordance with

reported downstream functions of Akt signaling mediating cellular growth [117]. However, the constitutively active Akt(E40K) mutant has not previously been studied for neurotrophic effects *in vivo*. Demonstration of this would serve three main purposes: 1) Validation of the mutant Akt(E40K) to mimic known downstream physiological effects of Akt signaling *in vivo* in a neuronal context, 2) Proof of principle to show that DD-Akt(E40K)-Flag retains the ability to activate signaling pathways *in vivo* that lead to known Akt cellular effects, and 3) Additional evidence that DD-Akt(E40K)-Flag is not inducible by TMP treatment in the SNpc of mice.

Here, we have unilaterally delivered Akt(E40K)-Flag to the SNpc of adult (8 week) C57BL/6 mice using AAV1. At 10 weeks post-injection, the SNpc were processed for TH expression to identify dopaminergic neurons and determine the trophic effects, if any, of Akt(E40K) signaling on dopaminergic neurons in the SNpc. Through visible observation, a clear and observable increase in average dopaminergic neuronal body size, as measured by area, was seen in addition to a thickening of neurites and increase in density of TH-stained neuropil surrounding the SNpc neurons (Figure 5.9).

The average cell body size was quantified for both control (non-injected) and experimental (injected with AAV1-Akt(E40K)) hemispheres, through a systematic method to randomly choose stained neurons within the region of interest across representative caudal, medial, and rostral sections of the SNpc. When the neuronal cell size was quantified as such, the average area of the neuronal cell body within the injected SNpc was found to be greater than 2-fold that of the control side, with the average area in the Akt(E40K)-injected hemisphere being $411 \pm 13\ \mu m^2$ and the average area in the control hemisphere being $201 \pm 5\ \mu m^2$ (Figure 5.10). This difference in neuronal cell size was found to be statistically significant ($p \leq 0.0001$, unpaired t-test).

The data also demonstrates a clear difference between neuronal cell sizes of the Akt(E40K) injected and uninjected hemispheres when presented as a frequency distribution of all measured neurons based on size (Figure 5.11). We see a clear shift in the distribution of dopaminergic neuronal cell body areas to the right when injected with AAV-Akt(E40K)-Flag, with the smallest measured TH-positive neuron from the injected hemisphere having an area approximately 11% larger than the smallest measured TH-positive neuron from the non-injected hemisphere. These results clearly demonstrate that Akt(E40K) is capable of inducing a trophic effect on neuron size within the SNpc, as would be expected from reported functions of Akt and our collaborator Dr. Robert Burke's work with myristoylated Akt [138].

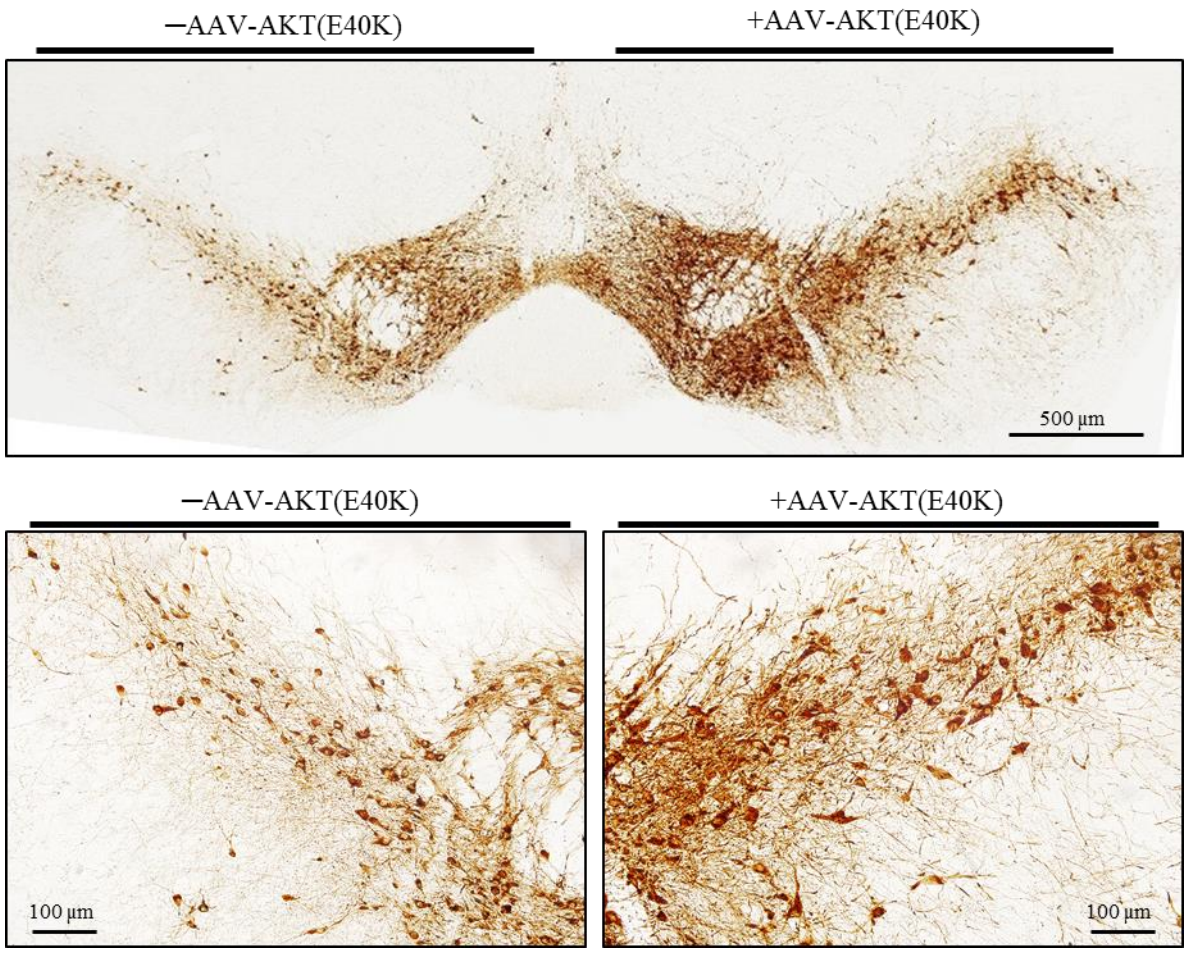


***Figure 5.9: Akt(E40K) has trophic effects on TH+ neurons in the SNpc***
AAV-Akt(E40K)-Flag with no DD domain was unilaterally injected into the SNpc of mice and processed 10 weeks post-injection for TH expression. Representative images are shown above.

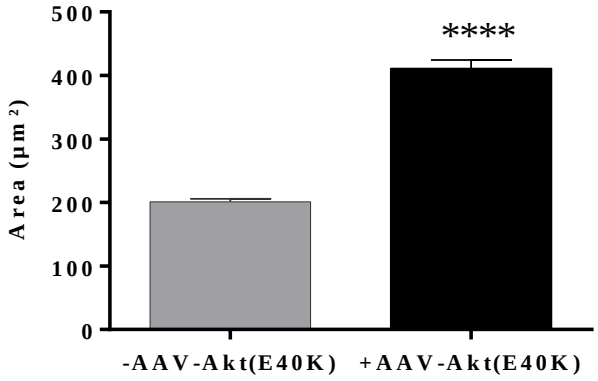


***Figure 5.10: Akt(E40K) doubles the average cell size of TH+ neurons in the SNpc***
The average cell body area of randomly chosen TH+ neurons in caudal, medial, and rostral sections of the SNpc was measured through the StereoInvestigator program. The contralateral, uninjected hemisphere was used as controls. The average increase in cell size was found to be 2-fold with injection of AAV-Akt(E40K), (****$p < 0.0001$, unpaired t-test). Graph is mean with SEM. N=105 neurons per condition (from 4 mice per condition).

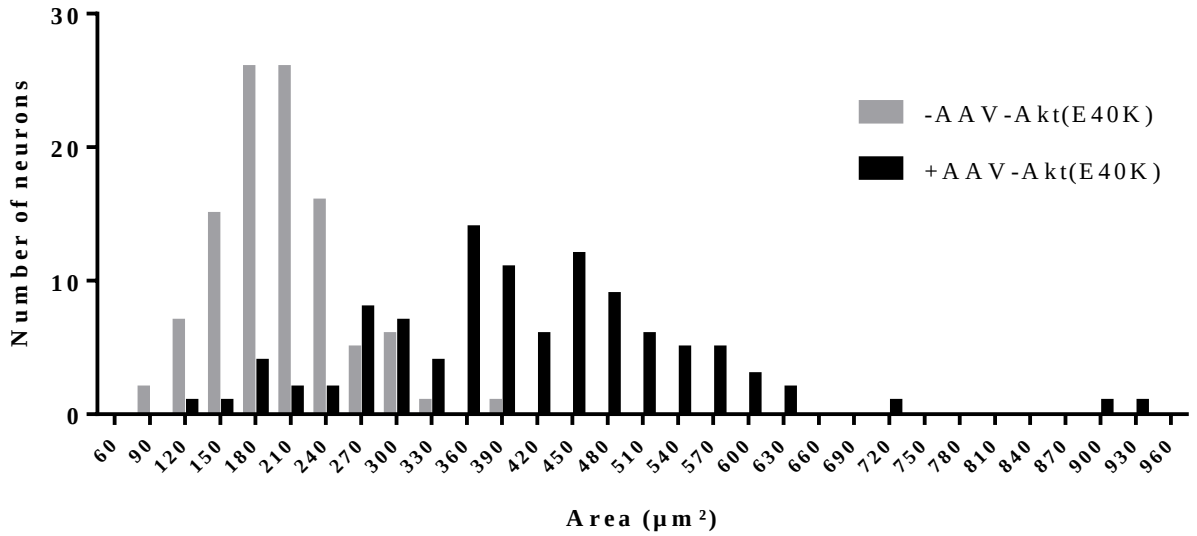


***Figure 5.11: Akt(E40K) expression increases dopaminergic neuron cell size***
The frequency distribution of all TH+ neuronal cell body areas demonstrates a clear trophic effect of Akt(E40K) expression on TH+ neurons in the SNpc.

The next question became whether DD-Akt(E40K)-Flag can exhibit a similar physiological effect. Our previous results had demonstrated that the protein was expressed at quantities large enough for clear detection by Flag staining, although expression levels were not detectably controlled by TMP administration. We therefore measured the cell size of neurons within the SNpc of mice that were unilaterally injected with AAV1-DD-Akt(E40K)-Flag and either given normal or TMP-treated water for 3 weeks (Figure 5.12). The average TH+ neuron cell size on the uninjected hemisphere was measured at 189.7 ± 4.8 $\mu m^2$ (-TMP) and 182.1 ± 4.2 $\mu m^2$ (+TMP), while on the injected hemisphere was measured at 232.2 ± 4.8 $\mu m^2$ (-TMP) and 227.0 ± 5.2 $\mu m^2$ (+TMP). Thus, we found that there was a significant increase in average TH+ neuron cell size by 23-25% with DD-Akt(E40K)-Flag injections compared to neurons of the uninjected hemisphere ($p < 0.0001$ vs. -AAV-DD-Akt(E40K)-Flag, 2-way ANOVA). In concordance with our results showing no apparent induction with TMP treatment, there was also

no difference found in cell size that correlated with TMP treatment (Figure 5.12, 2-way ANOVA).

Furthermore, the frequency distribution of all neuronal cell area measurements clearly show a shift upward in the range of neuron sizes in the hemisphere injected with the DD-Akt(E40K)-Flag compared to measurements from the uninjected hemisphere (Figure 5.13). These results reveal that DD-Akt(E40K)-Flag retains its trophic effect on neurons of the SNpc, even with the addition of the DD domain. However, the issue remains that the degradation of the protein within the SNpc is not controllable by orally administered TMP, in contrast to published results by other groups.

Further, it is interesting to note that the magnitude of the trophic effect found with expression of DD-Akt(E40K)-Flag was less than that of Akt(E40K). However, we cannot be sure that the expression levels of DD-Akt(E40K)-Flag and Akt(E40K) are equal. The two experiments were assessed for trophic effects at different lengths of time after injection (6 weeks for DD-Akt(E40K)-Flag and 10 weeks for Akt(E40K)). Additionally, the viral titer of DD-Akt(E40K)-Flag was $2.3 \times 10^{11}$ viral molecules/ml compared to the viral titer of Akt(E40K) at $4.9 \times 10^{12}$ viral molecules/ml. Although both of these differences could lead to the distinct results in trophic effect observed, it is worth nothing that the expression construct was identical with regards to the backbone plasmid and promoter. Given the drastic increase in average neuronal cell size by Akt(E40K) at 104% increase compared to an increase of 23-25% by DD-Akt(E40K)-Flag, the question remains whether the additional 4 weeks of time after injection and higher viral titer is sufficient to induce the 4-fold higher neuronal growth we observe with non-DD fusion Akt(E40K) expression.

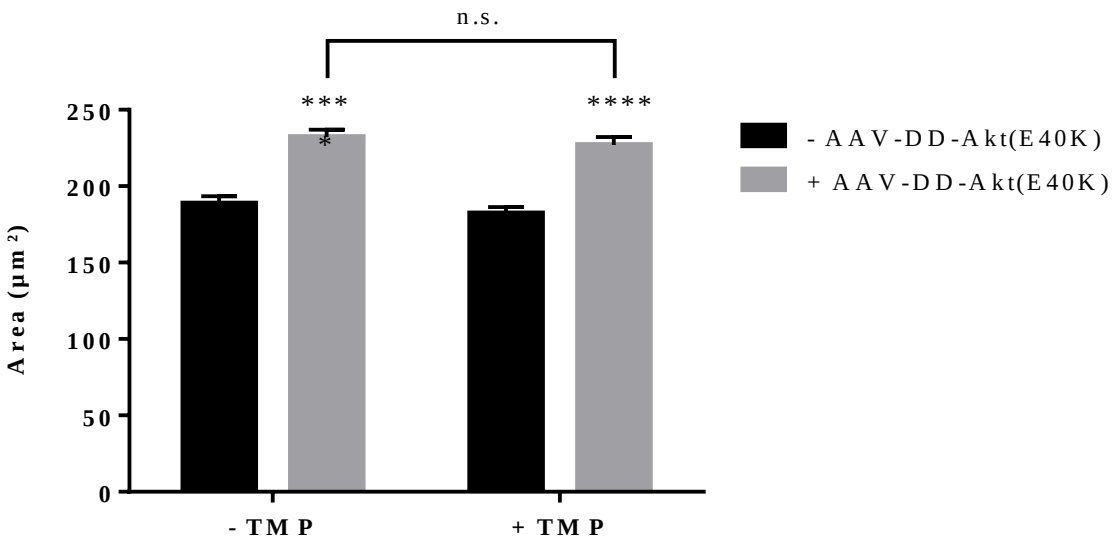


***Figure 5.12: DD-Akt(E40K)-Flag has trophic effects on dopaminergic neurons of the SNpc***
AAV-DD-Akt(E40K)-Flag was unilaterally injected into the SNpc of mice and processed 6 weeks post-injection for Flag expression. The average cell body area of randomly chosen Flag+ neurons in caudal, medial, and rostral sections of the SNpc in both non TMP-treated and TMP-treated mice was measured through the StereoInvestigator program. Neurons of the contralateral (uninjected) hemisphere was used as controls. Graph shows means with SEM. ****$p < 0.0001$; n.s. as determined by 2-way ANOVA with multiple comparisons. N=175 neurons from 7 –TMP mice, N=150 neurons from 6 +TMP mice.

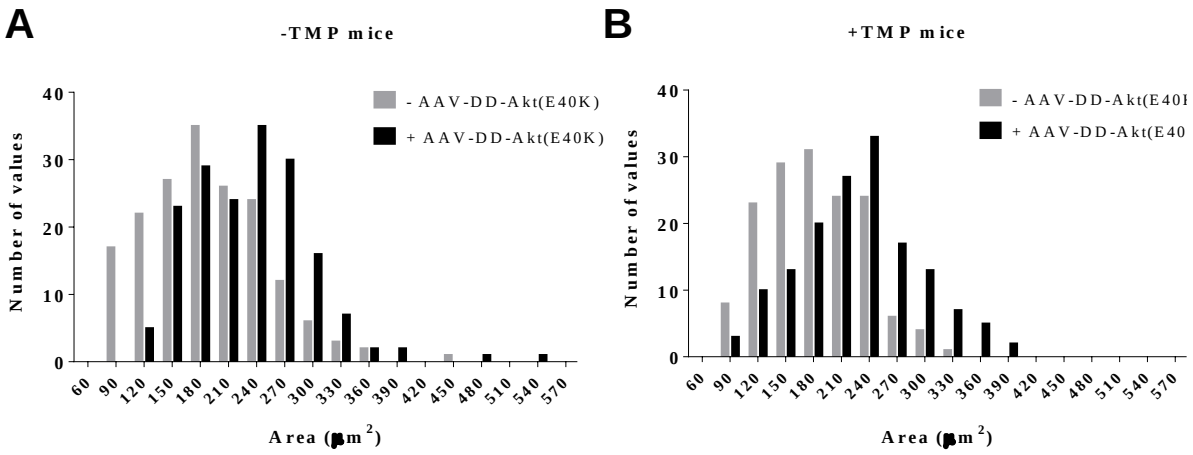


***Figure 5.13: DD-Akt(E40K)-Flag induces overall increases in dopaminergic neuron cell size***
The frequency distribution of all TH+ neuronal cell body areas demonstrates a clear trophic effect of DD-Akt(E40K)-Flag expression on TH+ neurons in the SNpc of (A) TMP-treated mice, N=175 neurons from 7 mice, and (B) non TMP-treated mice, N=150 neurons from 6 mice.

## 5.3: Discussion

In Chapter 5, we explored the feasibility of the DD-Akt(E40K) system as a Parkinson's disease therapy for clinical use by investigating its effects in an *in vivo* mouse model. Although previous studies in the literature had demonstrated robust induction of the DD system when fused to YFP, GDNF, and GTP cyclohydrolase 1 (GCH1) in rodent models with the oral administration of TMP [191, 211-213], we were not able to find any sign of induction of DD-Akt(E40K)-Flag with TMP treatment in the SNpc of mice. Interestingly, there was a detectable and statistically significant induction of DD-Akt(E40K)-Flag with TMP treatment that was observed in the striatum of mice, suggesting a regional difference in sensitivity of the DD system to TMP-mediated stabilization and induction. Additionally, significant physiological effects on the average size of the cell body were observed with the expression of DD-Akt(E40K)-Flag on the neurons of the SNpc. This trophic effect is in concordance with reported effects of Akt signaling on cell growth through mTORC1 [117].

The lack of TMP-mediated control over DD-Akt(E40K)-Flag in the SNpc is in contrast to previous published studies on the DHFR-derived DD system in the CNS of rodent models, which have demonstrated both clear induction of DD fusion proteins with YFP, GDNF, and GCH1 in the striatum as well as low baseline level expression[191, 211-213]. This could be due to a number of reasons, such as the potential inadequate sensitivity of our quantification method, the use of a different viral vector, differences in the protein of interest that is fused to the DD domain, issues with TMP administration (i.e. insufficient TMP reaching the region of expression), or regional differences that affect DD system behavior, all of which are explored below.

It is possible that our method of using the quantity of Flag-stained neurons as a readout of

DD-Akt(E40K)-Flag induction is not sensitive enough to detect 2.5 to 5-fold increases, as expected from our *in vitro* studies described in Chapter 3. Due to the nature of the enzymatic reaction used for immunohistochemical detection of Flag, it is difficult to ascertain the levels of Flag-tagged protein by intensity of staining. However, the successful detection of DD-Akt(E40K)-Flag induction in the striatum indicates that the quantification of Flag-stained neurons is an effective method to detect induction of DD-Akt(E40K)-Flag. Thus, the detection method is unlikely to account for the contrasting results of our studies from published data.

Viral vectors have a variety of unique characteristics, such as efficiency and specificity of infection, that may lead to differences in expression and potentially the behavior of a transgene [254]. As such, we considered the possibility that our use of an AAV vector may account for the contrasting results found with TMP-mediated inducibility of DD-Akt(E40K)-Flag. Within the literature, we found that most of the published studies of DHFR-derived DD have utilized lentiviral vectors to deliver their protein of interest to the striatum of rodents [191, 211, 212]. However, the most recent study in 2015 from the laboratory of Deniz Kirik utilized an AAV vector of serotype 5 with ITR sequences from serotype 2 (AAV2/5) [213]. This group demonstrated that delivery of DD-GCH1 using an AAV vector can lead to successful expression of DD fusion protein in the rodent CNS. Furthermore, their findings indicate that DD-GCH1 protein levels were regulatable by orally-administered TMP. There remains the important distinction between the AAV serotype used in their study (AAV2/5) and ours (AAV1). However, the AAV1 serotype used for our study has been validated by our collaborator Dr. Robert Burke's laboratory to efficiently induce expression of transgenes in mouse CNS [138, 140, 142, 174, 252]. Thus, we believe that the lack of TMP control over DD-Akt(E40K)-Flag is not likely due to differences in viral vector used.

There remains the possibility that the fusion of Akt to DD renders the system less efficient with regards to its regulation by TMP. Akt is by far the largest protein to be fused to DD and expressed in the CNS, with Akt having a molecular weight of approximately 60kDa compared to GCH1 at 28kDa, GDNF at 30kDa, and YFP at 26 kDa. The significantly larger size of the protein could potentially interfere with the DD domain's propensity to misfold and confer destabilizing function, contributing to the basal levels of DD-Akt(E40K)-Flag that we observe without TMP. However, the *in vitro* studies described in Chapters 3 and 4 exhibit robust induction of DD-Akt(E40K)-Flag, with an observable induction of protective effects against 6-OHDA and $MPP^+$ when treated with TMP and no protection found without TMP treatment, demonstrating that the DD-Akt fusion protein can be regulated by TMP within physiologically relevant levels in cell culture and have minimal basal levels. There also remains the possibility that the addition of a Flag tag to the C-terminus of DD-Akt(E40K) may affect its inducibility *in vivo*. However, we have demonstrated that at least in culture conditions, the additional Flag tag does not affect TMP-mediated induction (Figure 5.1). Thus, we believe it is likely that there is more at play than the difference in the protein that is fused to DD. It may be that the DD system behaves differently in culture compared to the full organismal level for reasons that may merit further exploration.

With regards to TMP administration being a potential contributor to the contrasting results from our studies with DD-Akt(E40K)-Flag inducibility in the SNpc, there are distinctions to the TMP treatment paradigm as well as the source of TMP used. However, we believe it is unlikely that these differences are enough to explain the lack of inducibility that we observe with DD-Akt(E40K)-Flag in the SNpc. The dosing of TMP in the drinking water of the animals in our studies was 1.0 mg/ml, 2 to 10-fold higher than published studies of DD-YFP and DD-GDNF in

the rodent striatum [191, 211, 212]. The most recent study by Deniz Kirik, published after we began our *in vivo* studies, utilizes a dose-escalation design with 3 doses beginning at 0.5 mg/ml and ending at 2.0 mg/ml, with 6 weeks spent at each dose. However, their motor behavioral assessment of the mice did not show significant differences between the middle dose of 1.0 mg/ml and ending dose of 2.0 mg/ml, suggesting that our TMP dose of 1.0 mg/ml should be sufficient to induce stabilization of DD-Akt(E40K)-Flag over untreated animals. Furthermore, the Kirik study demonstrated minimal basal expression of DD-GCH1 in untreated animals as detected by immunohistochemistry, thus suggesting that any difference in TMP treatment protocol would not explain the basal expression of DD-Akt(E40K)-Flag that we observe in our study. It is possible that our shorter length of TMP treatment time at 3 weeks compared to the full 18 weeks in the Kirik study could contribute to the lack of regulatory effect we observe with DD-Akt(E40K)-Flag in the SNpc. However, this 3-week treatment period has been demonstrated to efficiently induce stabilization and accumulation of DD fusion proteins in the earlier DHFR-derived DD studies [191, 211, 212]. Additionally, the TMP used in our *in vivo* studies was obtained from a different source as a TMP-lactate salt from ChemImpex International, Inc, whereas the other studies utilized an oral TMP suspension obtained from Meda AB, Solna, Sweden [191, 211-213]. However, based on our experimental verification of TMP-lactate in culture (Figure 5.3), it is unlikely that this would be a factor affecting inducibility of DD-Akt(E40K)-Flag in our hands. Thus, differences in our TMP treatment paradigm and source are unlikely to explain our conflicting results from previously published data.

Finally, we considered the possibility of a regional difference as an explanation for these contrasting data of TMP-mediated regulation of the DHFR-derived DD system. Among the above reasons explored, this region-specific sensitivity appears to be the most supported by our

data thus far. Our results showing induction with TMP in the striatum but not in the SNpc suggest that there is a region-specific effect that affects the sensitivity of DD system regulation by TMP such that there is detectable inducibility in the striatum but not the SNpc.

There are two possible general factors contributing to the observed lack of control over DD-Akt(E40K)-Flag protein with TMP in the SNpc: 1) high basal levels caused by inefficient degradation without TMP treatment, or 2) low stabilization levels with TMP administration as measured by a lack of increase in detectable DD fusion protein levels in TMP-treated groups. The results of the work described in this chapter suggest some combination of the two in the case of DD-Akt(E40K)-Flag in the SNpc, with three key supporting lines of evidence:

1) The detection of Flag staining in non TMP-treated animals reveals the sufficient presence of DD-Akt(E40K)-Flag protein even in the absence of the stabilizing ligand, supporting that high basal levels are a factor in the lack of detectable induction with TMP treatment,
2) The smaller magnitude of trophic effect by DD-Akt(E40K)-Flag at 23-25% increase in average cell size compared to myristoylated Akt at 50% increase [138] or Akt(E40K) at a little over 100% increase, supporting that increase of stabilization is insufficiently achieved with TMP compared to its fully activated potential, and
3) The lack of increase in trophic effect observed with TMP treatment for 3 weeks compared to untreated animals, thus suggesting that the TMP was not able to stabilize DD-Akt(E40K)-Flag above its baseline levels.

There are a few potential mechanisms through which regional differences could affect the DD system. First, the overall volume of the striatum is much larger than the SNpc, thus implicating the possibility that the concentration of virus on a per cell basis is higher in the SNpc

than in the striatum. This may contribute to higher basal expression levels of the transgene in the SNpc compared to the striatum. However, this mechanism assumes that the diffusion of viral particles during injection is confined to the target region, for which there is no supporting evidence to our knowledge. Furthermore, the extracellular space through which viral particles would diffuse has been estimated to be approximately 50% larger in the SN than in the striatum [255], suggesting that the overall concentration of viral particles after injection may actually be lower in the SNpc than in the striatum.

Second, there may be regional differences in the pharmacokinetics of TMP such that the TMP concentration in the striatum exceeds that in the SNpc. Our data presented in Chapter 3 established that TMP-mediated stabilization of DD-Akt(E40K) is dose-responsive, which implies that regional differences in TMP concentration within the CNS would directly lead to differences in stabilization and therefore accumulation of DD-Akt(E40K). Pharmacokinetics of drug target site distribution within the CNS depends on a large variety of factors, including drug transport across the blood-brain barrier, local metabolism, and regional tissue permeability, all of which may exhibit regional distinctions between the striatum and SNpc [256]. A recent study in 2016 assessing the regional distribution of antipsychotic drugs in rats found evidence of significant differences in region-specific blood-brain barrier penetration as well as intra-brain distribution and tissue binding [257]. The study further demonstrated evidence of the striatum as a brain region with one of the highest blood-brain barrier penetration. To test whether regional differences in TMP access might account for the contrasting inducibility in the striatum compared to the SNpc, we attempted to test inducibility of DD-YFP, as a positive control, within both of these brain regions. Unfortunately, we observed severe transduction toxicity with AAV-delivered DD-YFP, making our experiment inconclusive (data not shown). Thus, there remains

the possibility that regional TMP concentration differences may play a role in the regional inducibility of DD-Akt(E40K).

The last but perhaps most intriguing possibility is that the SNpc may be much poorer in protein degradation than the striatum, which could be related to selective vulnerability in Parkinson's disease [237, 238]. With the putative mechanism of DD-mediated destabilization being dependent on the ubiquitin-proteasome system (UPS) [214], a difference in proteasomal degradation efficiency between dopaminergic neurons of the SNpc and GABAergic neurons of the striatum could thus explain the insufficient degradation of the DD-Akt(E40K)-Flag in the SNpc, even in untreated animals. This mechanism is supported by our data presented in Chapter 3, demonstrating a greater than 250% increase in basal levels of DD-Akt(E40K) in dopaminergic neurons compared to neighboring non-dopaminergic cells *in vitro* (Figure 3.12). Additionally, there is much evidence supporting dysfunction of the UPS in Parkinson's disease [235, 236], and there have also been reports of decreased levels of proteasome activators, PA28 and PA700, in the SNpc compared to the striatum and cortex [237]. Furthermore, a study assessing the three catalytic activities (chymotrypsin-like, trypsin-like, and trypsin- and peptidylglutamyl-peptide hydrolase (PGPH)-like) of the proteasome across different species and brain regions revealed that two out of the three catalytic activities were significantly reduced in the striatum but only in the SN were all three catalytic activities significantly reduced [238]. Thus, the unexpected result of DD-Akt(E40K)-Flag inducibility in the striatum but not the SNpc may be due regionally reduced UPS activity, contributing to high basal levels of the protein off-TMP in the SNpc.

Another interesting result from the data presented in this chapter is the finding that the trophic effect of Akt(E40K) exceeded the reported effect of myristoylated Akt (myr-Akt) by approximately 2-fold, with Akt(E40K) having a 100% increase in average cell size compared to

the 50% increase found with myr-Akt expression [138]. This difference in the magnitude of effect contrasts with literature that suggests higher activity levels of myr-Akt than that of PH domain mutants, as is implied by much larger increases in heart size with overexpression of myr-Akt compared to Akt(E40K) in rats [232, 233]. Additionally, both myr-Akt and Akt(E40K) increased average cell size by a much larger proportion compared to that caused by DD-Akt(E40K). As discussed above, the length of time after viral injection that the animals were processed was distinct in each case; DD-Akt(E40K)-Flag injected mice were processed 6 weeks post-injection, myr-Akt injected mice were processed 7 weeks post-injection [138], and Akt(E40K) injected mice were processed 10 weeks post-injection. Thus, the increase in magnitude of trophic effect could potentially be explained by the differences in time that the active Akt was expressed in the brain before processing. Perhaps an even more convincing reason for the contrasting results lies in the viral titers – the titer of AAV-DD-Akt(40K)-Flag was estimated to be approximately 20-fold lower than the titer of AAV-Akt(E40K). Regardless, these contrasting results suggest that the trophic effect of DD-Akt(E40K)-Flag did not reach its maximum potential as suggested by the drastic increases in cell size with expression of myr-Akt and Akt(E40K).

The *in vivo* studies presented in this chapter reveal a number of important considerations. First, the utility of the DD system currently as a tool to control protein levels is limited in a clinical setting due to its variability of inducibility that may be affected by the region of expression. Second, this same variability of inducibility provides the possibility of further control over the levels of transgene or protein in gene therapy. If the reasons behind this variability are explored further, they could provide insights into very relevant considerations for any future therapies that aim to control levels of protein level, as well as alternative methods of fine tune

control in gene therapy in the CNS. Third, this study reemphasizes the physiological potential of Akt signaling that, if harnessed properly, presents a viable target to control cell growth and possibly other downstream effects of Akt including cell survival and neurite restoration.

# Chapter 6: Conclusions and Future Directions

This dissertation explores the applicability of a unique protein stabilization technique as a gene therapy tool in Parkinson's disease. This chapter will summarize the major achievements and future directions of this project.

## 6.1: Strategy for Control of Akt Signaling *In Vitro*

Here we have reported the development of a unique method for controlling Akt signaling *in vitro*. The use of DHFR-derived destabilizing domains (DD) for post-transcriptional control of protein levels by controlling protein stability was first reported by the Wandless group of Stanford University in 2010. Since then, the original publication has been cited 71 times by various groups utilizing the technique for control of diverse proteins as well as potential pairing with other innovative technologies, such as CRISPR/Cas9, for wider applications [191, 205, 211-213, 258-260].

We have applied this strategy to create a tool for the control of active Akt levels through the fusion of a DD domain to the N-terminus of Akt(E40K). This strategy employs the inexpensive, non-toxic, and commonly used antibiotic, Trimethoprim (TMP), to increase the levels of phosphorylated Akt kinase in a dose-responsive and reversible manner (Chapter 3.2.1 and Chapter 3.2.3). Furthermore, the full induction of active Akt with TMP treatment is achievable within 24 hours (Chapter 3.2.3). Importantly, we have presented evidence for the presence of DD-Akt(E40K) kinase activity through observations of increased phosphorylated FoxO4, a known Akt substrate, with TMP-mediated induction (Chapter 4.2.1).

As we have demonstrated the successful inducibility of this activateable Akt within multiple cellular contexts (human embryonic kidney cells, PC12 cells, rat cortical neurons, rat

dopaminergic neurons), this unlocks the possibility of utilizing this system in a variety of cellular studies regarding Akt signaling. Furthermore, if used in conjunction with gene editing technologies including CRISPR/Cas9, this tool could potentially be used to permit control of endogenous Akt signaling levels through an external ligand, TMP. Further studies could utilize this inducible Akt as a tool to potentially study unanswered questions about Akt signaling such as the timing of Akt downstream signaling events, the reliability of certain downstream events on the dose or level of active Akt, the distinctions of Akt signaling via recruitment to the plasma membrane compared to recruitment to other intracellular membrane structures, and the nuances of Akt regulation and feedback inhibition.

However, this strategy is not without limitations. As seen in our findings presented in Chapter 3, there exists a certain level of active Akt even in the absence of the stabilizing ligand. This is likely to always be the case due to the post-translational nature of the technology in which the protein is constantly expressed but tagged for proteasomal degradation. Although our data presented in Chapter 3 and Chapter 4 suggest that this basal level of DD-Akt(E40K) is not sufficient to induce detectable changes downstream in phosphorylation of FoxO4 or physiological pro-survival activity, there may exist certain cellular contexts in which the dependence of DD-Akt(E40K) inducibility on endogenous protein degradation systems is prohibitive. This last point is supported by our detection of higher basal DD-Akt(E40K) levels in dopaminergic neurons of the rat midbrain than non-dopaminergic neurons within the same cultures (Chapter 3.2.1), as well as our *in vivo* data demonstrating lack of detectable induction in the SNpc of mice, an area which has been suggested to have lower proteasomal activity (Chapter 5.2.2) [237, 238]. Further studies could directly assess basal proteasomal activities of different cellular contexts utilizing the basal activity levels of DD-Akt(E40K) or detected induction of this

system as a readout.

Overall, DD-Akt(E40K) presents a valuable tool for *in vitro* studies requiring dose-responsive control of Akt signaling.

### 6.2: Proof of Principle for Akt-Mediated Inducible Pro-Survival and Trophic Effects

In Chapter 4, we used this DD-mediated approach to demonstrate that Akt is capable of protecting cells against insults that lead to apoptotic death. This included protection of undifferentiated PC12 cells against growth factor removal-mediated death and neuronal cultures against PD mimetic neurotoxins, 6-OHDA and $MPP^+$, both in an inducible manner (Chapter 4.2.2 and Chapter 4.2.3).

In Chapter 5, we demonstrated further the capability of DD-Akt(E40K) to induce trophic effects in dopaminergic neurons of the SNpc in mice. This finding corroborates previous studies demonstrating significant trophic effects on neuronal cell size with the overexpression of myristoylated Akt [138].

Thus, our work achieves two major accomplishments:

First, we have validated the downstream physiological effects of Akt(E40K), which has been demonstrated to replicate certain Akt functions such as transformation of hematopoietic cells and inhibition of apoptosis induced by IL-3 withdrawal [222, 223], but never, to our knowledge, inhibition of apoptosis in PD models or trophic effects on neuronal cell size.

Second, we have provided evidence to further support the legitimacy of targeting Akt signaling as a strategy for Parkinson's disease therapies. Further studies should investigate this approach in promoting survival against additional PD models, particularly non-toxin models such as *in vitro* and *in vivo* α-synuclein fibrils or AAV-delivered α-synuclein overexpression *in*

*vivo* models [20, 32, 261].

Next steps may also include studies into the role of inducible Akt in neurite restoration, as this may open possibilities for DD-Akt(E40K) as a research tool to study this function of Akt activity as well as a clinical tool for nerve regeneration in brain disease.

### 6.3: Insights into the Clinical Utility of DD-Mediated Control of Akt

With continued development of gene therapy techniques as a therapy for Parkinson's disease, the DHFR-derived DD system provides great potential as a gene therapy tool to control protein levels within the CNS [262, 263]. The use of TMP as a regulator of this system lends a significant advantage to its clinical utility due to its ability to cross the blood brain barrier [215] and safety for long-term prophylactic use [216-219]. Thus, one may imagine a future treatment where the levels of a therapeutic protein are controlled by oral administration of a safe, approved antibiotic. In particular, with Akt dysfunction being implicated in various neurological disorders, including Parkinson's disease, our approach using DD-Akt(E40K) poses a promising therapeutic strategy if optimized for regulatability in animals [141, 143-148, 152, 162, 163].

In Chapter 5, we presented surprising findings into the contrasting behavior of the DD system depending on the target region of expression. More specifically, we identified detectable inducibility of DD-Akt(E40K)-Flag in the mouse striatum, but not in the mouse SNpc (Chapter 5.2.2). This finding is important in that it provides concrete evidence of the limitations on the clinical utility of the DD system, particularly its use as a therapeutic strategy for Parkinson's disease if dependent on expression of the system in the SNpc. However, the approach of targeting Akt activity as a therapy in Parkinson's disease may still be viable if further studies are done using alternative inducible methods, perhaps based on light-mediated protein stability [207]

or tetracycline-controlled inducible systems.

Furthermore, the potential for DD-mediated inducible Akt as a clinical tool remains strong for other diseases involving Akt dysfunction in various other brain regions, including other degenerative disorders such as Alzheimer's disease and prion disease [146-148], or even neuropsychiatric and neurodevelopmental disorders such as schizophrenia, autism spectrum disorder, epilepsy, and developing brain malformations [143-145]. Additionally, if a neurorestorative role of inducible Akt is validated as discussed above, DD-Akt(E40K) presents a potential clinical tool to treat diseases involving nerve damage and provide functional restoration in patients suffering from these diseases.

### 6.4: Insights into Parkinson's Disease Biology

Various mechanisms for selective neuronal vulnerability within Parkinson's disease have been explored but research has not been able to conclusively provide an explanation for selective degeneration of dopaminergic neurons within the SNpc [264, 265]. Our unexpected findings of the lack of apparent TMP-mediated DD-Akt(E40K)-Flag inducibility in the SNpc (Chapter 5.2.2) suggests an intriguing insight into the biology of Parkinson's disease with regards to its pathogenesis and selective vulnerability of SN dopaminergic neurons.

With reports of decreased proteasomal activity in the SN [237, 238], our data regarding lack of detectable inducibility in the SNpc of mice provide further evidence of decreased proteasomal function in the SNpc, even under non-disease contexts. Additionally, our findings demonstrate for the first time a concrete functional outcome of reported lower proteasomal activity in the SNpc, showing that the putative difference in proteasomal activity between the SNpc and striatum is sufficient to interfere with degradation of a protein that we have found to

be normally degraded in other cell types within culture (Chapter 3.2.1 and Chapter 5.2.2). This conclusion is supported by our *in vitro* data, showing that the measured DD-Akt(E40K) basal levels are greater than 250% higher in dopaminergic neurons than non-dopaminergic neurons within the same cultures (Chapter 3.2.2). We believe these results merit further investigation into the possibility of lower proteasomal activity within the dopaminergic neurons of the SNpc contributing to decreased ability to clear abnormal or misfolded proteins, including α-synuclein, and thus leading to the selective degeneration that is a key characteristic of Parkinson's disease. Further studies using basal expression levels of DD-Akt(E40K) as a readout of proteasomal degradation may be used to parse out differences in proteasomal activity across different neuronal subtypes, both in cell culture and *in vivo* utilizing viral vectors developed for the studies presented here. An intriguing next step would be to determine any differences in proteasomal degradation capability in SNpc neurons compared to VTA neurons through midbrain culture studies and viral injections of DD-Akt(E40K) in animals.

### 6.5: Closing Statement

This dissertation establishes a novel approach to control Akt activity, with particular emphasis on its utility as therapeutic tool in Parkinson's disease. We have demonstrated that although clinical utility of DD-Akt(E40K) may be limited in the context of Parkinson's, our innovation provides a new tool for the research of Akt signaling and opens new avenues of research regarding regional variability of proteasomal degradation and selective vulnerability in Parkinson's disease.

## Bibliography


1. Poewe, W., et al., *Parkinson disease.* Nat Rev Dis Primers, 2017. **3**: p. 17013.

2. Twelves, D., K.S. Perkins, and C. Counsell, *Systematic review of incidence studies of Parkinson's disease.* Mov Disord, 2003. **18**(1): p. 19-31.

3. Savica, R., et al., *Incidence and pathology of synucleinopathies and tauopathies related to parkinsonism.* JAMA Neurol, 2013. **70**(7): p. 859-66.

4. Van Den Eeden, S.K., et al., *Incidence of Parkinson's disease: variation by age, gender, and race/ethnicity.* Am J Epidemiol, 2003. **157**(11): p. 1015-22.

5. Chaudhuri, K.R. and A.H. Schapira, *Non-motor symptoms of Parkinson's disease: dopaminergic pathophysiology and treatment.* Lancet Neurol, 2009. **8**(5): p. 464-74.

6. Spillantini, M.G., et al., *alpha-Synuclein in filamentous inclusions of Lewy bodies from Parkinson's disease and dementia with lewy bodies.* Proc Natl Acad Sci U S A, 1998. **95**(11): p. 6469-73.

7. Dauer, W. and S. Przedborski, *Parkinson's disease: mechanisms and models.* Neuron, 2003. **39**(6): p. 889-909.

8. Burke, R.E. and K. O'Malley, *Axon degeneration in Parkinson's disease.* Experimental neurology, 2013. **246**: p. 72-83.

9. Ghebremedhin, E., et al., *Diminished tyrosine hydroxylase immunoreactivity in the cardiac conduction system and myocardium in Parkinson's disease: an anatomical study.* Acta Neuropathol, 2009. **118**(6): p. 777-84.

10. Singaram, C., et al., *Dopaminergic defect of enteric nervous system in Parkinson's disease patients with chronic constipation.* Lancet, 1995. **346**(8979): p. 861-4.

11. Li, Z., et al., *Essential roles of enteric neuronal serotonin in gastrointestinal motility and the development/survival of enteric dopaminergic neurons.* J Neurosci, 2011. **31**(24): p. 8998-9009.

12. Sulzer, D. and D.J. Surmeier, *Neuronal vulnerability, pathogenesis, and Parkinson's disease.* Mov Disord, 2013. **28**(6): p. 715-24.

13. Braak, H., et al., *Staging of brain pathology related to sporadic Parkinson's disease.* Neurobiology of aging, 2003. **24**(2): p. 197-211.

14. Dickson, D.W., et al., *Neuropathological assessment of Parkinson's disease: refining the diagnostic criteria.* Neuropathological assessment of Parkinson's disease: refining the diagnostic criteria, 2009.

15. Forno, L.S., *Neuropathology of Parkinson's disease.* J Neuropathol Exp Neurol, 1996. **55**(3): p. 259-72.

16. Olanow, C.W., et al., *Lewy-body formation is an aggresome-related process: a hypothesis.* Lancet Neurol, 2004. **3**(8): p. 496-503.

17. Ben Gedalya, T., et al., *Alpha-synuclein and polyunsaturated fatty acids promote clathrin-mediated endocytosis and synaptic vesicle recycling.* Traffic, 2009. **10**(2): p. 218-34.

18. Madine, J., et al., *The effects of alpha-synuclein on phospholipid vesicle integrity: a study using 31P NMR and electron microscopy.* Mol Membr Biol, 2008. **25**(6-7): p. 518-27.

19. Nemani, V.M., et al., *Increased expression of alpha-synuclein reduces neurotransmitter release by inhibiting synaptic vesicle reclustering after endocytosis.* Neuron, 2010. **65**(1): p. 66-79.

20. Koprich, J.B., et al., *Towards a Non-Human Primate Model of Alpha-Synucleinopathy for Development of Therapeutics for Parkinson's Disease: Optimization of AAV1/2 Delivery Parameters to Drive Sustained Expression of Alpha Synuclein and Dopaminergic Degeneration in Macaque.* PLoS One, 2016. **11**(11): p. e0167235.

21. Butler, B., et al., *Dopamine Transporter Activity Is Modulated by alpha-synuclein.* J Biol Chem, 2015.

22. Chu, Y., et al., *Alterations in axonal transport motor proteins in sporadic and experimental Parkinson's disease.* Brain, 2012. **135**(Pt 7): p. 2058-73.

23. Chung, C.Y., et al., *Dynamic changes in presynaptic and axonal transport proteins combined with striatal neuroinflammation precede dopaminergic neuronal loss in a rat model of AAV alpha-synucleinopathy.* J Neurosci, 2009. **29**(11): p. 3365-73.

24. Mazzulli, J.R., et al., *alpha-Synuclein-induced lysosomal dysfunction occurs through disruptions in protein trafficking in human midbrain synucleinopathy models.* Proc Natl Acad Sci U S A, 2016. **113**(7): p. 1931-6.

25. Tang, F.L., et al., *VPS35 in Dopamine Neurons Is Required for Endosome-to-Golgi Retrieval of Lamp2a, a Receptor of Chaperone-Mediated Autophagy That Is Critical for alpha-Synuclein Degradation and Prevention of Pathogenesis of Parkinson's Disease.* J Neurosci, 2015. **35**(29): p. 10613-28.

26. Singleton, A.B., et al., *alpha-Synuclein locus triplication causes Parkinson's disease.* Science, 2003. **302**(5646): p. 841.

27. Burke, R.E., W.T. Dauer, and J.G. Vonsattel, *A critical evaluation of the Braak staging scheme for Parkinson's disease.* Annals of Neurology, 2008. **64**(5): p. 485-491.

28. Rietdijk, C.D., et al., *Exploring Braak's Hypothesis of Parkinson's Disease.* Front Neurol, 2017. **8**: p. 37.

29. Kordower, J.H., et al., *Lewy body-like pathology in long-term embryonic nigral transplants in Parkinson's disease.* Nat Med, 2008. **14**(5): p. 504-6.

30. Li, J.Y., et al., *Lewy bodies in grafted neurons in subjects with Parkinson's disease suggest host-to-graft disease propagation.* Nat Med, 2008. **14**(5): p. 501-3.

31. Peelaerts, W., et al., *alpha-Synuclein strains cause distinct synucleinopathies after local and systemic administration.* Nature, 2015. **522**(7556): p. 340-4.

32. Volpicelli-Daley, L.A., et al., *Exogenous α-synuclein fibrils induce Lewy body pathology leading to synaptic dysfunction and neuron death.* Neuron, 2011. **72**(1): p. 57-71.

33. Volpicelli-Daley, L.A., K.C. Luk, and V.M. Lee, *Addition of exogenous alpha-synuclein preformed fibrils to primary neuronal cultures to seed recruitment of endogenous alpha-synuclein to Lewy body and Lewy neurite-like aggregates.* Nat Protoc, 2014. **9**(9): p. 2135-46.

34. Abdelmotilib, H., et al., *alpha-Synuclein fibril-induced inclusion spread in rats and mice correlates with dopaminergic Neurodegeneration.* Neurobiol Dis, 2017. **105**: p. 84-98.

35. Mao, X., et al., *Pathological alpha-synuclein transmission initiated by binding lymphocyte-activation gene 3.* Science, 2016. **353**(6307).

36. Gasser, T., J. Hardy, and Y. Mizuno, *Milestones in PD genetics.* Mov Disord, 2011. **26**(6): p. 1042-8.

37. Klein, C. and A. Westenberger, *Genetics of Parkinson's disease.* Cold Spring Harb Perspect Med, 2012. **2**(1): p. a008888.

38. Kalinderi, K., S. Bostantjopoulou, and L. Fidani, *The genetic background of Parkinson's disease: current progress and future prospects.* Acta Neurol Scand, 2016. **134**(5): p. 314-326.

39. Langston, J.W., et al., *Chronic Parkinsonism in humans due to a product of meperidine-analog synthesis.* Science, 1983. **219**(4587): p. 979-80.

40. Mostafalou, S. and M. Abdollahi, *Pesticides and human chronic diseases: evidences, mechanisms, and perspectives.* Toxicol Appl Pharmacol, 2013. **268**(2): p. 157-77.

41. Kamel, F., *Epidemiology. Paths from pesticides to Parkinson's.* Science, 2013. **341**(6147): p. 722-3.

42. Ascherio, A. and M.A. Schwarzschild, *The epidemiology of Parkinson's disease: risk factors and prevention.* Lancet Neurol, 2016. **15**(12): p. 1257-1272.

43. Cohen, G., *Oxy-radical toxicity in catecholamine neurons.* Neurotoxicology, 1984. **5**(1): p. 77-82.

44. McCann, S.J., et al., *The association between polymorphisms in the cytochrome P-450 2D6 gene and Parkinson's disease: a case-control study and meta-analysis.* J Neurol Sci, 1997. **153**(1): p. 50-3.

45. Landi, M.T., et al., *Gene-environment interaction in parkinson's disease. The case of CYP2D6 gene polymorphism.* Adv Neurol, 1996. **69**: p. 61-72.

46. Rostami-Hodjegan, A., et al., *Meta-analysis of studies of the CYP2D6 polymorphism in relation to lung cancer and Parkinson's disease.* Pharmacogenetics, 1998. **8**(3): p. 227-38.

47. Christensen, P.M., P.C. Gotzsche, and K. Brosen, *The sparteine/debrisoquine (CYP2D6) oxidation polymorphism and the risk of Parkinson's disease: a meta-analysis.* Pharmacogenetics, 1998. **8**(6): p. 473-9.

48. Riedl, A.G., et al., *P450 enzymes and Parkinson's disease: the story so far.* Mov Disord, 1998. **13**(2): p. 212-20.

49. Sandy, M.S., et al., *CYP2D6 allelic frequencies in young-onset Parkinson's disease.* Neurology, 1996. **47**(1): p. 225-30.

50. Tan, E.K., et al., *Variability and validity of polymorphism association studies in Parkinson's disease.* Neurology, 2000. **55**(4): p. 533-8.

51. Alonso-Navarro, H., et al., *Genomic and pharmacogenomic biomarkers of Parkinson's disease.* Curr Drug Metab, 2014. **15**(2): p. 129-81.

52. Connolly, B.S. and A.E. Lang, *Pharmacological treatment of Parkinson disease: a review.* JAMA, 2014. **311**(16): p. 1670-83.

53. Van Gerpen, J.A., et al., *Levodopa-associated dyskinesia risk among Parkinson disease patients in Olmsted County, Minnesota, 1976-1990.* Arch Neurol, 2006. **63**(2): p. 205-9.

54. Holloway, R.G., et al., *Pramipexole vs levodopa as initial treatment for Parkinson disease: a 4-year randomized controlled trial.* Arch Neurol, 2004. **61**(7): p. 1044-53.

55. Katzenschlager, R., et al., *Anticholinergics for symptomatic management of Parkinson's disease.* Cochrane Database Syst Rev, 2003(2): p. CD003735.

56. Friedman, J.H., et al., *Benztropine versus clozapine for the treatment of tremor in Parkinson's disease.* Neurology, 1997. **48**(4): p. 1077-81.

57. Crosby, N., K.H. Deane, and C.E. Clarke, *Amantadine in Parkinson's disease.* Cochrane Database Syst Rev, 2003(1): p. CD003468.

58. Ferreira, J.J., et al., *Summary of the recommendations of the EFNS/MDS-ES review on therapeutic management of Parkinson's disease.* Eur J Neurol, 2013. **20**(1): p. 5-15.

59. Pahwa, R. and K.E. Lyons, *Levodopa-related wearing-off in Parkinson's disease: identification and management.* Curr Med Res Opin, 2009. **25**(4): p. 841-9.

60. Ory-Magne, F., et al., *Withdrawing amantadine in dyskinetic patients with Parkinson disease: the AMANDYSK trial.* Neurology, 2014. **82**(4): p. 300-7.

61. Johnston, T.H., S.H. Fox, and J.M. Brotchie, *Advances in the delivery of treatments for Parkinson's disease.* Expert Opin Drug Deliv, 2005. **2**(6): p. 1059-73.

62. Bronstein, J.M., et al., *Deep brain stimulation for Parkinson disease: an expert consensus and review of key issues.* Arch Neurol, 2011. **68**(2): p. 165.

63. Hickey, P. and M. Stacy, *Deep Brain Stimulation: A Paradigm Shifting Approach to Treat Parkinson's Disease.* Front Neurosci, 2016. **10**: p. 173.

64. Verhagen Metman, L., G. Pal, and K. Slavin, *Surgical Treatment of Parkinson's Disease.* Curr Treat Options Neurol, 2016. **18**(11): p. 49.

65. Athauda, D. and T. Foltynie, *The ongoing pursuit of neuroprotective therapies in Parkinson disease.* Nat Rev Neurol, 2015. **11**(1): p. 25-40.

66. Fischer, D.L., et al., *Subthalamic Nucleus Deep Brain Stimulation Employs TrkB Signaling for Neuroprotection and Functional Restoration.* J Neurosci, 2017.

67. Ungerstedt, U., *6-Hydroxy-dopamine induced degeneration of central monoamine neurons.* Eur J Pharmacol, 1968. **5**(1): p. 107-10.

68. Schober, A., *Classic toxin-induced animal models of Parkinson's disease: 6-OHDA and MPTP.* Cell and tissue research, 2004. **318**(1): p. 215-224.

69. Seniuk, N.A., W.G. Tatton, and C.E. Greenwood, *Dose-dependent destruction of the coeruleus-cortical and nigral-striatal projections by MPTP.* Brain Res, 1990. **527**(1): p. 7-20.

70. Varastet, M., et al., *Chronic MPTP treatment reproduces in baboons the differential vulnerability of mesencephalic dopaminergic neurons observed in Parkinson's disease.* Neuroscience, 1994. **63**(1): p. 47-56.

71. Forno, L.S., et al., *Locus ceruleus lesions and eosinophilic inclusions in MPTP-treated monkeys.* Ann Neurol, 1986. **20**(4): p. 449-55.

72. Forno, L.S., et al., *Similarities and differences between MPTP-induced parkinsonsim and Parkinson's disease. Neuropathologic considerations.* Adv Neurol, 1993. **60**: p. 600-8.

73. Jellinger, K., et al., *Chemical evidence for 6-hydroxydopamine to be an endogenous toxic factor in the pathogenesis of Parkinson's disease.* J Neural Transm Suppl, 1995. **46**: p. 297-314.

74. Olanow, C.W., K. Kieburtz, and A.H. Schapira, *Why have we failed to achieve neuroprotection in Parkinson's disease?* Ann Neurol, 2008. **64 Suppl 2**: p. S101-10.

75. Blesa, J. and S. Przedborski, *Parkinson's disease: animal models and dopaminergic cell vulnerability.* Front Neuroanat, 2014. **8**: p. 155.

76. Kirik, D., et al., *Parkinson-like neurodegeneration induced by targeted overexpression of alpha-synuclein in the nigrostriatal system.* J Neurosci, 2002. **22**(7): p. 2780-91.

77. Klein, R.L., et al., *Dopaminergic cell loss induced by human A30P alpha-synuclein gene transfer to the rat substantia nigra.* Hum Gene Ther, 2002. **13**(5): p. 605-12.

78. Lo Bianco, C., et al., *alpha -Synucleinopathy and selective dopaminergic neuron loss in a rat lentiviral-based model of Parkinson's disease.* Proc Natl Acad Sci U S A, 2002. **99**(16): p. 10813-8.

79. Decressac, M., et al., *Progressive neurodegenerative and behavioural changes induced by AAV-mediated overexpression of alpha-synuclein in midbrain dopamine neurons.* Neurobiol Dis, 2012. **45**(3): p. 939-53.

80. Luk, K.C. and V.M. Lee, *Modeling Lewy pathology propagation in Parkinson's disease.* Parkinsonism Relat Disord, 2014. **20 Suppl 1**: p. S85-7.

81. Healy, D.G., et al., *Phenotype, genotype, and worldwide genetic penetrance of LRRK2-associated Parkinson's disease: a case-control study.* Lancet Neurol, 2008. **7**(7): p. 583-90.

82. Ramonet, D., et al., *Dopaminergic neuronal loss, reduced neurite complexity and autophagic abnormalities in transgenic mice expressing G2019S mutant LRRK2.* PLoS One, 2011. **6**(4): p. e18568.

83. Chen, C.Y., et al., *(G2019S) LRRK2 activates MKK4-JNK pathway and causes degeneration of SN dopaminergic neurons in a transgenic mouse model of PD.* Cell Death Differ, 2012. **19**(10): p. 1623-33.

84. Gautier, C.A., T. Kitada, and J. Shen, *Loss of PINK1 causes mitochondrial functional defects and increased sensitivity to oxidative stress.* Proc Natl Acad Sci U S A, 2008. **105**(32): p. 11364-9.

85. Kitada, T., et al., *Absence of nigral degeneration in aged parkin/DJ-1/PINK1 triple knockout mice.* J Neurochem, 2009. **111**(3): p. 696-702.

86. Hennis, M.R., et al., *Surprising behavioral and neurochemical enhancements in mice with combined mutations linked to Parkinson's disease.* Neurobiol Dis, 2014. **62**: p. 113-23.

87. Yao, R. and G.M. Cooper, *Requirement for phosphatidylinositol-3 kinase in the prevention of apoptosis by nerve growth factor.* Science, 1995. **267**(5206): p. 2003-6.

88. Dudek, H., et al., *Regulation of neuronal survival by the serine-threonine protein kinase Akt.* Science, 1997. **275**(5300): p. 661-5.

89. Miller, T.M., et al., *Inhibition of phosphatidylinositol 3-kinase activity blocks depolarization- and insulin-like growth factor I-mediated survival of cerebellar granule cells.* J Biol Chem, 1997. **272**(15): p. 9847-53.

90. Crowder, R.J. and R.S. Freeman, *Phosphatidylinositol 3-kinase and Akt protein kinase are necessary and sufficient for the survival of nerve growth factor-dependent sympathetic neurons.* J Neurosci, 1998. **18**(8): p. 2933-43.

91. Staal, S.P., J.W. Hartley, and W.P. Rowe, *Isolation of transforming murine leukemia viruses from mice with a high incidence of spontaneous lymphoma.* Proceedings of the National Academy of Sciences, 1977. **74**(7).

92. Staal, S.P., *Molecular cloning of the akt oncogene and its human homologues AKT1 and AKT2: amplification of AKT1 in a primary human gastric adenocarcinoma.* Proc Natl Acad Sci U S A, 1987. **84**(14): p. 5034-7.

93. Bellacosa, A., et al., *A retroviral oncogene, akt, encoding a serine-threonine kinase containing an SH2-like region.* Science, 1991. **254**(5029): p. 274-7.

94. Jones, P.F., et al., *Molecular cloning and identification of a serine/threonine protein kinase of the second-messenger subfamily.* Proc Natl Acad Sci U S A, 1991. **88**(10): p. 4171-5.

95. Coffer, P.J. and J.R. Woodgett, *Molecular cloning and characterisation of a novel putative protein-serine kinase related to the cAMP-dependent and protein kinase C families.* Eur J Biochem, 1991. **201**(2): p. 475-81.

96. Franke, T.F., et al., *The protein kinase encoded by the Akt proto-oncogene is a target of the PDGF-activated phosphatidylinositol 3-kinase.* Cell, 1995. **81**(5): p. 727-36.

97. Burgering, B.M. and P.J. Coffer, *Protein kinase B (c-Akt) in phosphatidylinositol-3-OH kinase signal transduction.* Nature, 1995. **376**(6541): p. 599-602.

98. Kohn, A.D., K.S. Kovacina, and R.A. Roth, *Insulin stimulates the kinase activity of RAC-PK, a pleckstrin homology domain containing ser/thr kinase.* EMBO J, 1995. **14**(17): p. 4288-95.

99. Bellacosa, A., J.R. Testa, and L. Larue, *A portrait of AKT kinases: human cancer and animal models depict a family with strong individualities.* A portrait of AKT kinases: human cancer and animal models depict a family with strong individualities, 2004.

100. Gonzalez, E. and T.E. McGraw, *The Akt kinases: isoform specificity in metabolism and cancer.* Cell Cycle, 2009. **8**(16): p. 2502-8.

101. Yang, Z.Z., et al., *Protein kinase B alpha/Akt1 regulates placental development and fetal growth.* J Biol Chem, 2003. **278**(34): p. 32124-31.

102. Datta, S., A. Brunet, and M.E. Greenberg, *Cellular survival: a play in three Akts.* Genes & Development, 1999. **13**(22): p. 2905-2927.

103. Kumar, C.C. and V. Madison, *AKT crystal structure and AKT-specific inhibitors.* Oncogene, 2005. **24**(50): p. 7493-501.

104. Engelman, J.A., J. Luo, and L.C. Cantley, *The evolution of phosphatidylinositol 3-kinases as regulators of growth and metabolism.* Nat Rev Genet, 2006. **7**(8): p. 606-19.

105. Manning, B.D. and A. Toker, *AKT/PKB Signaling: Navigating the Network.* Cell, 2017. **169**(3): p. 381-405.

106. Stokoe, D., et al., *Dual role of phosphatidylinositol-3,4,5-trisphosphate in the activation of protein kinase B.* Science, 1997. **277**(5325): p. 567-70.

107. Liu, P., et al., *PtdIns(3,4,5)P3-Dependent Activation of the mTORC2 Kinase Complex.* Cancer Discov, 2015. **5**(11): p. 1194-209.

108. Ebner, M., et al., *Localization of mTORC2 activity inside cells.* J Cell Biol, 2017. **216**(2): p. 343-353.

109. Jethwa, N., et al., *Endomembrane PtdIns(3,4,5)P3 activates the PI3K–Akt pathway.* J Cell Sci, 2015. **128**(18): p. 3456-3465.

110. Bellacosa, A., et al., *Activation of AKT kinases in cancer: implications for therapeutic targeting.* Adv Cancer Res, 2005. **94**: p. 29-86.

111. Alessi, D.R., et al., *Mechanism of activation of protein kinase B by insulin and IGF-1.* EMBO J, 1996. **15**(23): p. 6541-51.

112. Alessi, D.R., et al., *Characterization of a 3-phosphoinositide-dependent protein kinase which phosphorylates and activates protein kinase Balpha.* Curr Biol, 1997. **7**(4): p. 261-9.

113. Stephens, L., et al., *Protein kinase B kinases that mediate phosphatidylinositol 3,4,5-trisphosphate-dependent activation of protein kinase B.* Science, 1998. **279**(5351): p. 710-4.

114. Yang, J., et al., *Molecular mechanism for the regulation of protein kinase B/Akt by hydrophobic motif phosphorylation.* Mol Cell, 2002. **9**(6): p. 1227-40.

115. Brodbeck, D., M.M. Hill, and B.A. Hemmings, *Two splice variants of protein kinase B gamma have different regulatory capacity depending on the presence or absence of the regulatory phosphorylation site serine 472 in the carboxyl-terminal hydrophobic domain.* J Biol Chem, 2001. **276**(31): p. 29550-8.

116. Maehama, T. and J.E. Dixon, *The tumor suppressor, PTEN/MMAC1, dephosphorylates the lipid second messenger, phosphatidylinositol 3,4,5-trisphosphate.* J Biol Chem, 1998. **273**(22): p. 13375-8.

117. Manning, B.D. and L.C. Cantley, *AKT/PKB Signaling: Navigating Downstream.* Cell, 2007. **129**(7): p. 1261-1274.

118. Datta, S.R., et al., *Akt phosphorylation of BAD couples survival signals to the cell-intrinsic death machinery.* Cell, 1997. **91**(2): p. 231-41.

119. Tran, H., et al., *The many forks in FOXO's road.* Sci STKE, 2003. **2003**(172): p. RE5.

120. Tzivion, G., M. Dobson, and G. Ramakrishnan, *FoxO transcription factors; Regulation by AKT and 14-3-3 proteins.* Biochim Biophys Acta, 2011. **1813**(11): p. 1938-45.

121. Cross, D.A., et al., *Inhibition of glycogen synthase kinase-3 by insulin mediated by protein kinase B.* Nature, 1995. **378**(6559): p. 785-9.

122. Dajani, R., et al., *Crystal structure of glycogen synthase kinase 3 beta: structural basis for phosphate-primed substrate specificity and autoinhibition.* Cell, 2001. **105**(6): p. 721-32.

123. Frame, S. and P. Cohen, *GSK3 takes centre stage more than 20 years after its discovery.* Biochem J, 2001. **359**(Pt 1): p. 1-16.

124. Wullschleger, S., R. Loewith, and M.N. Hall, *TOR signaling in growth and metabolism.* Cell, 2006. **124**(3): p. 471-84.

125. Manning, B.D. and L.C. Cantley, *Rheb fills a GAP between TSC and TOR.* Trends Biochem Sci, 2003. **28**(11): p. 573-6.

126. Inoki, K., et al., *TSC2 is phosphorylated and inhibited by Akt and suppresses mTOR signalling.* Nat Cell Biol, 2002. **4**(9): p. 648-57.

127. Potter, C.J., L.G. Pedraza, and T. Xu, *Akt regulates growth by directly phosphorylating Tsc2.* Nat Cell Biol, 2002. **4**(9): p. 658-65.

128. Kovacina, K.S., et al., *Identification of a proline-rich Akt substrate as a 14-3-3 binding partner.* J Biol Chem, 2003. **278**(12): p. 10189-94.

129. Sancak, Y., et al., *PRAS40 is an insulin-regulated inhibitor of the mTORC1 protein kinase.* Mol Cell, 2007. **25**(6): p. 903-15.

130. Liang, J., et al., *PKB/Akt phosphorylates p27, impairs nuclear import of p27 and opposes p27-mediated G1 arrest.* Nat Med, 2002. **8**(10): p. 1153-60.

131. Shin, I., et al., *PKB/Akt mediates cell-cycle progression by phosphorylation of p27(Kip1) at threonine 157 and modulation of its cellular localization.* Nat Med, 2002. **8**(10): p. 1145-52.

132. Viglietto, G., et al., *Cytoplasmic relocalization and inhibition of the cyclin-dependent kinase inhibitor p27(Kip1) by PKB/Akt-mediated phosphorylation in breast cancer.* Nat Med, 2002. **8**(10): p. 1136-44.

133. Diehl, J.A., et al., *Glycogen synthase kinase-3beta regulates cyclin D1 proteolysis and subcellular localization.* Genes Dev, 1998. **12**(22): p. 3499-511.

134. Welcker, M., et al., *Multisite phosphorylation by Cdk2 and GSK3 controls cyclin E degradation.* Mol Cell, 2003. **12**(2): p. 381-92.

135. Mamane, Y., et al., *eIF4E--from translation to transformation.* Oncogene, 2004. **23**(18): p. 3172-9.

136. Markus, A., J. Zhong, and W.D. Snider, *Raf and Akt Mediate Distinct Aspects of Sensory Axon Growth.* Neuron, 2002. **35**(1): p. 65-76.

137. Kwon, C.H., et al., *Pten regulates neuronal arborization and social interaction in mice.* Neuron, 2006. **50**(3): p. 377-88.

138. Ries, V., et al., *Oncoprotein Akt/PKB induces trophic effects in murine models of Parkinson's disease.* Proceedings of the National Academy of Sciences, 2006. **103**(49): p. 18757-18762.

139. Kim, S., et al., *Dopaminergic pathway reconstruction by Akt/Rheb-induced axon regeneration.* Annals of Neurology, 2011. **70**(1): p. 110-120.

140. Kim, S., et al., *AAV transduction of dopamine neurons with constitutively active Rheb protects from neurodegeneration and mediates axon regrowth.* Molecular therapy : the journal of the American Society of Gene Therapy, 2012. **20**(2): p. 275-286.

141. Greene, L.A., O. Levy, and C. Malagelada, *Akt as a victim, villain and potential hero in Parkinson's disease pathophysiology and treatment.* Cell Mol Neurobiol, 2011. **31**(7): p. 969-78.

142. Ries, V., et al., *Regulation of the postnatal development of dopamine neurons of the substantia nigra in vivo by Akt/protein kinase B.* J Neurochem, 2009. **110**(1): p. 23-33.

143. Howell, K.R., K. Floyd, and A.J. Law, *PKBgamma/AKT3 loss-of-function causes learning and memory deficits and deregulation of AKT/mTORC2 signaling: Relevance for schizophrenia.* PLoS One, 2017. **12**(5): p. e0175993.

144. Zheng, W., et al., *The possible role of the Akt signaling pathway in schizophrenia.* Brain Res, 2012. **1470**: p. 145-58.

145. Wang, L., et al., *Brain Development and Akt Signaling: the Crossroads of Signaling Pathway and Neurodevelopmental Diseases.* J Mol Neurosci, 2017. **61**(3): p. 379-384.

146. Lu, T., et al., *REST and stress resistance in ageing and Alzheimer's disease.* Nature, 2014. **507**(7493): p. 448-454.

147. Song, Z., et al., *REST alleviates neurotoxic prion peptide-induced synaptic abnormalities, neurofibrillary degeneration and neuronal death partially via LRP6-mediated Wnt-beta-catenin signaling.* Oncotarget, 2016. **7**(11): p. 12035-52.

148. Song, Z., et al., *Downregulation of the Repressor Element 1-Silencing Transcription Factor (REST) Is Associated with Akt-mTOR and Wnt-beta-Catenin Signaling in Prion Diseases Models.* Front Mol Neurosci, 2017. **10**: p. 128.

149. Rickle, A., et al., *Akt activity in Alzheimer's disease and other neurodegenerative disorders.* Neuroreport, 2004. **15**(6): p. 955-9.

150. C, O.N., *PI3-kinase/Akt/mTOR signaling: impaired on/off switches in aging, cognitive decline and Alzheimer's disease.* Exp Gerontol, 2013. **48**(7): p. 647-53.

151. Mercado-Gomez, O., et al., *Inhibition of Wnt and PI3K signaling modulates GSK-3beta activity and induces morphological changes in cortical neurons: role of tau phosphorylation.* Neurochem Res, 2008. **33**(8): p. 1599-609.

152. Malagelada, C., Z.H. Jin, and L.A. Greene, *RTP801 is induced in Parkinson's disease and mediates neuron death by inhibiting Akt phosphorylation/activation.* The Journal of neuroscience : the official journal of the Society for Neuroscience, 2008. **28**(53): p. 14363-14371.

153. Timmons, S., et al., *Akt signal transduction dysfunction in Parkinson's disease.* Neuroscience letters, 2009. **467**(1): p. 30-35.

154. Elstner, M., et al., *Expression analysis of dopaminergic neurons in Parkinson's disease and aging links transcriptional dysregulation of energy metabolism to cell death.* Acta Neuropathol, 2011. **122**(1): p. 75-86.

155. Kim, W., et al., *miR-126 contributes to Parkinson's disease by dysregulating the insulin-like growth factor/phosphoinositide 3-kinase signaling.* Neurobiology of aging, 2014.

156. Anglade, P., et al., *Apoptosis and autophagy in nigral neurons of patients with Parkinson's disease.* Histol Histopathol, 1997. **12**(1): p. 25-31.

157. Hirsch, E.C., et al., *Glial cell participation in the degeneration of dopaminergic neurons in Parkinson's disease.* Adv Neurol, 1999. **80**: p. 9-18.

158. Tompkins, M.M., et al., *Apoptotic-like changes in Lewy-body-associated disorders and normal aging in substantia nigral neurons.* Am J Pathol, 1997. **150**(1): p. 119-31.

159. Mogi, M., et al., *Brain-derived growth factor and nerve growth factor concentrations are decreased in the substantia nigra in Parkinson's disease.* Neurosci Lett, 1999. **270**(1): p. 45-8.

160. Chauhan, N.B., G.J. Siegel, and J.M. Lee, *Depletion of glial cell line-derived neurotrophic factor in substantia nigra neurons of Parkinson's disease brain.* J Chem Neuroanat, 2001. **21**(4): p. 277-88.

161. Howells, D.W., et al., *Reduced BDNF mRNA expression in the Parkinson's disease substantia nigra.* Exp Neurol, 2000. **166**(1): p. 127-35.

162. Yang, Y., et al., *Inactivation of Drosophila DJ-1 leads to impairments of oxidative stress response and phosphatidylinositol 3-kinase/Akt signaling.* Proc Natl Acad Sci U S A, 2005. **102**(38): p. 13670-5.

163. Murata, H., et al., *A new cytosolic pathway from a Parkinson disease-associated kinase, BRPK/PINK1: activation of AKT via mTORC2.* J Biol Chem, 2011. **286**(9): p. 7182-9.

164. Zhao, J., et al., *Oxidative Modification and Its Implications for the Neurodegeneration of Parkinson's Disease.* Mol Neurobiol, 2017. **54**(2): p. 1404-1418.

165. Nair, V.D. and C.W. Olanow, *Differential modulation of Akt/glycogen synthase kinase-3beta pathway regulates apoptotic and cytoprotective signaling responses.* J Biol Chem, 2008. **283**(22): p. 15469-78.

166. Durgadoss, L., et al., *Redox modification of Akt mediated by the dopaminergic neurotoxin MPTP, in mouse midbrain, leads to down-regulation of pAkt.* FASEB J, 2012. **26**(4): p. 1473-83.

167. Heras-Sandoval, D., et al., *The role of PI3K/AKT/mTOR pathway in the modulation of autophagy and the clearance of protein aggregates in neurodegeneration.* Cell Signal, 2014. **26**(12): p. 2694-701.

168. Sanchez-Mora, R.M., H. Arboleda, and G. Arboleda, *PINK1 overexpression protects against C2-ceramide-induced CAD cell death through the PI3K/AKT pathway.* J Mol Neurosci, 2012. **47**(3): p. 582-94.

169. Aleyasin, H., et al., *DJ-1 protects the nigrostriatal axis from the neurotoxin MPTP by modulation of the AKT pathway.* Proc Natl Acad Sci U S A, 2010. **107**(7): p. 3186-91.

170. Malagelada, C., et al., *Rapamycin protects against neuron death in in vitro and in vivo models of Parkinson's disease.* J Neurosci, 2010. **30**(3): p. 1166-75.

171. Luo, L., et al., *L-F001, a Multifunction ROCK Inhibitor Prevents 6-OHDA Induced Cell Death Through Activating Akt/GSK-3beta and Nrf2/HO-1 Signaling Pathway in PC12 Cells and Attenuates MPTP-Induced Dopamine Neuron Toxicity in Mice.* Neurochem Res, 2017. **42**(2): p. 615-624.

172. Bao, X.Q., et al., *Squamosamide derivative FLZ protected dopaminergic neuron by activating Akt signaling pathway in 6-OHDA-induced in vivo and in vitro Parkinson's disease models.* Brain Res, 2014. **1547**: p. 49-57.

173. Wang, L., et al., *Insulin-like growth factor 1 protects human neuroblastoma cells SH-EP1 against MPP+-induced apoptosis by AKT/GSK-3beta/JNK signaling.* Apoptosis, 2010. **15**(12): p. 1470-9.

174. Cheng, H.-C.C., et al., *Akt suppresses retrograde degeneration of dopaminergic axons by inhibition of macroautophagy.* The Journal of neuroscience : the official journal of the Society for Neuroscience, 2011. **31**(6): p. 2125-2135.

175. Grider, M.H., et al., *Lipid raft-targeted Akt promotes axonal branching and growth cone expansion via mTOR and Rac1, respectively.* J Neurosci Res, 2009. **87**(14): p. 3033-42.

176. Foster, D.A. and A. Toschi, *Targeting mTOR with rapamycin: one dose does not fit all.* Cell Cycle, 2009. **8**(7): p. 1026-9.

177. Harkavyi, A. and P.S. Whitton, *Glucagon-like peptide 1 receptor stimulation as a means of neuroprotection.* British journal of pharmacology, 2010. **159**(3): p. 495-501.

178. Weinreb, O., et al., *Rasagiline: a novel anti-Parkinsonian monoamine oxidase-B inhibitor with neuroprotective activity.* Prog Neurobiol, 2010. **92**(3): p. 330-44.

179. Olanow, C.W., et al., *A double-blind, delayed-start trial of rasagiline in Parkinson's disease.* N Engl J Med, 2009. **361**(13): p. 1268-78.

180. Jo, H., et al., *Small molecule-induced cytosolic activation of protein kinase Akt rescues ischemia-elicited neuronal death.* Proceedings of the National Academy of Sciences of the United States of America, 2012. **109**(26): p. 10581-10586.

181. Carpten, J.D., et al., *A transforming mutation in the pleckstrin homology domain of AKT1 in cancer.* Nature, 2007. **448**(7152): p. 439-444.

182. Yi, K.H. and J. Lauring, *Recurrent AKT mutations in human cancers: functional consequences and effects on drug sensitivity.* Oncotarget, 2016. **7**(4): p. 4241-51.

183. Kordower, J.H., et al., *Neurodegeneration prevented by lentiviral vector delivery of GDNF in primate models of Parkinson's disease.* Science, 2000. **290**(5492): p. 767-73.

184. Scalzo, P., et al., *Serum levels of brain-derived neurotrophic factor correlate with motor impairment in Parkinson's disease.* J Neurol, 2010. **257**(4): p. 540-5.

185. Kordower, J.H., et al., *Delivery of neurturin by AAV2 (CERE-120)-mediated gene transfer provides structural and functional neuroprotection and neurorestoration in MPTP-treated monkeys.* Ann Neurol, 2006. **60**(6): p. 706-15.

186. Lang, A.E., et al., *Randomized controlled trial of intraputamenal glial cell line-derived neurotrophic factor infusion in Parkinson disease.* Ann Neurol, 2006. **59**(3): p. 459-66.

187. Bartus, R.T., et al., *Post-mortem assessment of the short and long-term effects of the trophic factor neurturin in patients with alpha-synucleinopathies.* Neurobiol Dis, 2015. **78**: p. 162-71.

188. Sullivan, A.M. and G.W. O'Keeffe, *Neurotrophic factor therapy for Parkinson's disease: past, present and future.* Neural Regen Res, 2016. **11**(2): p. 205-7.

189. Mittermeyer, G., et al., *Long-term evaluation of a phase 1 study of AADC gene therapy for Parkinson's disease.* Hum Gene Ther, 2012. **23**(4): p. 377-81.

190. Palfi, S., et al., *Long-term safety and tolerability of ProSavin, a lentiviral vector-based gene therapy for Parkinson's disease: a dose escalation, open-label, phase 1/2 trial.* Lancet, 2014. **383**(9923): p. 1138-46.

191. Iwamoto, M., et al., *A general chemical method to regulate protein stability in the mammalian central nervous system.* Chemistry & biology, 2010. **17**(9): p. 981-988.

192. Banaszynski, L.A., et al., *A rapid, reversible, and tunable method to regulate protein function in living cells using synthetic small molecules.* Cell, 2006. **126**(5): p. 995-1004.

193. Banaszynski, L.A., et al., *Chemical control of protein stability and function in living mice.* Nature medicine, 2008. **14**(10): p. 1123-1127.

194. Armstrong, C.M. and D.E. Goldberg, *An FKBP destabilization domain modulates protein levels in Plasmodium falciparum.* Nat Methods, 2007. **4**(12): p. 1007-9.

195. Brooks, C.F., et al., *The toxoplasma apicoplast phosphate translocator links cytosolic and apicoplast metabolism and is essential for parasite survival.* Cell Host Microbe, 2010. **7**(1): p. 62-73.

196. Herm-Gotz, A., et al., *Rapid control of protein level in the apicomplexan Toxoplasma gondii.* Nat Methods, 2007. **4**(12): p. 1003-5.

197. Dvorin, J.D., et al., *A plant-like kinase in Plasmodium falciparum regulates parasite egress from erythrocytes.* Science, 2010. **328**(5980): p. 910-2.

198. Madeira da Silva, L., et al., *Regulated expression of the Leishmania major surface virulence factor lipophosphoglycan using conditionally destabilized fusion proteins.* Proc Natl Acad Sci U S A, 2009. **106**(18): p. 7583-8.

199. Raj, D.K., et al., *Antibodies to PfSEA-1 block parasite egress from RBCs and protect against malaria infection.* Science, 2014. **344**(6186): p. 871-7.

200. Campeau, E., et al., *A versatile viral system for expression and depletion of proteins in mammalian cells.* PLoS One, 2009. **4**(8): p. e6529.

201. Dolan, B.P., et al., *MHC class I antigen processing distinguishes endogenous antigens based on their translation from cellular vs. viral mRNA.* Proc Natl Acad Sci U S A, 2012. **109**(18): p. 7025-30.

202. Gong, Y. and T. de Lange, *A Shld1-controlled POT1a provides support for repression of ATR signaling at telomeres through RPA exclusion.* Mol Cell, 2010. **40**(3): p. 377-87.

203. Kwan, M.D., et al., *Chemical control of FGF-2 release for promoting calvarial healing with adipose stem cells.* J Biol Chem, 2011. **286**(13): p. 11307-13.

204. Pruett-Miller, S.M., et al., *Attenuation of zinc finger nuclease toxicity by small-molecule regulation of protein levels.* PLoS Genet, 2009. **5**(2): p. e1000376.

205. Park, A., et al., *CRISPR/Cas9 Allows Efficient and Complete Knock-In of a Destabilization Domain-Tagged Essential Protein in a Human Cell Line, Allowing Rapid Knockdown of Protein Function.* PLoS ONE, 2014. **9**(4).

206. Miyazaki, Y., et al., *Destabilizing Domains Derived from the Human Estrogen Receptor.* Journal of the American Chemical Society, 2012. **134**(9): p. 3942-3945.

207. Bonger, K.M., et al., *General method for regulating protein stability with light.* ACS chemical biology, 2013. **9**(1): p. 111-115.

208. Liu, P., et al., *A bioorthogonal small-molecule-switch system for controlling protein function in live cells.* Angewandte Chemie (International ed. in English), 2014. **53**(38): p. 10049-10055.

209. Muralidharan, V., et al., *Plasmodium falciparum heat shock protein 110 stabilizes the asparagine repeat-rich parasite proteome during malarial fevers.* Nat Commun, 2012. **3**: p. 1310.

210. Muralidharan, V., et al., *Asparagine repeat function in a Plasmodium falciparum protein assessed via a regulatable fluorescent affinity tag.* Proc Natl Acad Sci U S A, 2011. **108**(11): p. 4411-6.

211. Tai, K., et al., *Destabilizing domains mediate reversible transgene expression in the brain.* PloS one, 2012. **7**(9).

212. Quintino, L., et al., *Functional neuroprotection and efficient regulation of GDNF using destabilizing domains in a rodent model of Parkinson's disease.* Molecular therapy : the journal of the American Society of Gene Therapy, 2013. **21**(12): p. 2169-2180.

213. Cederfjäll, E., L. Broom, and D. Kirik, *Controlled Striatal DOPA Production From a Gene Delivery System in a Rodent Model of Parkinson's Disease.* Molecular Therapy, 2015. **23**(5): p. 896-906.

214. Egeler, E.L., et al., *Ligand-switchable Substrates for a Ubiquitin-Proteasome System.* Journal of Biological Chemistry, 2011. **286**(36): p. 31328-31336.

215. Barling, R.W. and J.B. Selkon, *The penetration of antibiotics into cerebrospinal fluid and brain tissue.* J Antimicrob Chemother, 1978. **4**(3): p. 203-27.

216. Svensson, R., P. Larsson, and K. Lincoln, *Low dose trimethoprim prophylaxis in long term control of chronic recurrent urinary tract infection.* Scand J Infect Dis, 1982. **14**(2): p. 139-42.

217. Forna, F., et al., *Systematic review of the safety of trimethoprim-sulfamethoxazole for prophylaxis in HIV-infected pregnant women: implications for resource-limited settings.* AIDS Rev, 2006. **8**(1): p. 24-36.

218. Rungoe, C., et al., *Infections during induction therapy for children with acute lymphoblastic leukemia. the role of sulfamethoxazole-trimethoprim (SMX-TMP) prophylaxis.* Pediatr Blood Cancer, 2010. **55**(2): p. 304-8.

219. Zywiel, M.G., et al., *Prophylactic oral antibiotics reduce reinfection rates following two-stage revision total knee arthroplasty.* Int Orthop, 2011. **35**(1): p. 37-42.

220. Bellacosa, A., et al., *Akt activation by growth factors is a multiple-step process: the role of the PH domain.* Oncogene, 1998. **17**(3): p. 313-325.

221. Hyvonen, M. and M. Saraste, *Structure of the PH domain and Btk motif from Bruton's tyrosine kinase: molecular explanations for X-linked agammaglobulinaemia.* EMBO J, 1997. **16**(12): p. 3396-404.

222. Skorski, T., et al., *Transformation of hematopoietic cells by BCR/ABL requires activation of a PI-3k/Akt-dependent pathway.* EMBO J, 1997. **16**(20): p. 6151-61.

223. Ahmed, N.N., et al., *Transduction of interleukin-2 antiapoptotic and proliferative signals via Akt protein kinase.* Proc Natl Acad Sci U S A, 1997. **94**(8): p. 3627-32.

224. Greene, L.A. and A.S. Tischler, *Establishment of a noradrenergic clonal line of rat adrenal pheochromocytoma cells which respond to nerve growth factor.* Proc Natl Acad Sci U S A, 1976. **73**(7): p. 2424-8.

225. Liu, J., et al., *Activating transcription factor 4 (ATF4) modulates post-synaptic development and dendritic spine morphology.* Front Cell Neurosci, 2014. **8**: p. 177.

226. Rayport, S., et al., *Identified postnatal mesolimbic dopamine neurons in culture: morphology and electrophysiology.* J Neurosci, 1992. **12**(11): p. 4264-80.

227. Edinger, A.L. and C.B. Thompson, *Akt maintains cell size and survival by increasing mTOR-dependent nutrient uptake.* Mol Biol Cell, 2002. **13**(7): p. 2276-88.

228. Ceci, M., et al., *Cardiac-specific overexpression of E40K active Akt prevents pressure overload-induced heart failure in mice by increasing angiogenesis and reducing apoptosis.* Cell Death & Differentiation, 2007. **14**(5): p. 1060-1062.

229. Aoki, M., et al., *The akt kinase: molecular determinants of oncogenicity.* Proc Natl Acad Sci U S A, 1998. **95**(25): p. 14950-5.

230. Hart, J.R. and P.K. Vogt, *Phosphorylation of AKT: a mutational analysis.* Oncotarget, 2011. **2**(6): p. 467-76.

231. Pellman, D., et al., *An N-terminal peptide from p60src can direct myristylation and plasma membrane localization when fused to heterologous proteins.* Nature, 1985. **314**(6009): p. 374-7.

232. Shiojima, I. and K. Walsh, *Regulation of cardiac growth and coronary angiogenesis by the Akt/PKB signaling pathway.* Genes Dev, 2006. **20**(24): p. 3347-65.

233. Sussman, M.A., et al., *Myocardial AKT: the omnipresent nexus.* Physiol Rev, 2011. **91**(3): p. 1023-70.

234. Yang, J., et al., *Crystal structure of an activated Akt/protein kinase B ternary complex with GSK3-peptide and AMP-PNP.* Nat Struct Biol, 2002. **9**(12): p. 940-4.

235. Ebrahimi-Fakhari, D., L. Wahlster, and P.J. McLean, *Protein degradation pathways in Parkinson's disease: curse or blessing.* Acta neuropathologica, 2012. **124**(2): p. 153-172.

236. Olanow, C.W. and K.S. McNaught, *Ubiquitin-proteasome system and Parkinson's disease.* Mov Disord, 2006. **21**(11): p. 1806-23.

237. McNaught, K.S., et al., *Altered proteasomal function in sporadic Parkinson's disease.* Exp Neurol, 2003. **179**(1): p. 38-46.

238. Zeng, B.Y., et al., *Proteasomal activity in brain differs between species and brain regions and changes with age.* Mech Ageing Dev, 2005. **126**(6-7): p. 760-6.

239. van der Horst, A. and B.M. Burgering, *Stressing the role of FoxO proteins in lifespan and disease.* Nat Rev Mol Cell Biol, 2007. **8**(6): p. 440-50.

240. Dansen, T.B. and B.M. Burgering, *Unravelling the tumor-suppressive functions of FOXO proteins.* Trends Cell Biol, 2008. **18**(9): p. 421-9.

241. Brenkman, A.B., et al., *The peptidyl-isomerase Pin1 regulates p27kip1 expression through inhibition of Forkhead box O tumor suppressors.* Cancer Res, 2008. **68**(18): p. 7597-605.

242. Yang, H., et al., *Constitutively active FOXO4 inhibits Akt activity, regulates p27 Kip1 stability, and suppresses HER2-mediated tumorigenicity.* Oncogene, 2005. **24**(11): p. 1924-35.

243. Wang, W., P.H. Zhou, and W. Hu, *Overexpression of FOXO4 induces apoptosis of clear-cell renal carcinoma cells through downregulation of Bim.* Mol Med Rep, 2016. **13**(3): p. 2229-34.

244. Kops, G.J., et al., *Direct control of the Forkhead transcription factor AFX by protein kinase B.* Nature, 1999. **398**(6728): p. 630-4.

245. Takaishi, H., et al., *Regulation of nuclear translocation of forkhead transcription factor AFX by protein kinase B.* Proc Natl Acad Sci U S A, 1999. **96**(21): p. 11836-41.

246. Grau, C.M. and L.A. Greene, *Use of PC12 cells and rat superior cervical ganglion sympathetic neurons as models for neuroprotective assays relevant to Parkinson's disease.* Methods Mol Biol, 2012. **846**: p. 201-11.

247. Walkinshaw, G. and C.M. Waters, *Neurotoxin-induced cell death in neuronal PC12 cells is mediated by induction of apoptosis.* Neuroscience, 1994. **63**(4): p. 975-87.

248. Hartley, A., et al., *Complex I inhibitors induce dose-dependent apoptosis in PC12 cells: relevance to Parkinson's disease.* J Neurochem, 1994. **63**(5): p. 1987-90.

249. Weinberg, M.S., R.J. Samulski, and T.J. McCown, *Adeno-associated virus (AAV) gene therapy for neurological disease.* Neuropharmacology, 2013. **69**: p. 82-88.

250. Markakis, E.A., et al., *Comparative transduction efficiency of AAV vector serotypes 1-6 in the substantia nigra and striatum of the primate brain.* Mol Ther, 2010. **18**(3): p. 588-93.

251. Bartus, R.T., M.S. Weinberg, and R.J. Samulski, *Parkinson's disease gene therapy: success by design meets failure by efficacy.* Mol Ther, 2014. **22**(3): p. 487-97.

252. Jeon, M.-T.T., et al., *In vivo AAV1 transduction with hRheb(S16H) protects hippocampal neurons by BDNF production.* Molecular therapy : the journal of the American Society of Gene Therapy, 2015. **23**(3): p. 445-455.

253. Nam, J.H., et al., *Induction of GDNF and BDNF by hRheb(S16H) Transduction of SNpc Neurons: Neuroprotective Mechanisms of hRheb(S16H) in a Model of Parkinson's Disease.* Molecular neurobiology, 2015. **51**(2): p. 487-499.

254. Davidson, B.L. and X.O. Breakefield, *Viral vectors for gene delivery to the nervous system.* Nat Rev Neurosci, 2003. **4**(5): p. 353-64.

255. Cragg, S.J., et al., *Dopamine-mediated volume transmission in midbrain is regulated by distinct extracellular geometry and uptake.* J Neurophysiol, 2001. **85**(4): p. 1761-71.

256. Westerhout, J., M. Danhof, and E.C. De Lange, *Preclinical prediction of human brain target site concentrations: considerations in extrapolating to the clinical setting.* J Pharm Sci, 2011. **100**(9): p. 3577-93.

257. Loryan, I., et al., *In-depth neuropharmacokinetic analysis of antipsychotics based on a novel approach to estimate unbound target-site concentration in CNS regions: link to spatial receptor occupancy.* Mol Psychiatry, 2016. **21**(11): p. 1527-1536.

258. Rakhit, R., R. Navarro, and T.J. Wandless, *Chemical biology strategies for posttranslational control of protein function.* Chem Biol, 2014. **21**(9): p. 1238-52.

259. Czapinski, J., et al., *How to Train a Cell-Cutting-Edge Molecular Tools.* Front Chem, 2017. **5**: p. 12.

260. Senturk, S., et al., *Rapid and tunable method to temporally control gene editing based on conditional Cas9 stabilization.* Nat Commun, 2017. **8**: p. 14370.

261. Koprich, J.B., et al., *Expression of human A53T alpha-synuclein in the rat substantia nigra using a novel AAV1/2 vector produces a rapidly evolving pathology with protein*

*aggregation, dystrophic neurite architecture and nigrostriatal degeneration with potential to model the pathology of Parkinson's disease.* Mol Neurodegener, 2010. **5**: p. 43.

262. Chtarto, A., et al., *A next step in adeno-associated virus-mediated gene therapy for neurological diseases: regulation and targeting.* Br J Clin Pharmacol, 2013. **76**(2): p. 217-32.

263. Kordower, J.H., *Gene therapy for Parkinson's disease: still a hot topic?* Neuropsychopharmacology, 2015. **40**(1): p. 255-6.

264. Brichta, L. and P. Greengard, *Molecular determinants of selective dopaminergic vulnerability in Parkinson's disease: an update.* Front Neuroanat, 2014. **8**: p. 152.

265. Dickson, D.W., *Linking selective vulnerability to cell death mechanisms in Parkinson's disease.* Am J Pathol, 2007. **170**(1): p. 16-9.